Sensory Synaptic Mechanisms Within the Nucleus of the Solitary Tract

By

Mark Doyle

A Dissertation

Presented to the Department of Physiology and Pharmacology

And the Oregon Health Sciences University

School of Medicine

in partial fulfillment of

the requirement for the degree of

Doctor of Philosophy

March 2001

School of Medicine
Oregon Health Sciences University

Certificate of Approval

This is to certify the the Ph.D. thesis of

Mark Doyle

Has been approved

[redacted]
Professor in charge of thesis

[redacted]
Member

[redacted]
Member

[redacted]
Member

[redacted]
Member

TABLE OF CONTENTS

LIST OF FIGURES

CHAPTER 1

CHAPTER 2

CHAPTER 3

CHAPTER 4

ABBREVIATIONS

αβ-metATP	Alpha-Beta-Methylene Adenosine Triphosphate
ACSF	Artificial Cerebral Spinal Fluid
ACTH	Adreno Corticotropic Hormone
ADN	Aortic Depressor Nerve
ANP	Atrial Natriatic Peptide
AP-5	DL-2-Amino-5-Phosphonovaleric Acid
ATP	Adenosine Triphosphate
AV	Atrio-ventricular
CAP	Capsaicin
CGRP	Calcitonin Gene-Related Peptide
CNQX	6-Cyano-7-nitroquinoxaline- 2,3-dione
CNS	Central Nervous System
CSN	Carotid Sinus Nerve
CV	Cardiovascular
CVLM	Caudal Ventral Lateral Medulla
DiA	4-(4-(dihexadecylamino)styryl) -N-methylpyridinium iodide
DIC	Differential Interferance Contrast
DiI	1,1'-dioctadecyl-3,3,3',3'- tetramethylindocarbocyanine perchlorate
DMNX	Dorsal Motor Nucleus of the Vagus
EPSC	Excitatory Post-synaptic Current
EPSP	Excitatory Post-synaptic Potential
FDD	Frequency-Dependent Depression
GABA	Gamma Amino Butyric Acid
GLU	Glutamate
HR	Heart Rate
Hz	Hertz
IPSC	Inhibitory Post-synaptic Current
IPSP	Inhibitory Post-synaptic Potential

IR	Infared
mSec	Milliseconds
mV	Millivolt
NA	Nucleus Ambiguus
nA	Nanoamps
NBQX	2,3-Dioxo-6-nitro-1,2,3,4-tetrahydrobenzo[f]quinoxaline-7-)sulphonamide
NMDA	n-Methyl d-Aspartate
NTS	Nucleus of the Solitary Tract
P2X	Purinurgic Receptor
pA	Picoamps
PB&J	Peanut Butter and Jelly
PNS	Parasympathetic Nervous System
PSC	Post-synaptic Current
RVLM	Rostral Ventral Lateral Medulla
SA	Sino-atrial
SD	Standard Deviation
SEM	Standard Error on the Mean
SNS	Sympathetic Nervous System
SP	Substance P
ST	Solitary Tract
SV	Stroke Volume
TNP-ATP	2'-(or-3')-O-(trinitrophenyl) adenosine 5'-triphosphate, trisodium salt
TRH	Thyrotrophin-releasing hormone
TTX	Tetrodotoxin
uM	Micromolar
usec	Microseconds
Vh	Holding Potential
VIP	Vasoactive Intestinal Peptide
Vm	Membrane Potential

VR1	Vanilloid Receptor -1

ACKNOWLEDGEMENTS

I would like to thank my mentor, Dr. Michael Andresen, for providing support, encouragement and the opportunity to perform my graduate work in his laboratory. I would also like to thank all the other scientists who collaborated and shared this experience with me, especially Dr John Schild, and family, for his outstanding encouragement.

Most importantly, I would like to thank my wife, Beth for her incredible patience and support through this time in our lives.

PREFACE

In accordance with the guidelines set forth by the Graduate Program of the School of Medicine, Oregon Health Science University, Portland Oregon, I have prepared my dissertation, consisting of a general introduction, two chapters of original data, and a final chapter discussing the findings. References are listed separately in alphabetical order and follow the format of *J. Neurophysiol.*

Chapter two contains data figures and text as they appear in an original paper that has been published previously. Chapter three contains data, figures and text, as they would appear in an original paper that has been submitted for publication.

All work presented in this dissertation has been done by myself except the work done on dissociated NTS neurons. In order to increase resolution to discern pre- vs. post-synaptic effects, and to minimize the indirect responses from multiple synaptic connections within the slice, a dissociated neuron preparation was required. The lab was not set up to perform these experiments. As such a collaborative relationship was established with Professor Norio Akaike in Fukuoka, Japan.

ABSTRACT

Visceral sensory afferents, including those of the baroreflex, enter the brainstem via cranial nerves to form the solitary tract (ST) and terminate in NTS. NTS integrates this sensory information with descending inputs from higher brain areas. The information is distributed to multiple brainstem regions that have reciprocal connections with NTS. In reflex control of heart rate, the neuronal pathways within NTS may only involve a single synapse between the sensory afferent and an NTS second order neuron that projects out of NTS. As such, this first sensory synapse is a likely point of modulation by the multiple inputs into NTS. In order to understand the cellular mechanisms underlying this first synapse, monosynaptic sensory connections must be distinguished from polysynaptic connections within NTS and from monosynaptic connections originating from other sources.

This dissertation describes a unique preparation for studying the primary synapse of the baroreflex. The rat aortic depressor nerve contains only baroreceptor sensory afferents from the aortic arch. Lipophillic carbocyanine dyes, DiA or DiI were placed on the cervical ADN and fluorescently labeled sensory synaptic terminations on the NTS second order neurons. Fluorescent microscopy was used to identify specific neurons apposed to labeled ADN terminations within a horizontal brainstem slice. Recording electrodes were guided to these identified neurons using differential interference contrast (DIC) optics under infrared illumination. Synaptic responses evoked from ST

stimulation in these identified NTS second order neurons were characterized electrophysiologically.

To distinguish between mono- and polysynaptic postsynaptic currents (PSCs), we examined the temporal nature of the responses evoked by ST stimulation. We expected that absolute latency (the time between the stimulus and the onset of the synaptic event); the variability in the latency from one stimulus to the next (jitter, SD of latency); and the number of synaptic failures would increase with increasing neuronal pathway complexity. Increases in these temporal characteristics are often used to identify polysynaptic pathways.

ST evoked PSCs in identified NTS neurons challenged many of these expectations. Absolute latencies of PSCs in these neurons ranged from 1.3 to 4.8 msec (n=8). This range of latencies for identified neurons spanned 75% of the total range of latencies evoked by ST stimulation in this brainstem preparation. Of the EPSCs recorded from labeled second order neurons, jitter was uniformly minimal (<70 usec in 90% of responses tested). Absolute latency and jitter were significantly less for labeled EPSCs than for polysynaptic IPSCs (latency 3.25 ± 1.23 vs. 4.45 ± 0.76msec $p=0.041$ $n=6$; jitter 71.02 ± 51 vs. 273 ± 78 usec, $p=0.0001$, $n=6$), although these latencies overlapped. Some EPSC latencies recorded from identified neurons were longer than some polysynaptic IPSC latencies. Conversely, many EPSCs with latencies much shorter than the long latency EPSCs from labeled cells had such large jitter (equivalent to polysynaptic IPSC jitter) that they were likely polysynaptic EPSCs. Very

surprisingly, the prevalence of synaptic failure was not correlated ($p>0.147$; $n=49$) with either latency or jitter.

In conclusion, my findings suggest that jitter and not latency or failures best discriminates mono- from polysynaptic pathways. However, there is still ambiguity in discerning the synaptic order of some responses with intermediate temporal variability. Therefore multiple parameters should be considered in determining of the nature of the synaptic connection. Identification of the primary visceral sensory synapse within NTS will now allow a more complete characterization of the synaptic mechanisms involved in visceral sensory processing.

Chapter 1

Introduction

The upright posture of humans makes tremendous dynamic demands on the cardiovascular system to maintain blood flow to the brain and heart in the face of substantial gravitational challenges. The work conducted for this dissertation focused on portions of the brainstem region responsible for key aspects of the most rapid regulatory mechanisms of the cardiovascular regulation. The intent of this work was to improve our understanding of the mechanisms responsible for the earliest processing of sensory inputs to the brainstem and, as much as possible, the cellular mechanisms pertaining to the arterial baroreceptors that transduce and transmit the blood pressure information to the central nervous system. The following general introduction reviews important basic principles of the neural regulation of the cardiovascular system as a physiological context for this research.

Circulation in higher organisms. The evolution of increasingly larger and more complex organisms increased diffusion distances and general transport demands for nutrient distribution and waste dispersion. The development of multiple organ systems is possible only by improved mass transport as a means of maintaining cellular homeostasis at an organismic level. Circulatory systems dedicated to such tasks evolved into specialized systems of pumps and conduits for rapid and

efficient fluid transportation. The cardiovascular system of higher vertebrates performs these tasks and is also a key element in temperature regulation, hormonal communication among organs, and immune responses. Cardiovascular regulation must reliably coordinate these multiple tasks and still match blood flow to the varied needs of each individual organ system despite varying challenges from the internal and external environment.

Pump and flow. The basic circulatory scheme of higher vertebrates consists of a pump (heart) and a network of conduits for blood distribution (blood vessels). Regulating system-wide transport of blood relies on adjustments in blood volume, pump function and the caliber of the vessels. Most directly blood flow depends chiefly on two factors: the pressure gradient along the vessel path and the resistance to flow presented by the blood vessels. The system-level pressure gradient is effectively the pressure difference between the site where blood exits the heart at the aorta and the point where it returns to flow into the heart at the entrance to the right atrium. That pressure difference driving flow across the cardiovascular system of vessels is created by the pumping action of the heart. Vascular resistance is strongly dependent on vessel diameter that acutely changes with contraction of smooth muscle in the wall of the vessel. Thus, two of the most important effector targets for regulation of the overall circulation are vascular smooth muscle and cardiac muscle. Circulation throughout the body is coordinated by changes in vessel resistances while maintaining an adequate pressure gradient to meet circulatory flow demand. The pump outflow of the heart

is reflected in the total cardiac output (the product of heart rate and stroke volume).

Acute and chronic circulatory regulation. Three of the most important processes impacting the circulation work over different time frames but are mutually dependent. These are: 1) Autoregulation maintains or adjusts local blood flow across a range of pressures according to the metabolic demands of local tissue. 2) The kidney has the capacity to slowly correct for very large fluctuations in blood pressure via regulation of water and electrolytes and, therefore, total blood volume. This is accomplished through sodium and water balance that occurs slowly over hours to days. 3) The neural control of the cardiovascular system integrates both internal and external factors influencing circulatory needs. The autonomic nervous system quickly adjusts heart rate and contractile force as well as vessel diameter. Adjusting arterial diameter rapidly changes peripheral resistance while adjusting venous capacitance vessels redistributes blood between the peripheral vessels and central vessels where it affects cardiac filling volumes.

The nervous system control of the circulation is reflex in nature. Sensory neurons at key sites gather information about local conditions within and outside of the circulatory system. These sensory neurons carry their information through the cranial nerves to the brainstem or through sympathetic trunks to the spinal cord. Within the central nervous system (CNS), the sensory input is compared to an optimal level or set point by mechanisms that are not understood. Deviations from

the set point initiate compensatory changes that maintain cardiovascular function. Output of the reflex through efferent neurons directed toward cardiovascular targets (e.g. the heart and vasculature) compensate for these perturbations.

Autonomic cardiovascular control pathway. The nervous system is an important aspect of cardiovascular control. A series of neural reflexes rapidly adjust circulatory performance and provide for homeostatic control. Most neural cardiovascular regulation is organized on the principle of negative feedback in these reflex loops. The basic reflex **(Figure 1-1)** consists of three primary components: the sensory input, the central nervous system comparator/integrator and the efferent neural output to the cardiovascular effectors. The input from sensory neurons is compared centrally to an integrated set point around which regulation occurs and then efferent nerve pathways alter function of the heart and blood vessels. Efferent output is primarily accomplished through the sympathetic and parasympathetic limbs of the autonomic nervous system. Sympathetic outputs enhance cardiovascular function increasing cardiac function and constricting vessels. Parasympathetic outputs inhibit particularly cardiac function decreasing heart rate and cardiac output. Thus, note that the two limbs of the autonomic nervous system have opposite effects.

Arterial baroreflex and autonomic control One particularly important sensory afferent input to baroreceptor reflex loops is from stretch receptors found in the outer walls of major arteries (Coleridge and Coleridge 1980;Thoren 1979). These

baroreceptors have discharge directly related to blood pressure (Seagard et al. 1990;Thoren and Jones 1977) and as such the reflexes which are evoked by their activation are termed arterial baroreflexes. Activation of baroreceptors triggers depressor responses characterized by decreases in blood pressure and heart rate. Other mechanoreceptors are located in all of the chambers of the heart and in the major central veins. Sensory endings of chemically sensitive neurons are also located at similar cardiovascular sites and supply information about blood pH, oxygen and carbon dioxide levels (Sapru and Krieger 1977). Many other factors such as body temperature, hormonal milieu, muscle activity and emotional state can influence cardiovascular reflex control. The precise mechanisms of interaction among mixed visceral sensory modalities (e.g. cardiovascular, respiratory and gastrointestinal) are poorly understood. Changes in behavioral state or hormonal status can alter these reflexes presumably at brainstem sites.

Baroreflex pathway. Cranial visceral sensory axons enter the brain and synapse in the nucleus of the solitary tract (NTS), one of the most important CNS nuclei involved in cardiovascular control (Andresen and Kunze 1994). Baroreceptor input entering the NTS provides a common sensory pathway to both the sympathetic and parasympathetic efferent limbs of arterial baroreflexes. Only very general information is established about the connections between the NTS and the autonomic motor neurons. Autonomic efferent outflow follows the general pattern of a two-neuron path consisting of a preganglionic neuron within the CNS and a postganglionic neuron that innervate the target organ. Beyond the general circuit

similarities, each limb of the autonomic nervous system is quite distinct.

Parasympathetic. In the baroreflex pathway, the parasympathetic preganglionic neurons are generally directed toward the heart and located within two brainstem nuclei: the nucleus ambiguus and the dorsal motor nucleus of the vagus (Loewy and Spyer 1990). These parasympathetic preganglionic neurons are cholinergic neurons that project long axons that exit the medulla and travel through the vagus nerve to synapse on postganglionic neurons in ganglia adjacent to the heart. Parasympathetic postganglionic neurons release acetylcholine onto the sino-atrial and atrio-ventricular nodes altering heart rate and conduction. Activation of parasympathetic neurons results in decreases in cardiac output. These parasympathetic responses are fast and regulate heart rate on a beat-to-beat basis. The conduction time from activation of sensory inputs to activation of peripheral vagal cardiac efferents near the heart can be as short as 20 msec (Kunze 1972; McAllen and Spyer 1978). The heart is unique in that it receives both the parasympathetic and sympathetic input (Levy and Martin 1979). Normal control consists of a reciprocal activation of parasympathetic output with a reduced sympathetic output during baroreceptor activation and the opposite pattern occurs when baroreceptor activation decreases.

Sympathetic. Sympathetic preganglionic cell bodies are located in the intermediolateral cell column of the spinal cord and most send axons to sympathetic ganglia just outside the spinal cord. Sympathetic postganglionic

neurons are adrenergic and innervate both the heart and vasculature. At the heart, sympathetic activation has both inotropic and chronotropic effects. These combined effects act to increase cardiac output with increasing nerve activity. Sympathetic afferent activity strongly influences blood pressure through actions on the resistance and capacitance vessels. Sympathetic activation initiates vasoconstriction through noradrenergic stimulation of smooth muscle. Sympathetic responses are slower and sustained compared to parasympathetic responses (Levy and Martin 1979).

Autonomic Tone Even under normal resting conditions, both sympathetic and parasympathetic efferent motor outputs that project to cardiovascular targets are actively discharging. The reciprocal nature of parasympathetic (inhibitory) and sympathetic (excitatory) influence on the heart gives more precise control of the mean arterial pressure through the balance of these outputs. The mechanisms that underlie the sympathetic and parasympathetic tonic activity at rest are suggested to result from two distinctly different circuits of generating the ongoing activity of autonomic output.

The tonic discharge of sympathetic postganglionic neurons appears to be generated by a group of neurons within the brainstem and reflex inputs modify their basic sympathetic rhythm (**Figure 1-1**). The ongoing sympathetic activity is thought to be initiated through a group of interconnected neurons within the rostral ventrolateral medulla (RVLM) loosely described as the pattern generating circuit.

This circuit may include spontaneously active or pacemaker cells (Allen et al. 1993;Huangfu and Guyenet 1997). Output neurons from the sympathetic generator circuit act as premotor neurons and project to the preganglionic cell bodies within the intermediolateral cell column of the spinal cord. Normally, the activity of the sympathetic pattern generator appears to be restrained by inhibitory projections originating from GABAergic neurons in the caudal ventrolateral medulla (CVLM, Spyer 1990). Thus, sympathetic tone at rest appears to be the net effects of the sympathetic pattern generator and ongoing inhibitory activity, which includes centrally inhibitory reflex inputs from the baroreflex, transmitted through CVLM neurons. The activity of these inhibitory neurons within CVLM is partly determined by glutamatergic projections from NTS (Ito and Sved 1997).

Figure 1-1 Overall organization of cardiovascular reflexes. Pressure information is gathered from sensors within a variety of sites within the circulatory system, predominantly from the aortic arch and carotid sinus. The central nervous system integrates this information and then efferent neuron responses are directed toward several target organs. Sympathetic efferent activity induces vasoconstriction and increases contractile strength of cardiac muscle. Parasympathetic efferent activity slows heart rate at the SA node. These responses affect arterial pressure completing a reflex circuit. SA, Sinoatrial node AV, Atrioventricular node; SV, Stroke volume.

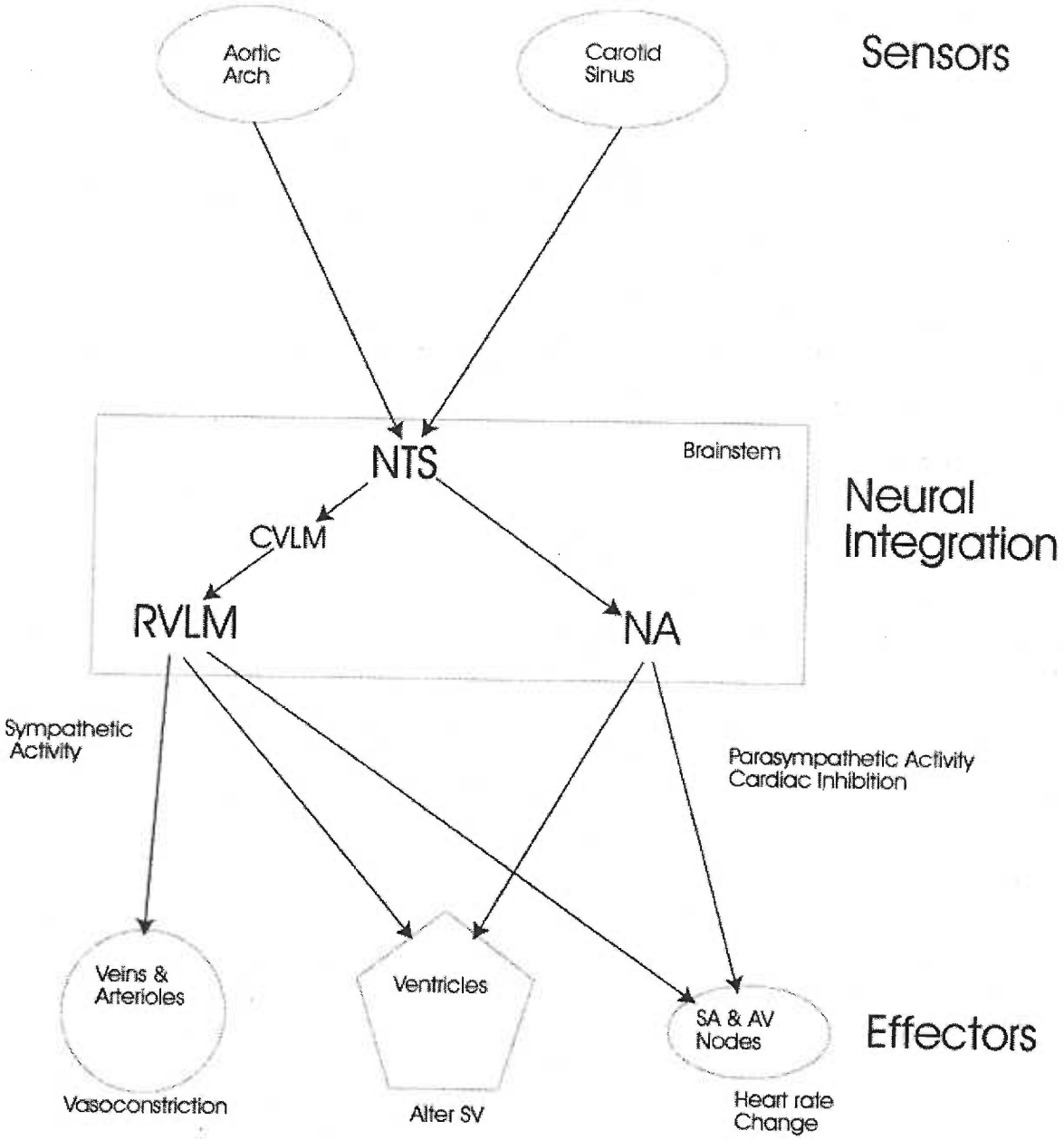
Aortic Arch
Carotid Sinus
Sensors
NTS
Brainstem
CVLM
RVLM
NA
Neural Integration
Sympathetic Activity
Parasympathetic Activity Cardiac Inhibition
Veins & Arterioles
Ventricles
SA & AV Nodes
Effectors
Vasoconstriction
Alter SV
Heart rate Change

For parasympathetic activity to the heart, vagal tone appears to result primarily from a simple mechanism requiring activation of sensory afferents that drive a reflex activation of central parasympathetic neuron activity. In humans for example, cardiac tone strongly depends on the baroreflex activation and baroreflex sensitivity is directly related to the degree of resting autonomic tone – as reflected in resting heart rate (Kollai et al. 1994). Blood pressure reductions to levels at which arterial baroreceptors fail to be activated eliminates discharge in parasympathetic efferents (Kunze 1972). Likewise, pharmacological blockade of excitatory synaptic transmission eliminates discharge in cardiac preganglionic neurons in nucleus ambiguous (NA) (Mendelowitz 1996). Thus, cardiac parasympathetic tone appears to be strongly dependent on arterial baroreflex feedback to maintain normal resting heart rate. Preganglionic parasympathetic motor neurons within NA are driven by excitatory projections from glutamatergic neurons within NTS (Neff et al. 1998). In preparations with sensory inputs eliminated, these NA neurons become silent despite patent connections between NTS and NA suggesting a lack of intrinsic pacemaker activity. Normally, NTS neurons are activated by sensory afferents including arterial baroreceptors that enter the brainstem and course through the solitary tract (ST) to synapse on neurons within NTS. At normal mean blood pressures, arterial baroreceptor discharge excites this circuit resulting in ongoing parasympathetic output and decreased sympathetic tone. Thus, the pattern of connections and activity suggests that the second-order sensory driven neurons within NTS are the key link between sensory transduction of blood pressure and the integration of autonomic

motor output. But how essential is NTS to circulatory control?

NTS role in cardiovascular regulation. In whole animals, anatomical lesions that specifically remove NTS abolish the depressor responses elicited by physiological or electrical activation of cardiovascular afferents (Reis and Talman 1984; Andresen and Kunze 1994). Bypassing the sensory neurons, activation of neurons within NTS directly by electrical stimulation or by microinjection of excitatory neurotransmitters (**Figure 1-2**) evokes robust decreases in heart rate and arterial pressure, thus mimicking baroreflex activation (Leone and Gordon 1989;Colombari et al. 1996). Despite recognition of the important role of NTS in cardiovascular regulation, relatively little is known about the mechanisms of sensory afferent integration (e.g. baroreceptor, chemosensory, respiratory and/or gastrointestinal) or the mechanisms that mediate descending supramedullary inputs to NTS.

Figure 1-2 Microinjection of glutamate into NTS decreases heart rate and mean arterial pressure. These responses were dose dependent. Injection volumes were given in a random order.

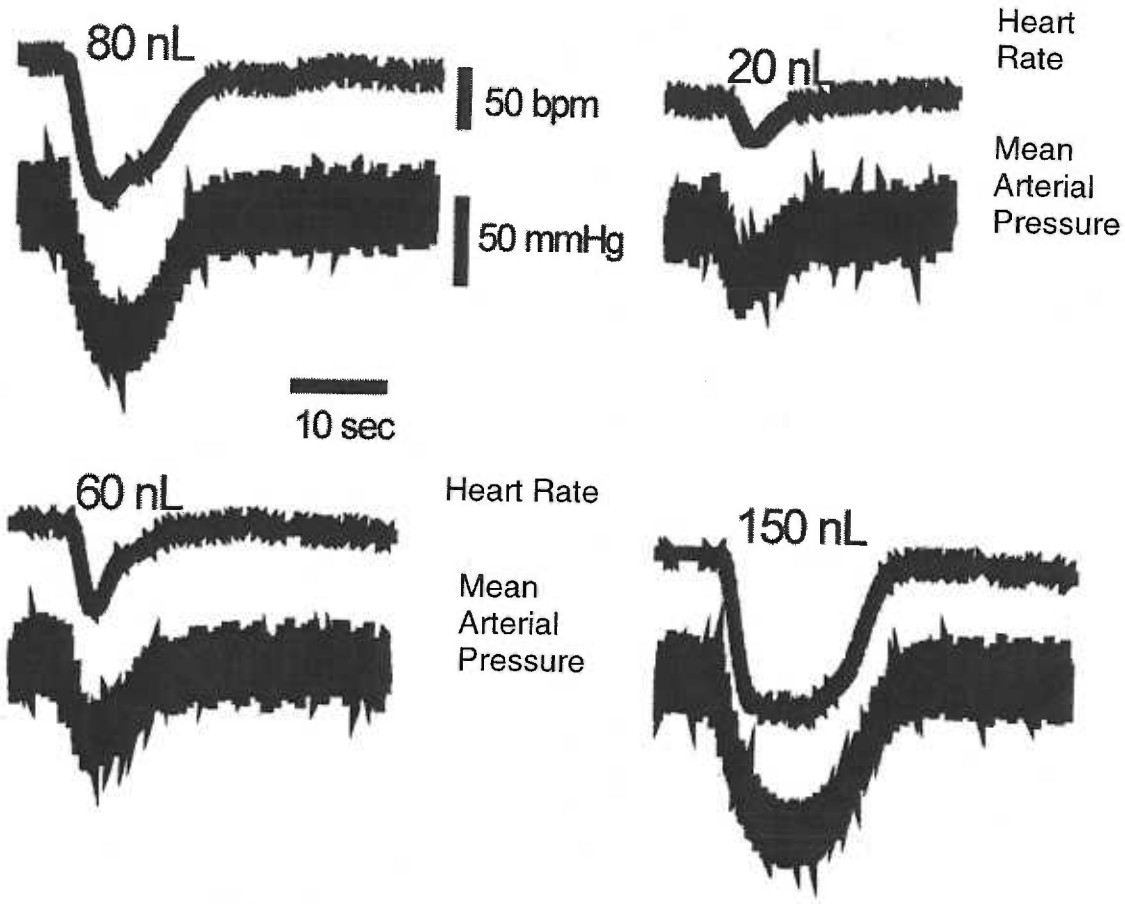
80 nL
50 bpm
50 mmHg
10 sec
Heart Rate
20 nL
Mean Arterial Pressure
60 nL
Heart Rate
Mean Arterial Pressure
150 nL

Viscerotopic NTS. NTS is a bilateral nucleus that extends rostrocaudally for several millimeters in the rat brain. Sensory afferent inputs from many visceral organs terminate predominantly in the caudal portions of NTS. (Andresen and Kunze 1994) Such sensory inputs are loosely organized viscerotopically with arterial baroreceptor afferents found in highest density in dorsomedial NTS, respiratory afferent terminations concentrated in ventrolateral NTS, the peripheral chemoreceptors spreading to lateral aspects of NTS and gastrointestinal afferents in parvocellular groups concentrated in sub postremal portions of medial NTS. Rostral NTS contains extensive gustatory afferent terminations (Loewy 1990)

Sensory innervation of NTS. Cranial visceral sensory afferents including baroreceptors enter the central nervous system at the brainstem and their axons form the solitary tract (ST; Ciriello 1983). In the rat, arterial baroreceptor information is carried predominantly in two nerve trunks, the aortic depressor nerve (ADN) and the carotid sinus nerve (CSN). CSN baroreceptors innervate the carotid sinus at the bifurcation of the internal and external carotid arteries. The baroreceptor fibers are intermixed within the CSN with afferent fibers from chemoreceptor afferents. This CSN bundle of afferents with mixed modalities travels to cell bodies located in the petrosal ganglia and enters the brainstem via the IX cranial nerve where it becomes part of the ST (Spyer 1990). In contrast, the rat ADN carries only baroreceptor afferents innervating the aortic arch (Sapru et al. 1981) which enter the medulla through the 10^{th} cranial nerve (Kobayashi et al. 1999).

As with somatic sensory innervation (Willis, Jr. and Coggeshall 1991b), two broad classes of afferent axons are found innervating NTS and are divided according to their myelination or conduction velocity. These subtypes are associated with specific expression of ion channels, neurotransmitters, and transmitter receptors (Lawson 1992). These cellular properties may contribute to the overall impact each phenotype has on reflex performance. At the level of NTS, very little is known about these afferent subtypes and the distinct neurons or pathways that they innervate within NTS. Much more is known about the distinct characteristics of the reflex responses based on activation of each afferent subtype, particularly arterial baroreceptors.

A-fiber baroreceptors Baroreceptors with A-delta type axons (A-fibers) are lightly myelinated and thus have a faster action potential conduction velocity (10-18 m/sec) compared to those with unmyelinated C-fibers (<2.5 m/sec). A-fiber baroreceptors have lower pressure thresholds for initiation of action potentials and repetitive discharge with frequencies that can exceed 100-200 Hz (Kunze and Andresen 1991). Discharge of A- fiber baroreceptors is patterned typically as trains of quite regularly spaced action potentials. A-fibers respond with bursts of high frequency discharge with each cardiac cycle and are slowly adapting on the order of seconds (Aars et al. 1978;Douglas and Ritchie 1956).

C-fiber baroreceptors In contrast, the unmyelinated C-type fiber baroreceptors require, on average, much higher pressures to reach threshold for discharge than the A-type baroreceptors. C-type baroreceptors respond with relatively low frequencies (1 Hz) and exhibit an irregular discharge pattern (Thoren et al. 1977). While discharge trains of single A- fibers closely follow the form of the arterial pressure profile within each cardiac cycle, the sparse and irregular discharge of single C-fibers is only loosely correlated with arterial pressure. Because of this discharge property of C- fibers, they may more faithfully encode information about mean arterial pressure rather than moment-to-moment hemodynamic status (Seagard et al. 1990). Interestingly, C- fibers outnumber A-fibers by as much as 10 fold and have a greater impact on reflex responses (Aars et al. 1978;Douglas and Ritchie 1956;Fan and Andresen 1998;Fan et al. 1999).

Evidence for sensory integration. A- and C-fiber baroreceptors may provide unique information to the NTS. Blood pressure responses (**Figure 1-3**) show different frequency dependence from stimulation of A- fibers within the ADN than from stimulation of C-fibers (Douglas and Ritchie 1956;Fan and Andresen 1998;Fan et al. 1999). Thus, information from each fiber type input may be integrated separately within the central nervous system. In terms of simple integration into baroreflex heart rate and blood pressure responses, electrical activation of both A- and C-fibers together results in smaller reflex responses than the simple sum of the effect expected from maximal stimulation of each A- and C-input individually. Selective maximal activation of A-fiber baroreceptors alone has

little impact on heart rate whereas even moderate activation of C-fiber baroreceptors alone decreases heart rate substantially (Fan et al. 1999). Interestingly, activation of both A- and C- fibers together impact heart rate more than C- fibers alone. Since the cardiac parasympathetic pathway is as short as four neurons, this important integration may occur at the earliest synaptic processing within NTS including presynaptic modulation (Fan et al. 1999).

Figure 1-3 Changes in mean arterial pressure in response to ADN stimulation. Low intensity stimulation activates A-type fibers. High intensity stimulation activates both A-type and C-type afferents initiating a more robust reflex response at lower frequencies. The combination of high stimulation with the application of capsaicin (C-fiber blockade) initiates a frequency response similar to A-type activation at low stimulation (from Fan and Andresen 1998).

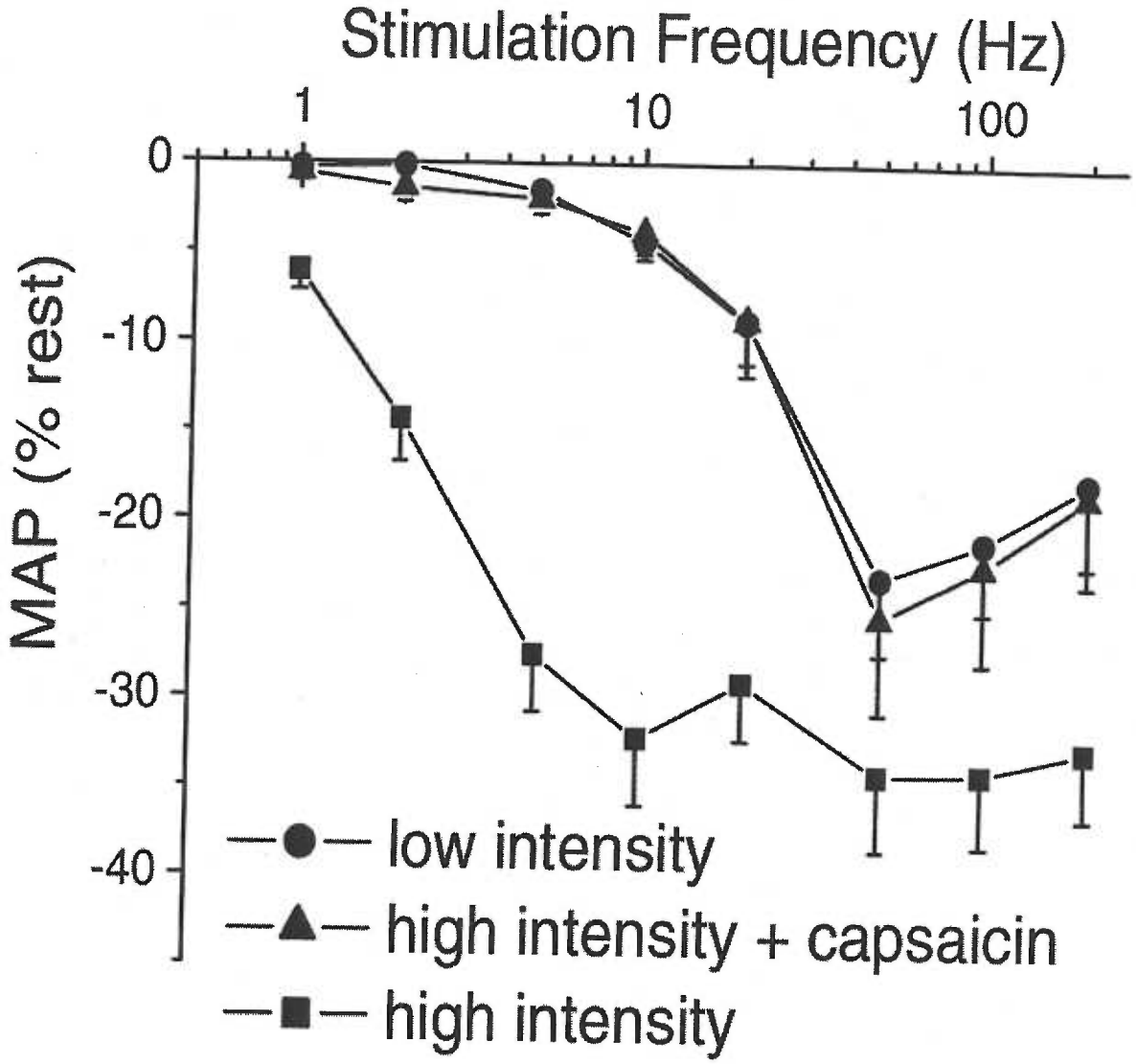
Stimulation Frequency (Hz)
1
10
100
0
-10
-20
-30
-40
MAP (% rest)
low intensity
high intensity + capsaicin
high intensity

Beyond the basic input and output of the neural pathways involved in baroreflex responses, few details about the mechanisms responsible for the behavior of the baroreflex loop are understood. The baroreceptor inputs are well defined. Many of the outputs and their performance characteristics are well known. Since NTS is the first stage at which central integration might occur within the baroreflex, studies of afferent mechanisms within NTS is a practical approach to understanding more about central processing of baroreflex mechanisms.

Integration within NTS In the rat, NTS consists of roughly 42,000 neurons and over 10^6 synapses (Van Giersbergen et al. 1992; Andresen and Kunze 1994). Many of these neurons in NTS are second-order neurons, which are neurons that received primary visceral sensory afferent inputs. Still other neurons are local interneurons whose processes are confined within NTS and many of these do not receive direct sensory inputs (Andresen and Kunze 1994). Which of these neurons that project out of NTS (second or higher order neurons) is not fully understood. In addition to visceral sensory afferents, NTS receives projections from a wide range of supramedullary areas of the brain. Most commonly, NTS connections to other CNS regions are reciprocal projections that establish two-way communication. The functional ramifications of such a pattern of connectivity among autonomic neurons is also open for investigation (Loewy 1990). Thus, pathways across multiple CNS nuclei feed information back into NTS and likely also contribute to integration (Andresen and Kunze 1994;Andresen and Mendelowitz 1996).

The functional organization of such interconnections is only beginning to emerge. One possible mechanism of sensory integration is convergence. At the light microscopy level, tracer studies identified anatomical convergence of sensory terminals arising from neurons across multiple modalities into specific subnuclei of NTS (Loewy 1990). Such studies support possible connections but cannot identify functional convergence onto individual neurons. Within NTS, nerve signals from separate afferent inputs can sum, facilitate, or occlude each other (Mifflin and Felder 1990). It is not clear whether these convergent interactions occur at second-order neurons or through serial NTS connections. Thus the nature of sensory integration within NTS and its cellular mechanisms needs to be determined.

The combined effect of multiple sensory inputs that eventually elicits a reflex output likely encompasses interconnections with numerous NTS interneurons. In recordings from individual NTS neurons, sensory afferent stimulation evokes multiple synaptic responses with many arriving at some time after the primary afferent synaptic response. Very commonly in NTS, for example, a single shock to the sensory fibers evokes a combination excitatory postsynaptic potential followed at a fixed delay by an inhibitory postsynaptic potential (Andresen and Yang 1990;Mifflin and Felder 1990). One explanation is that one sensory pathway inhibits another parallel sensory pathway by activation of a local NTS inhibitory circuit that projects back to the second-order neuron. For example,

cardiac and respiratory afferents that have opposing effects on autonomic output may interact through such a mechanism. Although the presence of NTS interneurons is anatomically clear, local circuits are difficult to study due to their multiple and diverse connections within NTS.

Many NTS neurons project to other CNS regions that are influential in cardiovascular function. NTS neurons project in a reciprocal fashion with brain regions responsible for release of hormones involved in cardiovascular regulation (Loewy 1990). Thus, baroreceptive inputs can potentially alter the humoral state of circulatory control through NTS. Likewise, neurons within NTS are sensitive to many of these hormonal mediators. Two important examples are angiotensin and vasopressin. Both of these hormones alter cardiovascular function when injected into NTS (Matsumura et al. 1998;Brattström et al. 1988;Matsuguchi et al. 1982). These hormones, and other circulating compounds can access receptors on NTS neurons through a partial blood brain barrier (Gross et al. 1990;Gross et al. 1991;Shaver et al. 1991). Thus the humoral state of the animal is integrated together with sensory and higher order information at the level of NTS.

Neurotransmitters of the NTS Microinjection, immunohistochemical and electrophysiological studies have implicated numerous neurotransmitters and neuromodulators within medial NTS (Andresen and Kunze 1994). This list includes biogenic amines, peptides and amino acids **(Table 1)**. The diversity of neurochemicals that are active within NTS reflects the heterogeneity of neurons

and the multiple functional roles that are mediated through NTS neurons. Little is known about the functions of these putative transmitters within NTS. At the neuron level, such transmitters are expected to alter the excitability of these neurons by alterations of voltage and ligand-gated ion channels as well as potential changes in receptor sensitivity and localization. In the context of the baroreflex, the two most prominent transmitters are glutamate and gamma amino butyric acid (GABA).

Table 1 Neurotransmitters and neuromodulators implicated in NTS		
Glutamate		ACTH
Non NMDA		ANP
NMDA		CGRP
Metabotropic		Beta Endorphin
GABA		Enkephalins
Glycine		Gastrin
Biogenic amines		Oxytocin
Dopamine		Vasopressin
Epinephrine		Alpha-MSH
Norepinephrine		Substance P
Histamine		Neuropeptide Y
Serotonin		VIP
Acetylcholine		TRH
Opioids		Neurophysins
Purinergics		Neurotensin
Adenosine		Bradykinin
Angiotensin		Cannabinoids
Somatostatin		Vanilloid

Primary transmitter Multiple lines of evidence suggest that glutamate is involved in baroreflex function in NTS. Removal of the nodose ganglia decreases glutamate release from sensory areas within NTS (Talman et al. 1980). Afferent nerve stimulation evokes several types of glutamate dependent synaptic responses in medial NTS neurons (Mifflin and Felder 1990). Glutamate analogues that effectively mimic afferent activated changes in heart rate and blood pressure when microinjected into NTS **(Figure 1-2).** Similarly, glutamate receptor antagonists microinjected into NTS completely block afferent activation of cardiovascular reflexes (Gordon and Leone 1991). Glutamate appears to be acting at both NMDA and Non-NMDA postsynapic receptors.

Although it is clear that glutamate plays a role in baroreflex regulatory mechanisms within NTS, several potential sites of action may contribute to the responses that have been observed especially with microinjection of agonists and antagonists. These include direct actions on second and higher order neurons within cardiovascular paths. Additional actions at non-baroreceptor sensory synapses could affect the integrated baroreflex output. Indirect actions include activation of local inhibitory feedback networks and glutamate-evoked excitation that triggers release of other transmitters that then alter cardiovascular reflex pathways. The complexity of the neuronal connections within NTS makes isolating the specific actions of glutamate difficult. The primary sensory synapse of the baroreflex is the most accessible for localization and activation. The role of glutamate at this primary synapse is the most likely candidate for initial isolation

and investigation.

Study Goals At the outset of my studies in NTS, I was interested in focusing on the cellular mechanisms of synaptic transmission and particularly of those signals between the sensory afferents onto the second-order NTS neurons. My interest in the actions and interactions of neurotransmitters meant that intracellular recordings would be necessary in order to assess excitatory and inhibitory neurotransmitter actions particularly if modulation of these signals was important. Considerable supporting evidence suggested that glutamate was the main or primary transmitter released by visceral sensory neurons. What was less clear at the outset of my work was the role of other glutamate receptors and, in particular, NMDA receptors (Aylwin et al. 1997;Ohta and Talman 1994;Leone and Gordon 1989). NMDA receptors are major contributors to plasticity (Collingridge and Bliss 1995;Cotman et al. 1988) but evaluations are complicated by the voltage dependent block of these channels by Mg^{++}.

Additionally with regard to sensory inputs to NTS, another goal was to better understand the impact of differences between the cellular characteristics of A- and C-type visceral sensory afferents to the nature of their actions in NTS. A fundamental question related to the A- and C-sensory inputs concerned the question of whether all of these peripheral sensory differences as well as their different reflex responses were reflected in synaptic mechanisms within NTS.

My beginning work started with the foundation of sharp electrode recordings in brainstem slices (Andresen and Yang 1990) that existed in the Andresen lab when I began my graduate studies. To address the critical limitations of the sharp electrode approach, I developed new experimental approaches with greater resolution to apply to NTS and to address hypotheses concerning sensory synaptic transmission. These new methods are an important part of my dissertation work and the following sections outline the rationales, problems and decisions that stimulated these developments in my approach to NTS.

Experimental strategy. The aortic depressor nerve (ADN) in the rat represents a unique sensory nerve bundle with important advantages for studying sensory inputs to NTS. The ADN carries only baroreceptor afferents innervating the aortic arch (Sapru and Krieger 1977). ADN has been studied extensively with single fiber techniques to understand pressure transduction by the afferent baroreceptor endings (Andresen and Yang 1989); (Kunze and Andresen 1991;Thoren et al. 1983) Electrical activation of ADN has been used to study baroreflex responses including those in conscious intact animals (De Paula et al. 1999). Alternatively, the other major nerve trunk carrying baroreceptors, the CSN, contains chemoreceptor afferents and sympathetic efferent fibers along with baroreceptor axons. This combination of efferents and afferents of different modalities within this nerve complicates interpretation of CSN activation.

Whole animal perspectives Much of what we have learned about neural control of the cardiovascular system and the role of NTS has come from whole animal models(Andresen and Kunze 1994). These experiments in intact animals have the major advantage that baroreflexes can be selectively activated using physiological stimuli making such observations highly relevant to understanding normal function. A common tool to assess CNS mechanisms is microinjection of selective agonists and antagonists into portions of NTS. Cardiovascular control related responses (e.g. blood pressure, heart rate, regional blood flow, and sympathetic nerve activity) could be easily measured with the complete reflex present. Such pharmacological manipulations can be divided into two general categories: 1) Activation or inhibition of regional NTS function (e.g. medial NTS), or 2) alterations of reflex responses evoked by blood pressure challenges or afferent stimulation.

In some respects, the presence of multiple control systems (e.g. cardiovascular and respiratory) affecting a measured variable such as blood pressure complicates interpretation of such an apparently simple parameter. Careful consideration of potential multiple interactions and the complexity of interventions, which may have multiple sites of action, are required. Reflex changes in blood pressure resulting from the experimental manipulation are translated and incorporated into the final output. Separating the primary experimental change from secondary compensatory effects due to other reflexes is often difficult. Part of this difficulty arises from the indirect measurement of the experimental variable. For example,

microinjections alter activity of neurons within NTS that do not normally contribute to baroreflex responses yet they indirectly affect the measured cardiovascular changes.

Another potential difficulty with microinjections is the accuracy of control over the local concentration of injected pharmacological agents. Diffusion of the pharmacological agent can affect several cells. Conclusions from these studies are helpful in recognizing neurotransmitter participation at the level of the nucleus or general region. Resolving the nature of the participation of a given receptor within a brain nucleus can be more difficult.

Electrophysiological recordings offer direct evidence of the cellular responses of neurons and can help resolve important aspects of cellular physiology. Such whole animal preparations maintain the ability to selectively activate discrete sensory inputs often with natural stimuli. Unfortunately, such recordings are for the most part limited to extracellular recordings in NTS due to the small size of the neurons and less than optimal recording conditions such as respiratory and cardiovascular movements. Such extracellular recordings yield valuable descriptions of intact function of NTS neurons (Seagard et al. 1995;Scheuer et al. 1996). *In vivo* intracellular NTS recordings have been limited in duration which compromises both the experimental yields as well as the protocols that can be successfully completed (Miura 1975;Mifflin and Felder 1988;Granata and Kitai 1989). These recordings utilize sharp electrodes with high access resistances that

make voltage control through voltage clamp impractical. Despite the intact nature of the afferent activation of these *in vivo* recordings from NTS, the identity of the recorded neuron within the baroreflex context is remains difficult to characterize clearly in these experiments.

The necessary presence of anesthetics in *in vivo* preparations raises the additional consideration that the intact responses are altered in variable or unpredictable ways by the anesthetic. For example, the common anesthetic agent pentobarbital increases inhibitory synaptic transmission via the GABAa receptors. These receptors play an important role in inhibitory pathways within NTS and baroreceptor pathways. Thus, anesthetics alter the operation of brainstem neural pathways that are known to alter the neural control of cardiovascular function. Hybrid, reduced preparations are beginning to emerge that combine an intact brainstem with a truncated torso, which includes lungs and heart (Paton et al. 1994). Such an approach eliminates the need for anesthetic and offers improved access for intracellular recording and ability to activate sensory inputs by manipulation of the life support apparatus.

Brain slice approach Brain slice preparations were introduced some thirty years ago to offer improved cellular access to neurons and local circuits of neurons contained within the isolated portion of the brain (Kerkut and Wheal 1981;Collingridge 1995). Such preparations offer increased ability to investigate cellular and molecular processes but often lack important physiological

connections that give them context. The key to these limitations is selection of the best method to match the appropriate resolution to answer the experimental question. Investigation of synaptic transmission within the baroreflex requires both the high resolution of a cellular preparation and the ability to identify and isolate the synapse in the context of the reflex.

Brainstem slices containing NTS offer a reduced preparation as a simple model while retaining sufficient connections to investigate mechanisms of synaptic transmission. These slices clearly lack the ongoing activity of sensory afferents and inputs from other brain areas. However, sensory axons can be activated by stimulation of the solitary tract (ST) within the slice to evoke a synaptic response in NTS second-order neurons. Such responses are free of the compensatory changes that may arise in the intact system and can confound interpretation of the nature of primary sensory transmission.

These brainstem slices have sufficient anatomical landmarks to appropriately identify the borders of the nucleus. For localizing baroreceptive medial regions of NTS, the edge of the fourth cerebral ventricle and the distinct white appearance of myelinated sensory afferent fibers within the ST are key features retained within slices containing NTS. Visualizing these landmarks in the slice aids in placing stimulating electrodes and in the selection of appropriate portions of NTS for recording electrode placement.

Improved experimental control and more direct physical access to the neurons of study are the two major advantages of such brain slice preparations. Conditions such as the temperature and composition of the external solutions surrounding the neurons of interest are under strict experimental control and can be used as investigational tools. Drug concentrations can be tightly controlled by perfusion of the slice. Rapid turnover of the bath solution offers a means of removing a drug completely after it has been applied. Washing out a drug and reestablishing a baseline condition establishes clear controls and allows serial pharmacological protocols. This method can distinguish multiple post-synaptic receptors involved in an evoked response. The absence of anesthesia removes a potentially substantial confounding factor.

Physical access to neurons allows improved manipulation and placement of electrodes for studies activating central portions of sensory processes found in the ST. Synaptic physiology can be investigated under voltage clamp conditions. Isolation of the neurons from movements inherent in more physiological settings provides extended access over long periods of time. Depending on the thickness of the slice used, neurons are available for direct visualization using optical methods such as differential interference microscopy (DIC) and other imaging techniques. Along with general anatomical landmarks, cellular morphology can be distinguished directly in the living neurons during experiments. Visual inspection of the signs of the general health of the neurons can be used to assess and improve experimental yields. For example, unhealthy neurons can become

visibly spherical with increased transparency and the appearance of distinct nucleoli. There is also a unique morphological appearance to NTS neurons. Neurons in nuclei adjacent to medial NTS are different in shape and size (e.g. commissural NTS and dorsal motor nucleus of the vagus). Visualizing neuron shape and proximal processes provides an additional basis for directing recording electrodes toward appropriate medial NTS neurons.

Despite these advantages, the brainslice preparation of NTS has several intrinsic limitations beyond the general aspect of a portion of the brain isolated from the rest of the nervous system and the body. The process of isolating the brainstem and slicing sections can damage the fragile neuronal tissue. Extreme caution must be exercised to minimize such trauma in order to preserve neuron function. Oxygen and pH fluctuations must also be carefully monitored to maintain conditions as close to a physiological environment as possible.

Neurons can send processes that extend beyond the limits of a slice of isolated brain. Eliminating portions of neurons can thus truncate normal connections among neurons. The orientation of the sectioning of the slice likely greatly affects neuron integrity. This can impact the synaptic processing by the neuron and eliminate some contacts. Additionally, the nonselective nature of electrical stimulation means that such stimulation can activate both fibers passing near the electrode as well as local neurons with connections that may feed back on the neuron under study. As such, electrically evoked synaptic responses may arise

from an undefined source due to current spread of the stimulus.

To minimize the potential for stimulus spread in the brainstem slices containing medial NTS, we used a nearly horizontal cutting orientation for our slices (Andresen and Yang 1990). As described in the manuscript chapters, this preserves a long segment of the ST so that electrical stimuli can be isolated with increased distance from the recorded neurons **(Figure 1-4)**. NTS neurons filled intracellularly appear to have a general orientation of their processes that are relatively planar and most are aligned parallel to the ST.

Figure 1-4 Low power photomicrograph of the horizontal medullary slice. The stimulus electrode is placed on the ST away from the recording region. This minimizes activation of local circuits within the recording region of NTS (ellipse).

ST and Horizontal Slice of Medial NTS

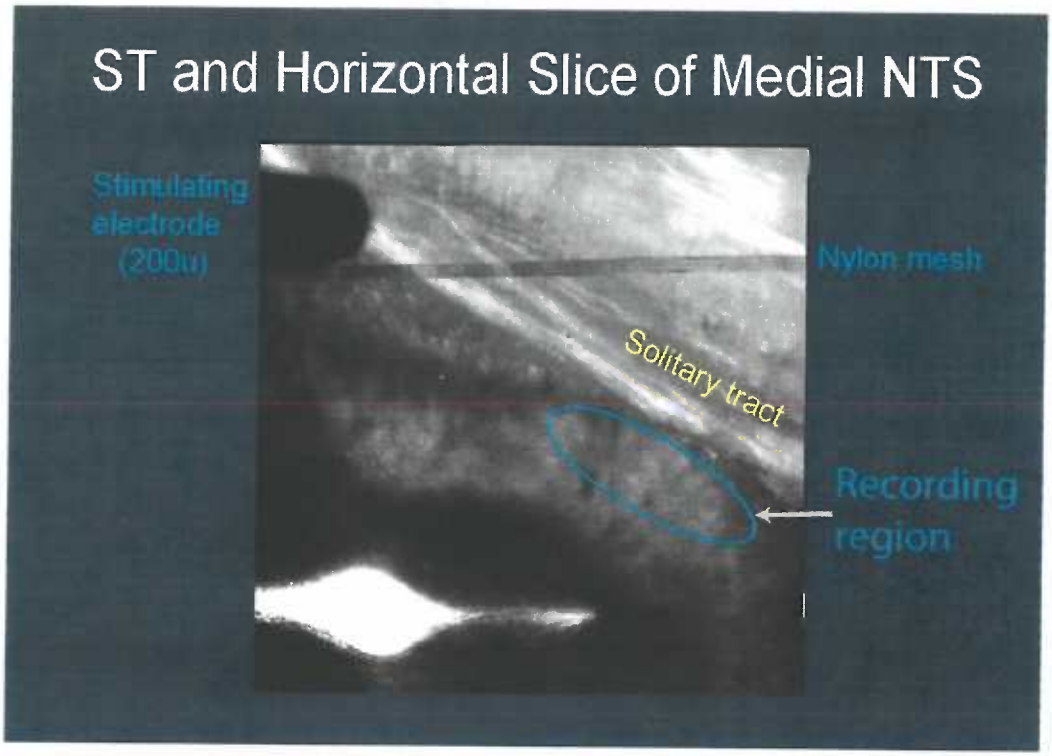

From Microelectrodes to Visualized Patch Recording. At the beginning of my graduate work, I used sharp microelectrodes to impale neurons in medial NTS. The ST was activated electrically from a site 1-3 mm away from the region in which neurons were recorded intracellularly. While this approach took advantage of the brainslice, lengthy recordings from NTS neurons in which ST stimuli evoked synaptic responses were difficult to obtain. Voltage clamp recordings were technically possible using a switching circuit with these sharp electrodes, but space clamp problems limited the values of such recordings and made voltage control suspect.

I had a background experience with voltage clamp techniques applied to isolated cardiac myocytes before graduate school and I decided to attempt to adapt patch recording to the medial NTS slice. To facilitate this transition in methodology, I visited the lab of Dr. David Mendelowitz in Memphis; a training visit funded by my Tartar Fellowship. This experience helped me to combine patch recording with the direct visualization of neurons within the NTS slice using infrared (IR) illumination with DIC optics and an IR sensitive video camera. As such, I was able to maneuver recording electrodes around structures like capillaries. Capillaries and other non-neuronal tissue are a source of tip contamination that prevents gigaohm seal formation with the membrane of the target neuron. Healthy neurons were easily identified.

To improve contrast under IR illumination, I cut somewhat thinner slices; 250 μm

compared to 400 µm for the sharp electrode experiments. Long segments of the ST were much harder to maintain within a thinner slice due to the complicated trajectory of the ST both in the rostral-caudal and medial-lateral orientations. The thin slice was physically more susceptible to stretching and thus inadvertent damage to synaptic connections. Stringent, careful slicing and handling procedures had to be developed in order to preserve function and a number of important improvements were made in joint efforts with Drs. William Cameron and David Robinson.

Continued improvements provided progressively better quality slices and increased experimental productivity. Foremost among these was the switch from conventional steel blades to a sapphire microtome blade (Diamond Delaware Knives). These knives at the time were not used for cutting fresh tissue. Sapphire blades are sharper and have an evenly and finely polished at the cutting edge. The final cutting edge on conventional steel blades has very small serrations that would tear the tissue and would be likely more traumatic than the sapphire blade. This change to the sapphire blade was accompanied by switching to an improved vibratome. The Leica VT 1000 has a mechanical vibration mechanism that minimizes knife movement along axis other than the horizontal cutting axis. This stable back and forth motion in the plane of the cutting edge visibly reduced tissue damage. We also equipped the microtome with a refrigerated cutting chamber to maintain the brainstem at a more uniform, very cold temperature (0-2° C) throughout the slicing procedure. Lowering the temperature both increases the

firmness of the tissue, a major cutting advantage, but also slows down metabolic processes and likely minimizes the anoxic effects while the tissue block is diffusion limited by thickness.

To promote the best possible voltage control, we increased tip diameter of the patch electrodes as much as possible. The resulting low access resistance of such pipettes increases their current passing characteristics and improves voltage control over the neuron. With improved space clamp, studies of large excitatory synaptic currents had fewer problems with contamination by uncontrolled voltage activated channels (e.g. Na^+ currents).

Live microscopy of the slices opened new methodological approaches that were not practical with my previous "blind" approaches. With the addition of fluorescence microscopy it was possible to visualize anatomical labeled baroreceptor endings within the slice. The lipophillic dyes (DiA and DiI, Molecular Probes) placed on aortic sensory afferents in the periphery labeled their processes within NTS (Mendelowitz et al. 1992). Previously, such dye localization had been performed after the electrophysiological experiments by examining neurons filled intracellularly and recovered in fixed sections. Success in recovering and documenting dye labeling was limited due to many technical difficulties and the complexity of the multiple procedures. Visualized patch recording provided a much more direct and straightforward experimental approach that permitted identification of the second-order baroreceptor neurons within the slice.

Carbocyanine Dye Afferent Labeling. The carbocyanine backbone is the basis for a series of versatile lipophillic trace dyes that can be detected with fluorescence microscopy. When placed on a nerve trunk, these dyes diffuse into the axon membrane and are internalized from the plasma membrane into the intracellular compartment in living nervous tissue. Such dye is stable for years (Lichtman et al. 1985). Work has shown that, in the case of the ADN for example, dye applied to the peripheral axon is then transported to both the central and peripheral ends of the baroreceptor neurons and is also trapped in the cell body (Mendelowitz et al. 1992;Mendelowitz and Kunze 1992). Thus, central terminal processes of aortic baroreceptors can be made fluorescently visible within NTS by application of peripheral carbocyanine dye on the ADN.

The fluorescent signals from ADN labeling consist of what appear to be spots or spatially narrow sources of the fluorescent emissions. Confocal images of these spots suggest that they have a similar size range and distribution to other tracers such as horseradish peroxidase labeling of ADN (personal communications from Diana Kunze, Case Western University). The size of each putative synaptic bouton is roughly 2 μm and corresponds to electron microscopic images of ADN synaptic terminal contacts (Drewe et al. 1988). (Studies are underway in collaboration with Sue Aicher to elaborate on the electron microscopic structure of these dye labeled terminals.) For simplicity, however, I will refer to these fluorescent spots as afferent ADN boutons or terminals, although it should be

appreciated that the dye observed at the light microscopy level is more accurately identifying close appositions by ADN terminal axons in these studies.

Studies with tracer dye were initiated in young rats (20 day old) so that a substantial period of dye migration (at least two months) could be allowed before the terminal electrophysiological experiments. The surgery to locate and isolate the nerve trunk of the ADN (100 μm) was performed using a stereomicroscope at 60-100x. Following a cervical incision, careful microdissection under the stereomicroscope freed approximately one cm of ADN from surrounding tissue beginning one cm peripheral to where ADN joins the superior laryngeal nerve near the nodose ganglion. Early failures to see transported dye were attributed to nerve damage from inadvertent crushing or stretching the nerve during surgery that prevented dye migration. Considerable care, therefore, was taken to minimize stretching the nerve during isolation.

The close proximity of other nerve trunks containing afferent axons that synapse in NTS was a potential problem for these experiments. The cervical portions of ADN lie immediately adjacent to the vagus. The vagal trunk contains both afferent and efferent nerve axons that travel in the ST. Misplaced dye entering the vagus could potentially label a range of sensory NTS terminals including those from cardiac, pulmonary, gastrointestinal and other visceral organs. In addition, since efferent axons are also present in the vagal trunk, cell bodies within dorsal motor nucleus of the vagus and nucleus ambiguus would be labeled. Initially, retrograde labeling

from the vagus brightly illuminated the brainstem and provided a critical clue about the very different appearance of afferent label within NTS. From this positive, if unintended, dye result, I learned that delicate care was required in handling the ADN. However, the finding of retrograde staining in dorsal motor nucleus of vagus was a clear indication of uncontrolled dye migration from the surgical site into the vagus and was considered an indicator of "non-specific", i.e. non-ADN, labeling. Since vagal contact with the dye could also likely produce anterograde label of non-baroreceptor afferents, such findings would contradict the specificity of aortic baroreceptor labeling.

To prevent migration of the dye from the site of placement, I developed a containment device for use during the dye implant procedure **(Figure 1-5).** This containment system consisted of a prefabricated sheath of dental impression compound. A small crystal of carbocyanine dye was placed on the ADN making sure visually that the dye remained within the containment system. Fresh dental impression compound was applied to the ADN and sheath in order to seal in and isolate the dye from the rest of the tissue. The material was allowed to cure in place before closing of the surgical wound.

Figure 1-5 Schematic of the ADN labeling technique. DiA or DiI was placed on the ADN in the periphery, isolated and fixed in place with a dental molding compound. After several weeks the fluorescent label concentrated in the sensory terminations of the ADN within NTS.

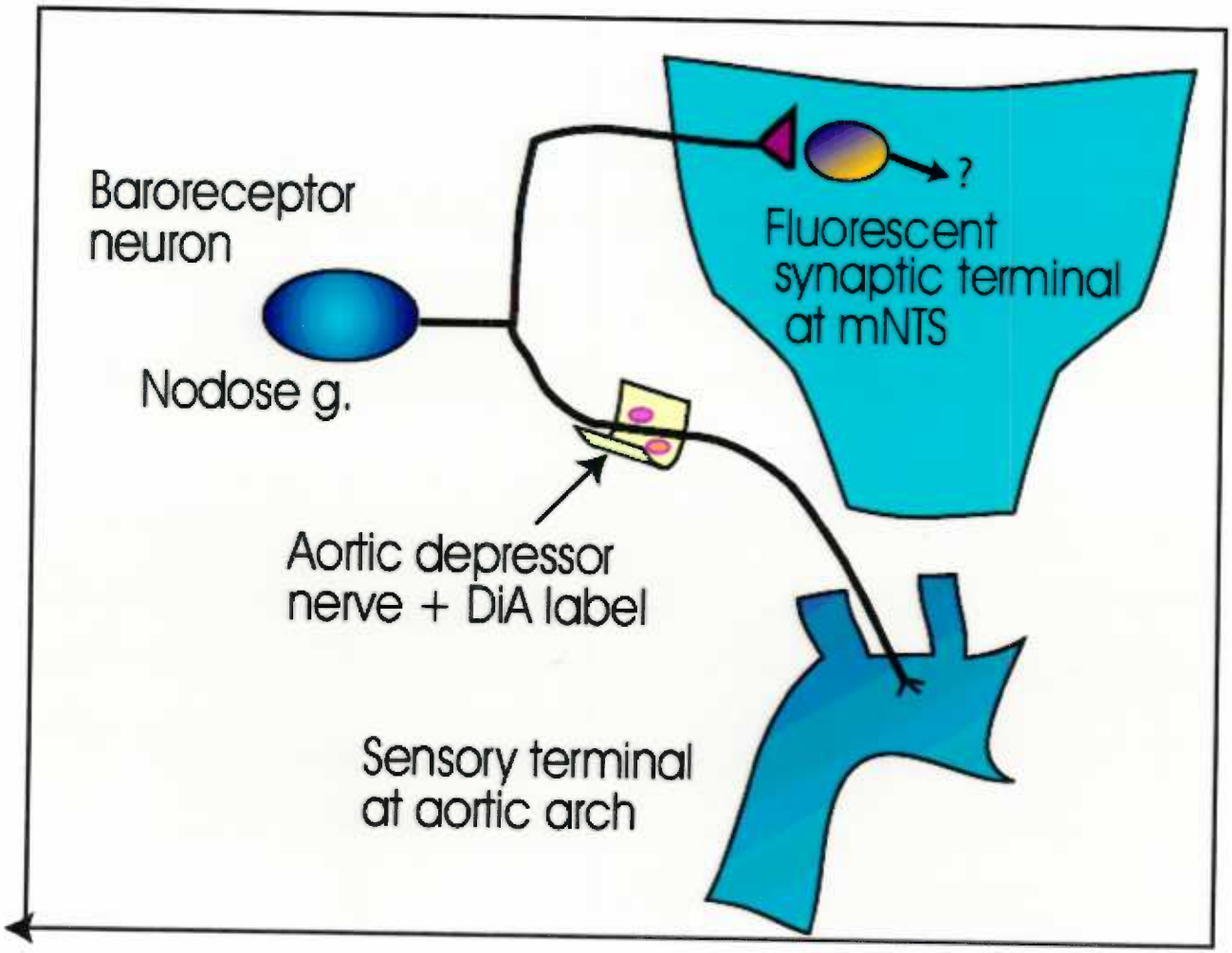
Baroreceptor
neuron
Nodose g.
?
Fluorescent
synaptic terminal
at mNTS
Aortic depressor
nerve + DiA label
Sensory terminal
at aortic arch

A period of 2-8 months was allowed before animals were sacrificed. During the development of this technique, animals were sacrificed after different periods of time to examine dye migration. An extended timeframe permitted dye to concentrate in the synaptic terminals forming punctate labeling surrounding cell bodies within NTS **(Figure 1-6)**. When animals were sacrificed after shorter periods of dye migration, fiber tracts within the ST and NTS fluoresced. This signal, although specific to the ADN, could not clearly identify second-order neurons in the slice since the fluorescent processes often did not align with identifiable cell bodies. As a result, my studies focused on relatively large (400-500g) adult rats to allow full dye travel. Viable horizontal slices from these large animals were more difficult to obtain and record from successfully.

Figure 1-6 Fluorescent ADN terminals within NTS. The fluorescent label identified second-order NTS neurons when overlaid with real time DIC images. Patch electrodes were then visually guided to these neurons.

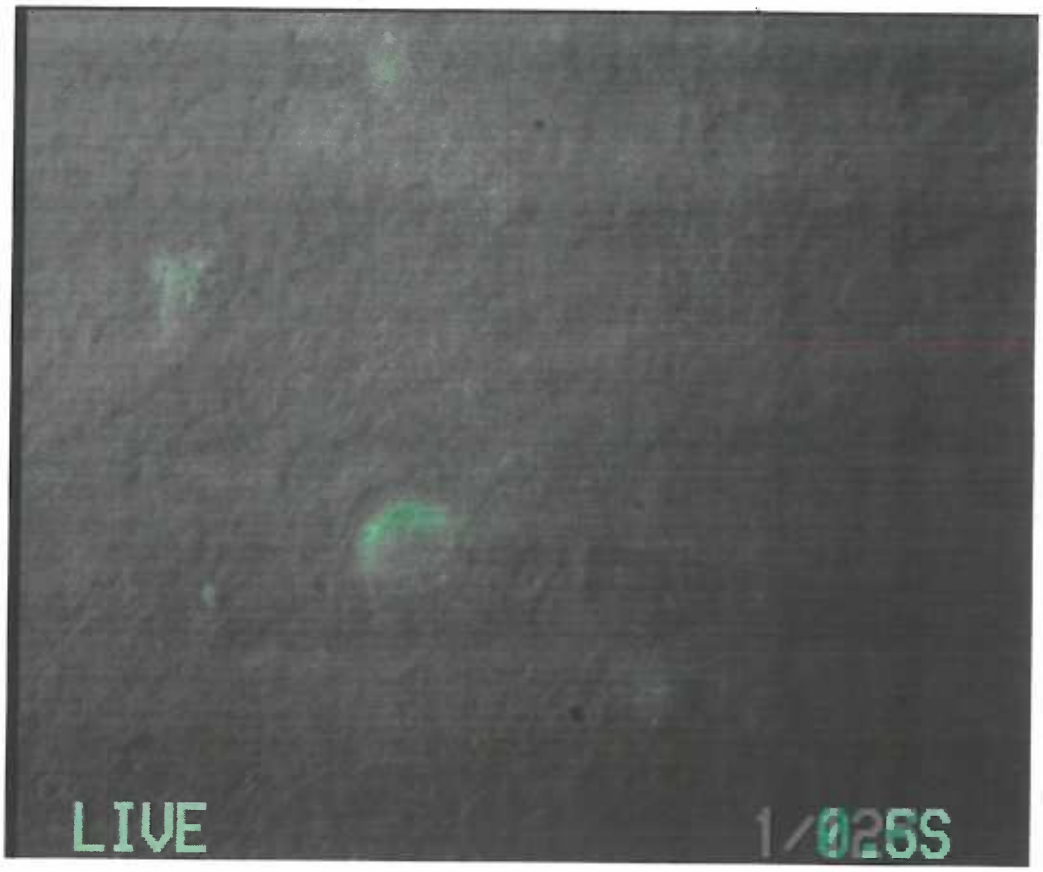
LIVE
1/026S

Quality control. Successful ADN labeling was found on mNTS neurons just medial to the ST and within 200-µm rostral or caudal from obex. Dim auto fluorescence often occurred and could be seen only when long exposure times were required. However, unlike specific label, auto fluorescence did not diminish with exposure to the excitation wavelengths of light and could be seen in unlabeled animals. Auto fluorescent signals in unlabeled slices were associated with particular structures visible within the slice under IR DIC. The two most common sources were small cells located around arteriole walls **(Figure 1-7)** and the nylon in the strands used to hold the slice in place. Neurons with specific labeling close to these auto fluorescent structures were rejected from study because the weaker signal was obscured.

For each animal, slices containing dorsal motor nucleus of the vagus were examined for evidence of retrograde dye labeling of cell bodies. Despite our strategy of containment of DiA, some small degree of cell body labeling in dorsal motor nucleus was clearly evident and is attributed to the fact that minor anatomical interchange of axons across the vagal and aortic depressor nerve trunks is commonly observed **(Figure 1-8)**. Somatic intracellular labeling produced a characteristic dye distribution within the soma that was often quite uniform and diffuse. The distribution of dye through a wide span of focal planes was indicative of such intracellular retrograde label and this label corresponded to the IR DIC profile of the soma. Large numbers of such retrogradely labeled vagal motor neurons indicated that dye exposure was not limited to the ADN. This retrograde

label of the efferent cell bodies was brighter than the anterograde labeling of afferent terminals due to the presence of much greater amounts of dye in the large cell body. Clearly, if dye had migrated to the vagus peripherally then not only were dorsal motor neurons labeled, but at least some of the DiA terminals were likely from vagal sensory afferents. Such contamination meant that labeled terminals could not be unambiguously interpreted as of aortic baroreceptor origin. Animals with dorsal motor nucleus labeling were rejected from further study. As a further control, the nodose ganglia were removed for examination on the day of sacrifice in some animals. Specific ADN labeling was limited to less than10% of the cell bodies within the ganglia. Greater than 50% of labeled nodose cell bodies was considered evidence for non-baroreceptor afferent labeling. In one animal examined, there was no labeling observed in the nodose ganglia but clear labeling within NTS. Such results emphasize that lack of dye at the ganglion cell bodies is not always indicative of terminal labeling at medial NTS.

Figure 1-7 Auto-fluorescence within NTS. Small cells surrounding arterioles were a common source of fluorescent noise (upper trace). This signal did not decrease during exposure to excitation wavelengths. Specifically labeled neurons with punctate labeling (arrow, lower panel) close to or within fluorescent noise were rejected from study.

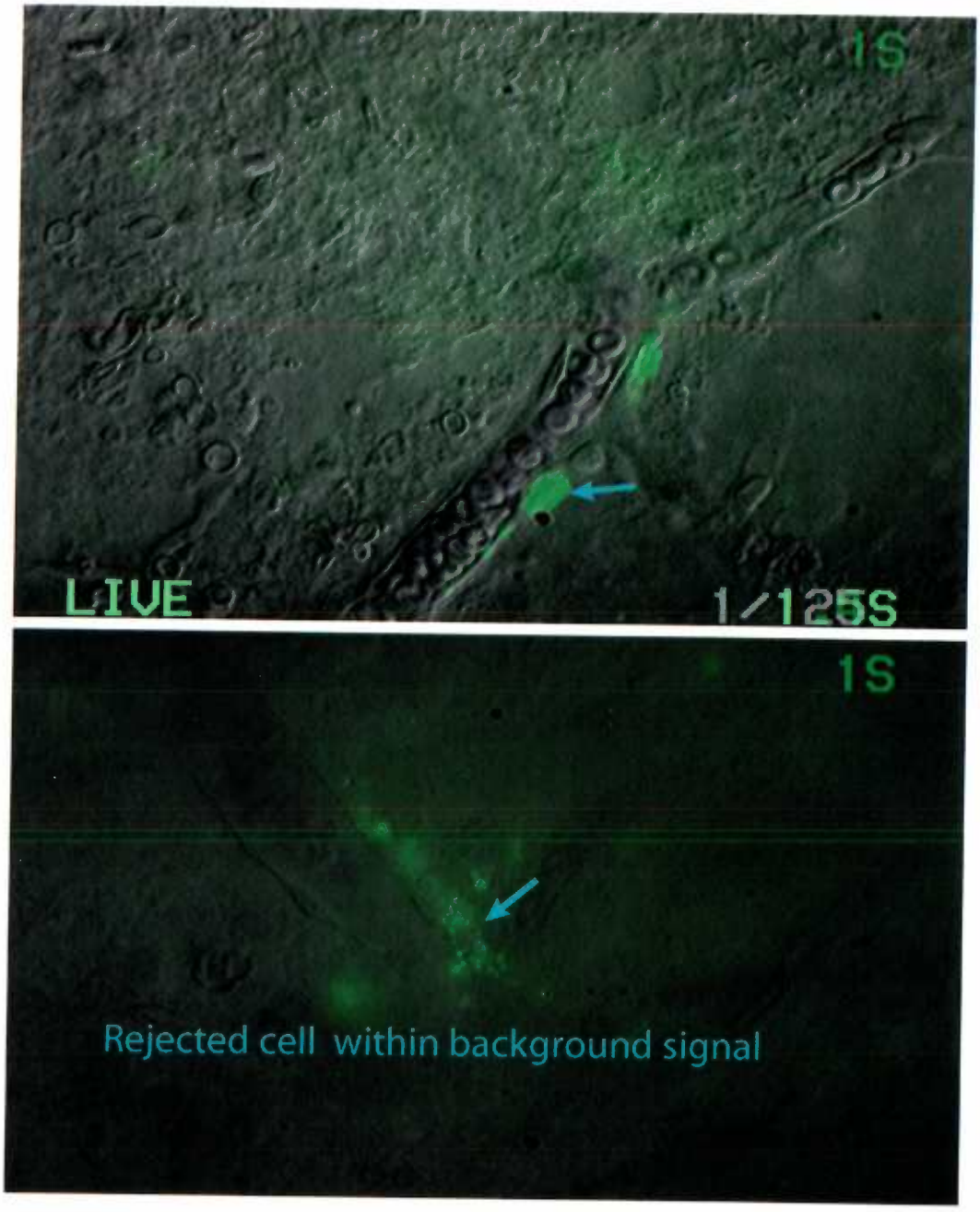
1S
LIVE
1/125S
1S
Rejected cell within background signal

Figure 1-8 A fluorescently labeled cell body within dorsal motor nucleus of the vagus. This slice was the next consecutive medullary slice ventrally after the NTS slice was removed. Labeled cell bodies outside NTS indicated that the dye labeled other fibers in the periphery (e.g. motor efferents within the vagus).

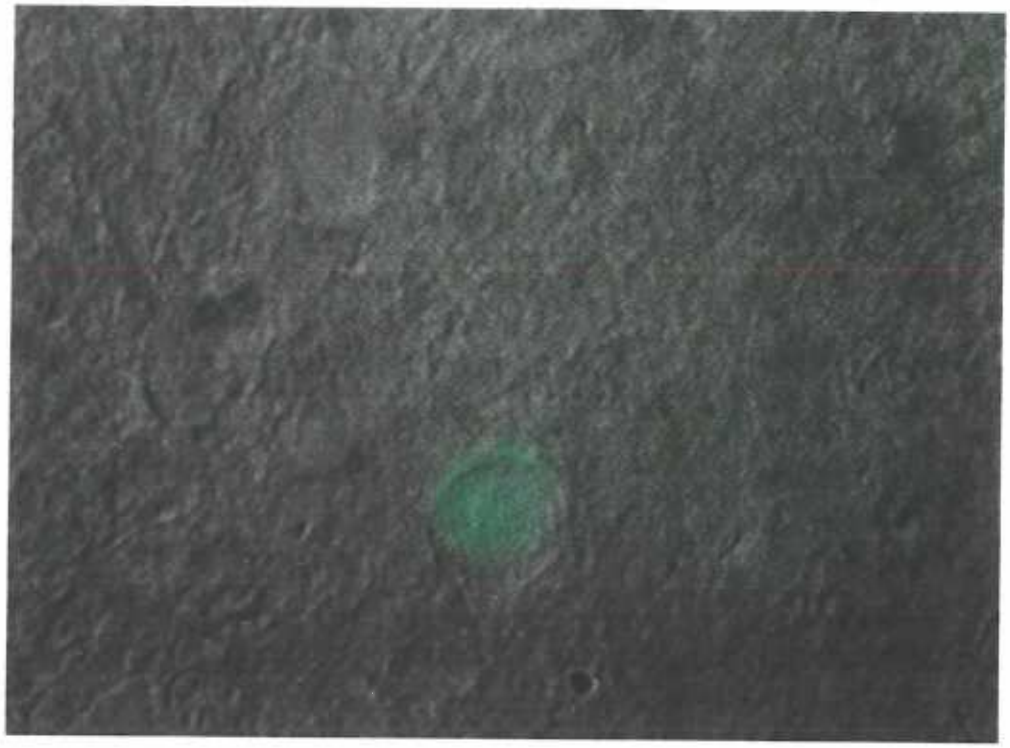

Image processing IR-DIC requires using a video camera to observe these images since IR is not in the visible spectrum. I used two models of the fixed stage Zeiss Axioskop microscope equipped with appropriate fluorescence cubes and DIC optics. Using the earliest model of the Axioskop, fluorescent images of ADN fluorescent signals were located visually through the eyepieces with brief excitation exposures and then captured by time integrating the signal for intervals of 1 to 8 seconds using an Argus 20 image processor (Hammamatsu) to acquire digital images from the video camera. Fluorescent ADN terminals close to the surface of the slice appear as very small spots of fluorescence and are distributed in space following a profile outline of the neuronal soma observed in IR DIC (**Figure 1-9**). The punctate character of the signal appeared blurred with neurons relatively deep within the slice. This is presumably due to the increased scatter of the fluorescent signal as it travels through the tissue. Unlike the infrared light, the fluorescent light is filtered with a polarizer and is therefore more susceptible to scatter. Light scatter increased with integration time. Scattering of the fluorescent signal resulted in images that were less distinct and their punctate quality often degraded into neuron shaped splotches of fluorescence (**Figure 1-10**). While such labeling was useful for identifying neurons with ADN contacts, the distribution of contacts was poorly resolved with this microscope. Interestingly, the direct visual observation through the eyepieces was much more sensitive than the camera and even faint labeling appeared distinctly punctate via the eyepieces.

Figure 1-9 Labeled ADN boutons appear as punctate fluorescence around the perimeter of the cell in superficial neurons. Note the translational shift in the images due to mechanical perturbation. This was due to moving the microscope while changing over from fluorescence to DIC optics.

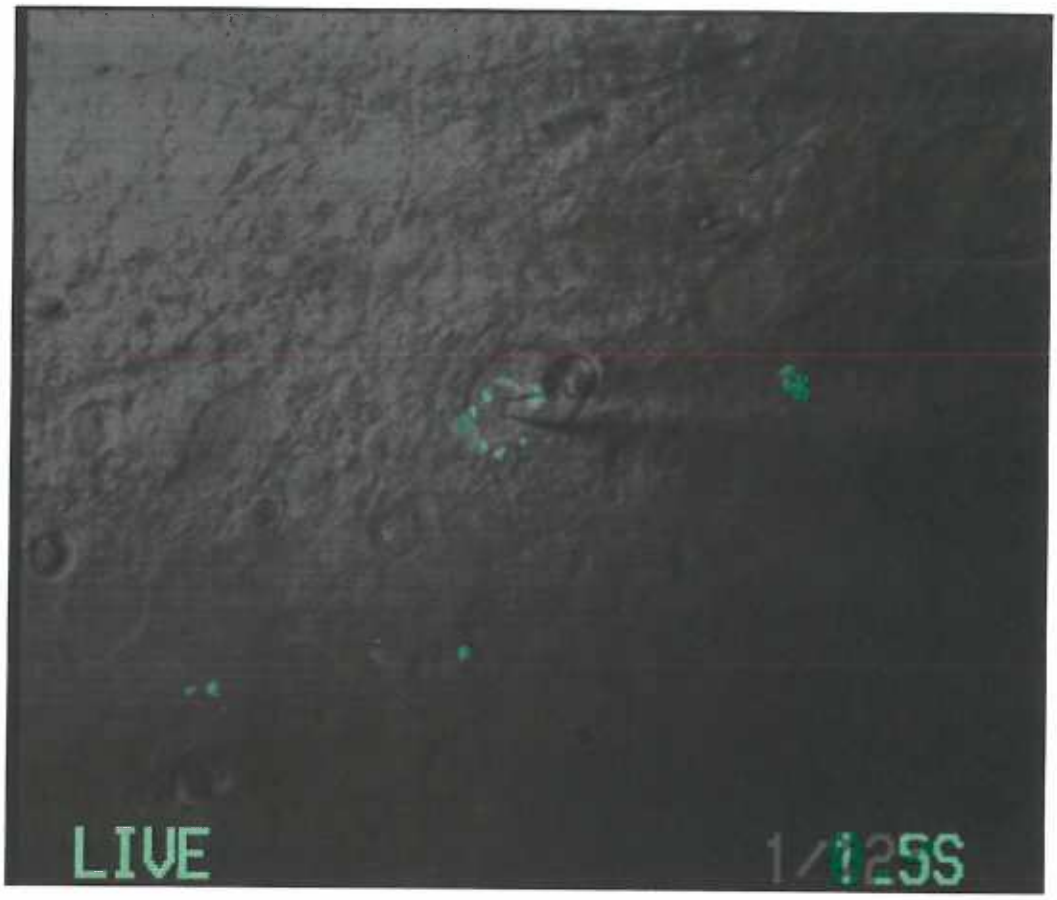
LIVE
1/125S

Figure 1-10 DiA labeling on neurons deep within the slice often appeared as fluorescent splotches. This is most likely due to signal scatter through the tissue and long integration times. The fluorescent signal in this picture is blue.

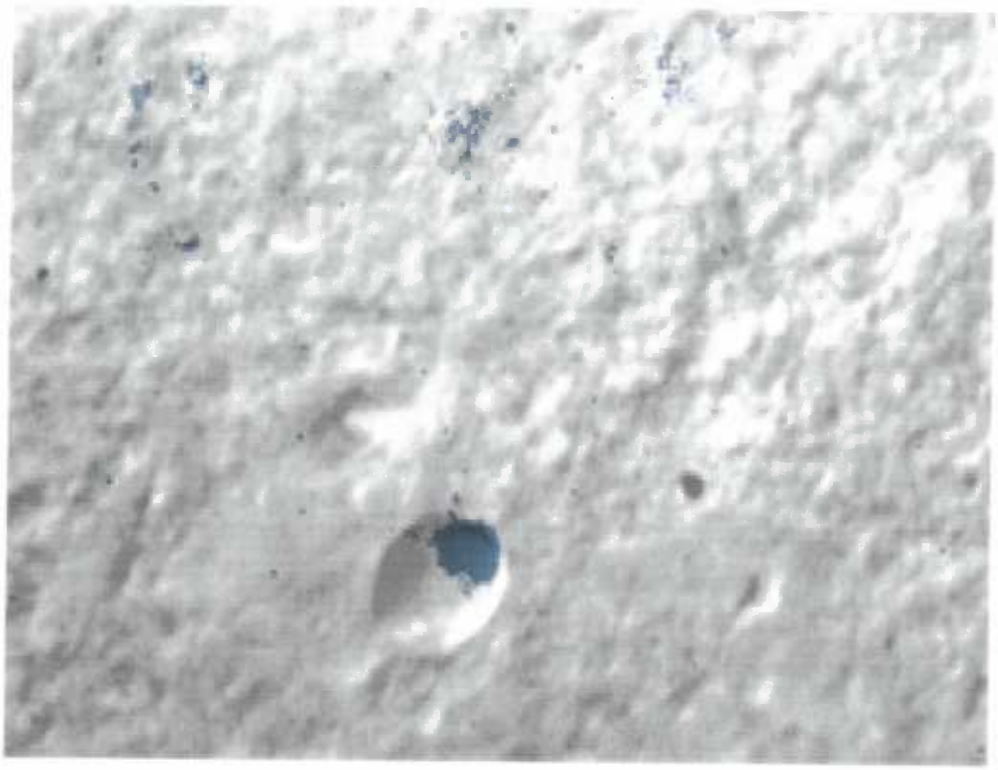

The fluorescent images of ADN contacts were captured and the digital image was overlaid with a real time IR DIC image of the neuron using the Argus 20 image processor and a Hammamatsu software plugin for Photoshop 5.0. Once an ADN positive neuron was identified, the live IR DIC image was used to direct the recording pipette to the identified neuron. In this manner, I could now record from neurons that received ADN contacts and study synaptic transmission from ST-activation in these neurons.

In later experiments, the laboratory acquired a Zeiss Axioskop2 microscope. This microscope was expressly purchased because in refining this model substantial improvements were made to the fluorescence efficiency of the optical path. In addition, image acquisition switch to use of a frame grabber with the video camera and Openlab software running on a Macintosh G4. This provided several clear advantages. First, the superior optics of the Axioskop 2 was immediately evident with our low light level ADN signals. I could reduce exposure/integration time to 1 second on average and thus minimized bleaching of the label. This more than tripled the number of labeled fields that I could capture in a slice before the fluorescent signal bleached (45 seconds). This, in turn, allowed several more attempts to patch identified second-order neurons. Second, the relatively short integration time also increased the spatial resolution of the fluorescent signal by reducing the effects of scattering. This improved resolution allowed me to more clearly establish the focal plane for the labeled terminals (**Figure 1-11**). Third, the

filter cubes on this microscope are mounted on a turret allowing more stable changeover to the IR DIC configuration. This improved the registry between fluorescent (terminal field) and IR DIC (neuron soma) images and helped determine the correspondence necessary to identify second-order baroreflex neurons. Fewer possible second-order neurons per slice were rejected as ambiguously identified when the images did not fully correspond. Fourth, the OpenLab software provided a user-friendly interface that minimized errors in the capturing command sequence. OpenLab minimized the number of steps and, more importantly, provided a means to overlay several different live IR DIC images over a single captured fluorescent image. This feature provided a means to reassess a label field under live IR DIC after an attempt was made to patch a neuron. Overall, the new equipment provided greater efficiency in coupling the label protocols with the electrophysiology within the slice.

Figure 1-11 The superior optics of the Axioskop 2 combined with the stronger fluorescent signal from DiI allowed much shorter integration times. As such, visualization of the label at several focal planes was possible. In panel A, the microscope is focused on the top of the cell. Each consecutive panel is focused 1 to 2 micrometers deeper than the previous.

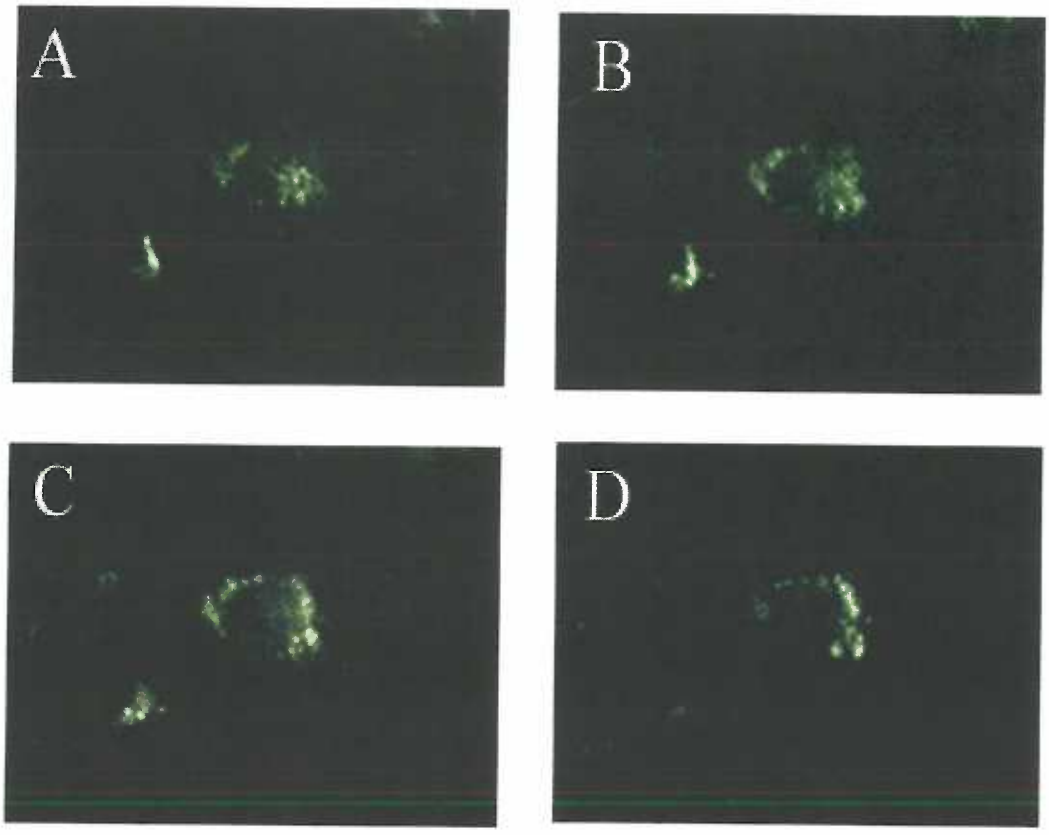
A
B
C
D

Formal Studies. These technical developments occurred as part of my research studies of NTS and the synaptic responses initiated by ST-activation. The advent of patch recording from visualized NTS neurons enabled me to approach several fundamental issues concerning synaptic transmission along these brainstem pathways. The improvements in resolution of time and signal to noise afforded by low resistance whole cell access to these neurons initiated several very basic studies addressing conventional expectations and assumptions about sensory processing in NTS. In addition to these studies, however, and in the period of my research work toward this dissertation, I have completed several other studies of NTS including work on anesthetics and voltage activated currents (Andresen et al. 2001;Bailey et al. 2001;Doyle et al. 1997;Doyle and Andresen 1997;Schild et al. 1997). The remainder of this dissertation will focus on two comprehensive studies that reflect the bulk of the work that I have completed.

The first study, which is now in press (Doyle and Andresen 2001), concerned the use of multiple complementary experimental strategies to identify neurons within NTS that received direct, i.e. monosynaptic connections from ST visceral sensory afferents. These studies relied on characterizations of the dynamic performance of ST evoked synaptic responses and a comparison to synaptic responses in neurons anatomically identified as second-order by the presence of dye labeled terminals on the cell body in NTS. A detailed temporal analysis and postsynaptic receptor identification using antagonists characterized monosynaptic responses to electrical activation of the tract. The first manuscript (Doyle and Andresen 2001)

concludes that commonly accepted operating definitions of monosynaptic and polysynaptic appear to be poorly predictive in NTS. The characteristics of ST evoked excitatory postsynaptic currents (EPSCs) in second-order neurons and the potential impact of recurrent inhibition during bursts of afferent activity was also discussed.

The second major project is presented as the second manuscript and concerns the chemical manipulation of the pool of primary afferents to NTS. As outlined above, cranial sensory afferents share many similarities with their more studied sensory counterparts in the spinal dorsal root ganglion. Earlier experiments had established that the ADN responded to capsaicin (CAP), the pungent ingredient of hot peppers (Fan and Andresen 1998). CAP excites sensory neurons of the somatic sensory system associated with nociception. CAP affected only the C-type axons in the ADN studies (Fan and Andresen 1998). As outlined in the manuscript, considerable evidence suggested that the recently cloned vanilloid receptor (VR1) at which CAP binds was strongly expressed in cranial visceral afferents and their terminal fields in NTS. My studies tested whether CAP selectively depolarizes these central sensory terminals in our brain stem slices and its mechanism of action. The second manuscript describes studies to test the hypothesis that CAP effects on second-order NTS neurons were mediated by glutamate release from ST axons.

Chapter 2

Reliability of monosynaptic sensory transmission in brain stem neurons *in vitro*

Mark W. Doyle and Michael C. Andresen [§]

Department of Physiology and Pharmacology

Oregon Health Sciences University

Portland, Oregon 97201-3098[§]

Abstract

The timing of events within the nervous system is a critical feature of signal processing and integration. In neurotransmission, the synaptic latency, the time between stimulus delivery and appearance of the synaptic event, is generally thought to be directly related to the complexity of that pathway. In horizontal brain stem slices, we examined synaptic latency and its shock-to-shock variability (synaptic jitter) in medial nucleus tractus solitarius (NTS) neurons in response to solitary tract (ST) electrical activation. Using a visualized patch recording approach, we activated ST 1-3 mm from the recorded neuron with short trains (50-200 Hz) and measured synaptic currents under voltage clamp. Latencies ranged

from 1.5 to 8.6 msec and jitter values (SD of intraneuronal latency) ranged from 26 to 764 μsec (n=49). Surprisingly, frequency of synaptic failure was not correlated with either latency or jitter ($p>0.147$; n=49). Despite conventional expectations, no clear divisions in latency were found from the earliest arriving excitatory postsynaptic currents (EPSCs) to late pharmacologically polysynaptic responses. Shortest latency EPSCs (<3 msec) were mediated by non-NMDA glutamate receptors. Longer latency responses were a mix of excitatory and inhibitory currents including non-NMDA EPSCs and GABAa receptor mediated currents (IPSC). All synaptic responses exhibited prominent frequency dependent depression. In a subset of neurons, we labeled sensory terminals by the anterograde fluorescent tracer, DiA, from aortic nerve baroreceptors and then recorded from anatomically identified second-order neurons. In identified second-order NTS neurons, ST-activation evoked EPSCs with short to moderate latency (1.9 to 4.8 msec) but uniformly minimal jitter (31 to 61 μsec) that were mediated by non-NMDA receptors but had failure rates as high as 39%. These monosynaptic EPSCs in identified second-order neurons were significantly different in latency, and jitter than GABAergic IPSCs (latency 2.95±0.71 vs. 5.56±0.74 msec $p=0.027$; jitter 42.3±6.5 vs. 416.3±94.4 μsec, $p=0.013$, n=4, 6, respectively) but failure rates were similar (27.8±9.0 vs. 9.7±4.4%, $p=0.08$, respectively). Such results suggest that jitter and not absolute latency or failure rate is the most reliable discriminator of mono- vs. polysynaptic pathways. The results suggest that brain stem sensory pathways may differ in their principles of integration compared to cortical models and that this importantly impacts synaptic performance. The unique performance

properties of the sensory-NTS pathway may reflect stronger axosomatic synaptic processing in brain stem compared to dendritically weighted models typical in cortical structures and thus may reflect very different strategies of spatio-temporal integration in this NTS region and for autonomic regulation.

Introduction

Timing is perhaps one of the most critical features of signal processing and integration in neural communication (Ferster and Spruston 1995). The distribution in time of action potentials and synaptic events critically determines interactions between groups of neurons in both the peripheral and central nervous system. In synaptic transmission, the time between activation of a pathway by a stimulus until its arrival as a synaptic response, the latency, is thought to be directly related to the nature and complexity of that pathway. This timing of events dictates the impact of the convergence of multiple synaptic inputs on single neurons and thus contributes to regulation of neuron excitability and the overall performance characteristics of a network or circuit of neurons. Understanding the mechanisms that shape synaptic timing is then a basic building block to understanding the cellular basis of function in any brain region.

The nucleus of the solitary tract (NTS) provides an interesting model for investigating synaptic performance and interactions. NTS is a major integrative site where visceral sensory information enters the brain and projections originate to a variety of brain stem and supra medullary nuclei with reciprocal projections

back to NTS (Loewy 1990). The sensory axons from cranial nerves traverse the brainstem through the bundle of the solitary tract (ST) to their synapses within NTS. This anatomical feature of ST offers direct access to afferent axons for electrical stimulation within brainstem slices (Andresen and Yang 1990). ST-stimulation evokes several synaptic responses within NTS neurons reflecting both activation of visceral sensory synapses as well as responses via indirect polysynaptic paths initiated in local circuits by ST-activation (Andresen and Yang 1995;Andresen and Yang 1990;Zhang and Mifflin 1998b;Miles 1986).

The most common approach to distinguishing monosynaptic from polysynaptic pathways relies on the shortness of the absolute latency and whether evoked synaptic events faithfully follow pairs of closely timed shocks (Miles 1986;Yoshimura and Jessell 1989;Gil et al. 1999;Berger and Averill 1983;Andresen and Yang 1995;Zhang and Mifflin 2000;Aylwin et al. 1997; Deuchars et al. 2000). In the present study, we assessed whether these commonly used electrophysiological criteria clearly distinguish mono- from polysynaptic responses. To do this, we examined synaptic responses to bursts of ST-activation in NTS neurons displaying a wide range of absolute latencies and assessed their response variability. We also determined the synaptic failure rates in these neurons. Lastly, we compared these synaptic performance characteristics to those of NTS neurons that were anatomically identified as second-order neurons by the presence of tracer-labeled sensory terminals on their cell bodies. Together, the results suggest that, contrary to conventional expectations, only

synaptic jitter, and the intraneuronal variability of the synaptic latency, reliably indicated monosynaptic contacts.

Methods

Slice Preparation Brainstem slices were prepared from adult (100 - 300 g) male Sprague Dawley Rats (Charles River). Rats were deeply anesthetized with ether and quickly killed by cervical dislocation. The hindbrain was removed and placed for one minute in freezing (-3 to 0 ° C) artificial cerebrospinal fluid (ACSF) containing: (mM) 125 NaCl, 3 KCl, 1.2 KH_2PO_4, 1.2 $MgSO_4$, 25 $NaHCO_3$, 10 dextrose, 2 $CaCl_2$, bubbled with 95%O_2 / 5%CO_2, The medulla was trimmed rostrally and caudally to yield a 1 cm block centered on the obex. The cerebellum was removed and a wedge of tissue was cut from the ventral surface to orient the brainstem such that 250 µm slices contained lengthy segments of sensory axons in the ST and their terminations on neurons within NTS (Mendelowitz et al. 1992). Slices were cut with a sapphire knife (Delaware Diamond Knives) mounted in a vibrating microtome (Leica VT-1000). Slices were placed in a custom perfusion chamber and secured with a nylon mesh on a platinum frame so that no strands crossed the ST or medial portions of NTS. This prevented compression of the sensory axons and minimized fluorescent background light emitted from the nylon fibers. The slices were perfused with ACSF at 34-37 ° C; pH 7.4; 300 mOsm. Recordings were made from NTS neurons located just medial to the ST and within 200 µm rostral or caudal from obex, the area of densest aortic baroreceptor afferent terminations (Mendelowitz et al. 1992).

Visualized patch recordings. Neurons were visualized using a Zeiss Axioskop microscope equipped with fluorescence, differential interference contrast (DIC) optics (40x water immersion lens) and an infrared (IR) sensitive camera. Patch electrodes were guided using IR DIC microscopy to neurons that were voltage clamped in the whole cell configuration (Axopatch 200A). Recording electrodes (1.8 to 3.5 MΩ) were filled with an intracellular solution containing (in mM): 10 NaCl, 130 K Gluconate, 11 EGTA, 1 $CaCl_2$, 2 $MgCl_2$, 10 HEPES; pH 7.3; 295 mOsm. In some experiments (noted in the text), 130 K Gluconate in the internal solution was replaced with 125 KCl (high internal Cl solution) in order to displace the chloride reversal potential away from the resting membrane potential. Data were filtered at 5 kHz and sampled at 10-20 kHz using p-Clamp7 software (Axon Instruments). Neurons were accepted for recording if they had an initial seal resistance greater than 1 GΩ and over the initial 10 minutes required no more than 100 pA to hold the neuron at -70 mV.

Stimuli were delivered by placing a 200 µm diameter concentric bipolar stimulating electrode (F. Haer) on the visible ST 1-3 mm from the site of the recorded neuron soma and recorded ST evoked post-synaptic currents (PSCs). Bursts of 5 ST stimuli every 4 or 5 seconds at frequencies of 50, 100, or 200 Hz were generated with a Master-8 isolated programmable stimulator (A.M.P.I. Jerusalem, Israel). At the cycle rate of 4-5 seconds, consistent synaptic responses were sustained for many tens of minutes with no burst-to-burst changes. Stimulus

duration was set at 0.1 ms based both on experience activating myelinated and unmyelinated afferent volleys in the aortic depressor nerve (Fan and Andresen 1998) and on preliminary tests of the ST stimulus duration to evoke maximum synaptic responses. Neurons were rejected from further study if the evoked synaptic currents initiated fast sodium current at clamped potentials more negative than -40 mV indicating inadequate voltage control. All drugs were dissolved in 100 µL DMSO, diluted with external solution and bath applied. NBQX was purchased from Tocris-Cookson (Ballwin, MO) and all other drugs were purchased from Sigma (St. Louis, MO). Application of the highest concentration of vehicle used for dissolving drugs had no effect on neuron properties or synaptic responses (data not shown).

Labeling of the aortic depressor nerve. In 20 day old, pentobarbital anesthetized (50 mg/ kg) rats, the aortic depressor nerve (ADN) was located and separated from the surrounding tissue one cm peripheral to joining the superior laryngeal nerve and entering the nodose ganglion (Mendelowitz et al. 1992). The nerve trunk was then placed within a pre-formed molded shell of dental impression compound (Coltene, Mahwah, NJ). The lipophilic fluorescent dye, DiA (Molecular Probes, Eugene, OR), was carefully placed on ADN making sure that dye did not contact adjacent nerves and structures. To prevent dye migration to adjacent nerves, the ADN was then sealed in place by application of additional dental impression compound and allowed to cure in place. Animals were sacrificed for experiments 2-3 months following dye implantation. Previous studies suggest that

this procedure fills synaptic terminals belonging to aortic arch baroreceptors and these are concentrated over cell bodies in medial portions of caudal NTS (Mendelowitz et al. 1992). For electrophysiological experiments, fluorescent ADN terminals within NTS were located visually under brief exposures to excitation wavelengths (Chroma, PN31024, DiA) and then images captured digitally using camera integration time intervals of 2 to 5 seconds. Captured fluorescent terminal images were then overlaid with real time IR DIC images using an ARGUS 20 image processor (Hammamatsu Bridgewater, NJ) to establish co-localization of fluorescence with the underlying neural structure. The presence of fluorescent ADN sensory terminals coincident with the neuron soma identified second-order neurons within NTS with anatomically monosynaptic connections and the synaptic responses to ST-activation were then studied in these neurons under voltage clamp (see Figure 8).

Synaptic performance was assessed by measuring the synaptic latency as the time between the onset of the stimulus artifact and the onset of synaptic current. For improved precision, the membrane current trace was first differentiated and these two onset times were taken as crossing points of a set threshold level (see Results for details). For clarity, only the synaptic responses to the first ST shock in each burst were analyzed for the jitter calculation. Jitter was calculated as the standard deviation of the shock-to-shock variation in latency within each neuron averaged over multiple trials (25-50 trials). The absence of a synaptic current deflection following a stimulus shock to the ST was taken as a synaptic failure and

the rate of failure calculated as the number of failed synaptic responses to bursts of stimuli (>50 Hz) across multiple trials. Failure rate was calculated as the number of absent synaptic responses divided by the number of stimulus shocks delivered and expressed as a percentage. Derived synaptic parameters (latency, jitter and failure rate) were compared across groups using two sample t-tests (Snedecor and Cochran 1980) and groups were considered significantly different at p-values less than 0.05. In addition, correlations were tested as described in the Results using linear models with least squares fitting (Origin 6.1, OriginLab Corp.).

Results

Trains of electrical shocks to the ST (**Figure 2-1a**) most often evoked large excitatory post-synaptic currents (EPSCs) in medial NTS neurons. Increases in the shock intensity of ST-stimulation did not further increase the EPSC amplitude suggesting that recruitment of additional fibers was minimal. If the ST shocks were repeated at short intervals (<2 seconds), the amplitudes of successive EPSCs within a burst of stimuli declined substantially. The decrease in amplitude was greater at higher frequencies and this frequency dependent depression (FDD) was similar in all neurons tested.

Figure 2-1 ST-stimulation in different medial NTS neurons evoked EPSCs with different latencies. Successive shocks (•) induced a similar frequency dependent depression of EPSC amplitude in these two examples of different neurons. Traces are averages of 5 consecutive sweeps. **A**: Short latency EPSC (latency = 2.2msec; jitter =46 μsec) had no observable failures in individual traces (not shown). **B**: Long latency EPSC (latency = 7.5msec; jitter =152 μsec) had several observable failures particularly on the fifth pulse of the train so that the average trace has little net deflection. In both cases, ST stimulus trains consisted of 5 pulses at 100 Hz and neurons were voltage clamped at -70 mV.

Doyle and Andresen: Figure 1

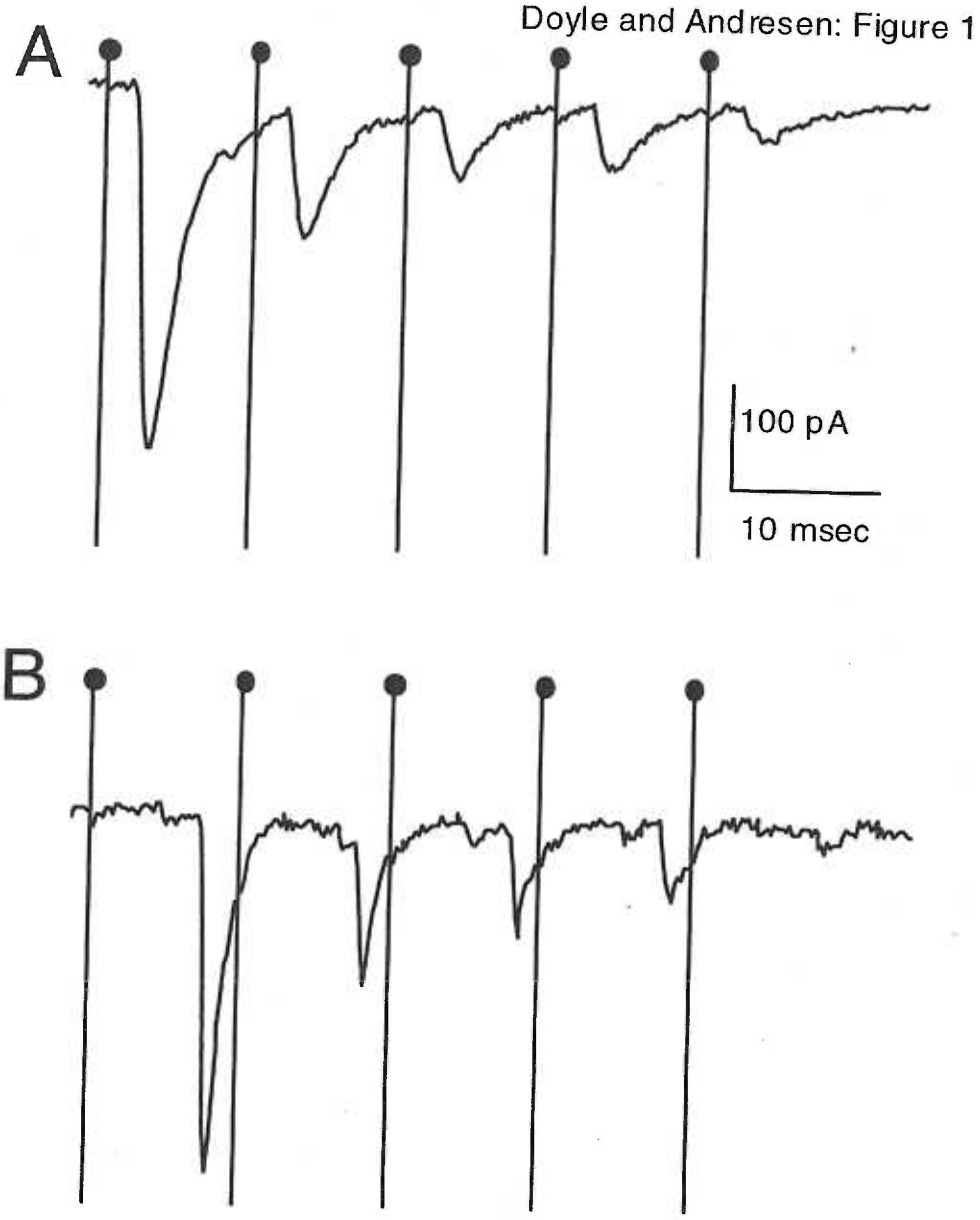

To improve the precision in assessment of synaptic latency, the individual synaptic current traces were mathematically differentiated with respect to time (**Figure 2-2a**). Differentiation accentuated the initial phase of the PSC onset. Latencies were calculated as the time between initiation of the ST shock until the time at which the differentiated signal trace crossed a horizontal noise threshold level. This threshold was set at a level equal to the greatest transient value of the fluctuations in the differentiated signal trace for 1-50 msec preceding the PSC. The first point of the PSC differential to exceed a noise threshold was designated as the beginning the synaptic event (**Figure 2-2a**, left small arrow). This technique provides a simple, precise measurement of the latency. Absolute latency values for a given neuron were calculated over a 30 to 60 minute period of recording as one measure of synaptic performance.

The range of absolute PSC latencies to ST-stimulation across NTS neurons was quite broad and the distribution was fairly unimodal with no clear divisions across our sample of 49 neurons (**Figure 2-2b**). All of the shortest latency PSCs (<3 msec) were excitatory. The longer latency (>3 msec) PSC group, however, included both excitatory and inhibitory PSCs (IPSCs). Given the distribution and mixture of excitatory and inhibitory events, the pathway underlying moderate latency events is ambiguous based on the absolute latency. Thus, we examined the shock-to-shock variation in latency (jitter) for repeated ST evoked PSCs within neurons as an additional measure of synaptic performance.

Figure 2-2 Analysis of synaptic jitter. **A:** Raw digitized current records were differentiated (middle trace) to facilitate accurate identification of the onset of the PSC. Time points for the onset of the stimulus and PSC were determined by differentiating current traces with respect to time (*dI/dt*). Short arrows (left and right) indicate data points in the differentiated signal which first exceed a noise threshold level (dashed line) indicated the beginning time points for stimulus (left arrow) and PSC (right arrow). The total latency between the ST shock and the PSC (double headed, horizontal arrow) was determined by subtracting the time of the stimulus onset from the onset time of the PSC. **B:** The unimodal distribution of the histogram of absolute latency for 36 NTS neurons reveals no distinction for mono- or polysynaptic events. Absolute latency is expressed as the mean of the latency of 20 to 50 individual PSCs measured over a 30 - 60 minute period.

Doyle and Andresen: Figure 2

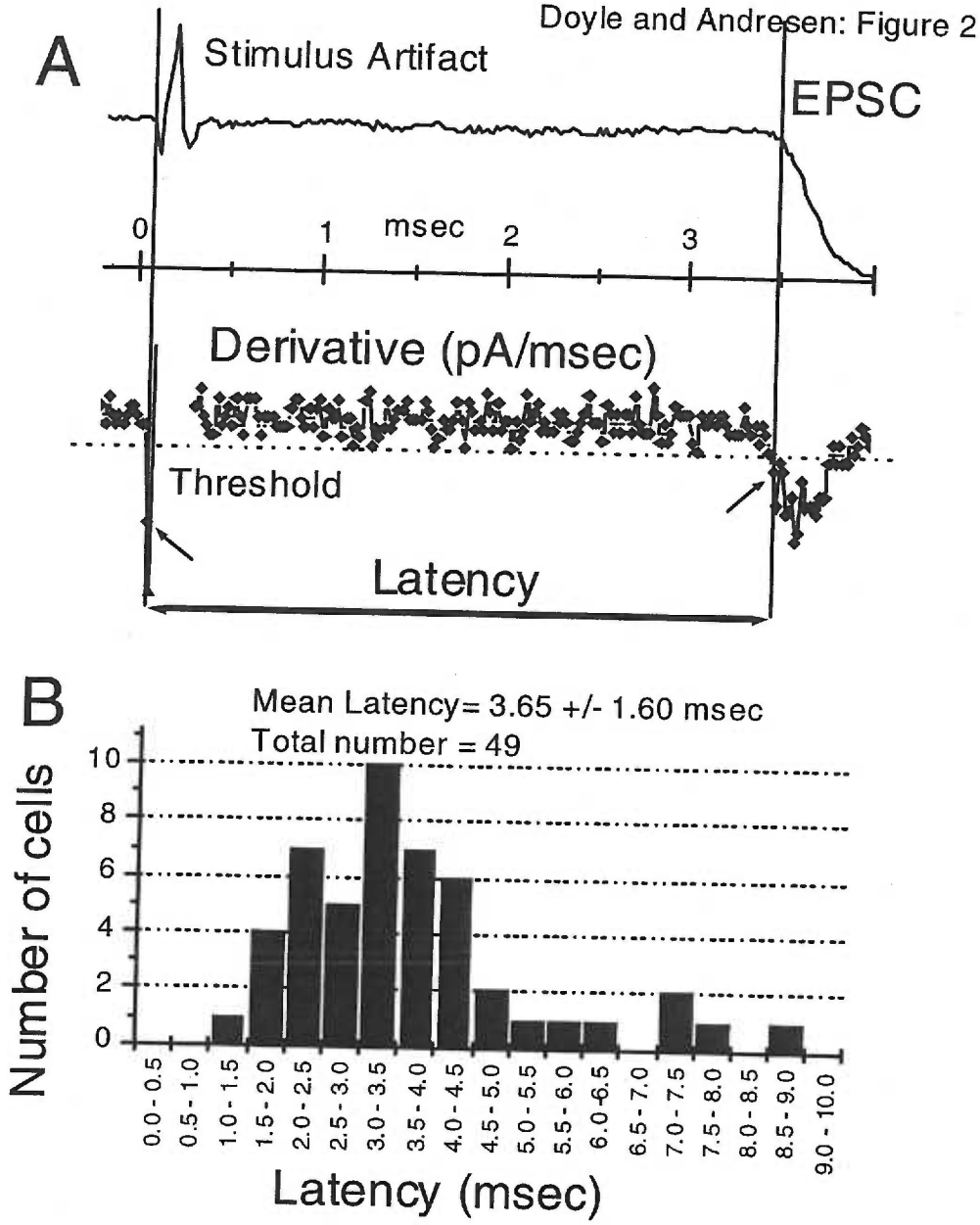

EPSCs in neurons with the shortest absolute latencies (**Figure 2-3a**) had remarkably low jitter (<100 µsec). This quantitatively high degree of temporal stability in synaptic performance is consistent with transmission via a monosynaptic pathway. Most highly consistent synaptic responses reliably evoked EPSCs with fewer than 5% failures. These low-jitter synaptic responses were fast, excitatory inward currents that reversed near zero mV and their pharmacological profile was similar to previous reports from medial NTS neurons (Andresen and Yang 1995). The non-NMDA selective glutamate receptor antagonist NBQX completely blocked such EPSCs. Recording such responses at depolarized membrane potentials or in extracellular solutions nominally free of Mg^{++} (**Figure 2-3b**) failed to reveal any contribution of NMDA receptor activation by synaptically released glutamate.

Figure 2-3. Short latency EPSCs with minimal jitter were mediated by glutamate acting at non-NMDA receptors. **A.** Short absolute latency EPSCs recorded from a medial NTS neuron voltage clamped at -70 mV. Five individual EPSC traces are overlaid to show shock-by-shock variation in latency to ST-stimulation. Each trace is the first EPSC of a burst. Every ST shock (•) evoked an EPSC with the high reliability of a monosynaptic connection (latency = 2.6 msec; jitter =68 μs and no observable failures, train of 5 pulses at 200 Hz). **B.** Successive, high frequency shocks reveal a frequency dependent depression of EPSC amplitude. EPSCs were completely blocked with 50 μM NBQX without extracellular Mg^{++} suggesting that no NMDA component was activated by ST shocks.

Doyle and Andresen: Figure 3

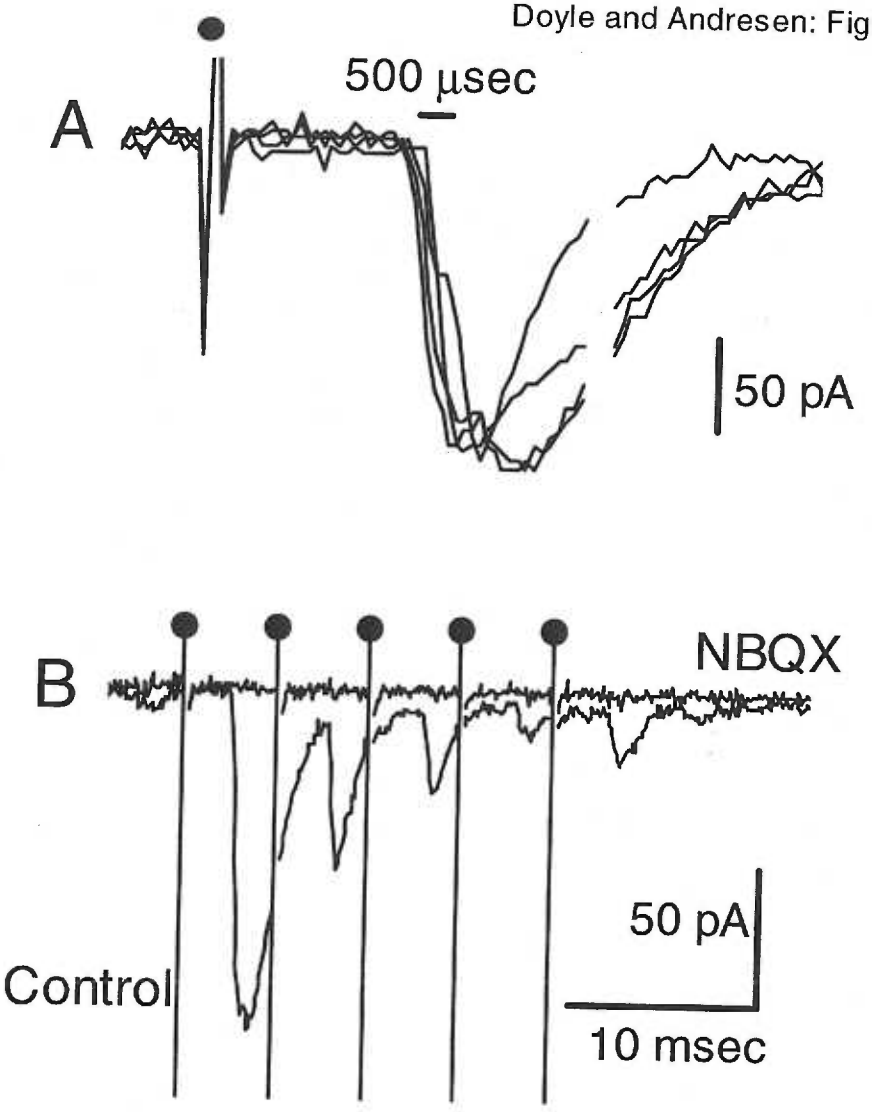

In contrast, the synaptic performance of longer latency EPSCs often displayed substantial temporal variation. Synaptic jitter of long latency responses increased as much as ten fold over those with short latencies (**Figure 2-4a**). Interestingly, despite these highly variable synaptic responses, failures to bursts of ST stimuli were infrequent or absent in these neurons. In some neurons with these intermediate latency EPSCs (3 out of 5), pharmacological blockade with NBQX in solutions with zero extracellular Mg^{++} revealed a small, slow inward synaptic response (**Figure 2-4b,c**). Note that such NBQX -insensitive inward synaptic currents always had a longer absolute latency (**Figure 2-4c**) than the NBQX sensitive EPSC and failed to follow 50 Hz trains of ST stimuli. The NBQX insensitive currents were blocked with the NMDA receptor antagonist AP-5 (**Figure 2-4b,c**). These observations (short latency non-NMDA event and longer latency, NMDA event) are consistent with two events of separate origin activated at different synapses on the same neuron. Thus, in neurons that appear to be polysynaptically linked to the ST (long latency with high jitter), a mix of synaptic responses was found which could include participation of non-NMDA and NMDA receptors.

Figure 2-4 Moderate latency EPSCs evoked by ST-stimulation have greater temporal variability and a different pharmacological profile. **A.** Moderate latency EPSC evoked by ST-stimulation (Vm=-70mV; 0 mM extracellular Mg^{++}). There is greater sweep-to-sweep variation in latency (Jitter = 120 µsec). Five EPSCs are overlaid to show differences in latency between stimuli (left panel). Each trace is the first EPSC of a burst of stimuli. **B.** There are no observable failures to 100 Hz ST-stimulation. Note the frequency dependent depression. **C.** In a time-expanded view of the initial portion of this same case as **B.**, a small, slow, NBQX (50 µM) insensitive response remains which was blocked by the NMDA receptor antagonist AP-5 (100 µM). The NBQX sensitive response had a shorter latency than the NMDA response (3.3 msec vs. 6 msec) suggesting origin from different synapses.

Doyle and Andresen: Figure 4

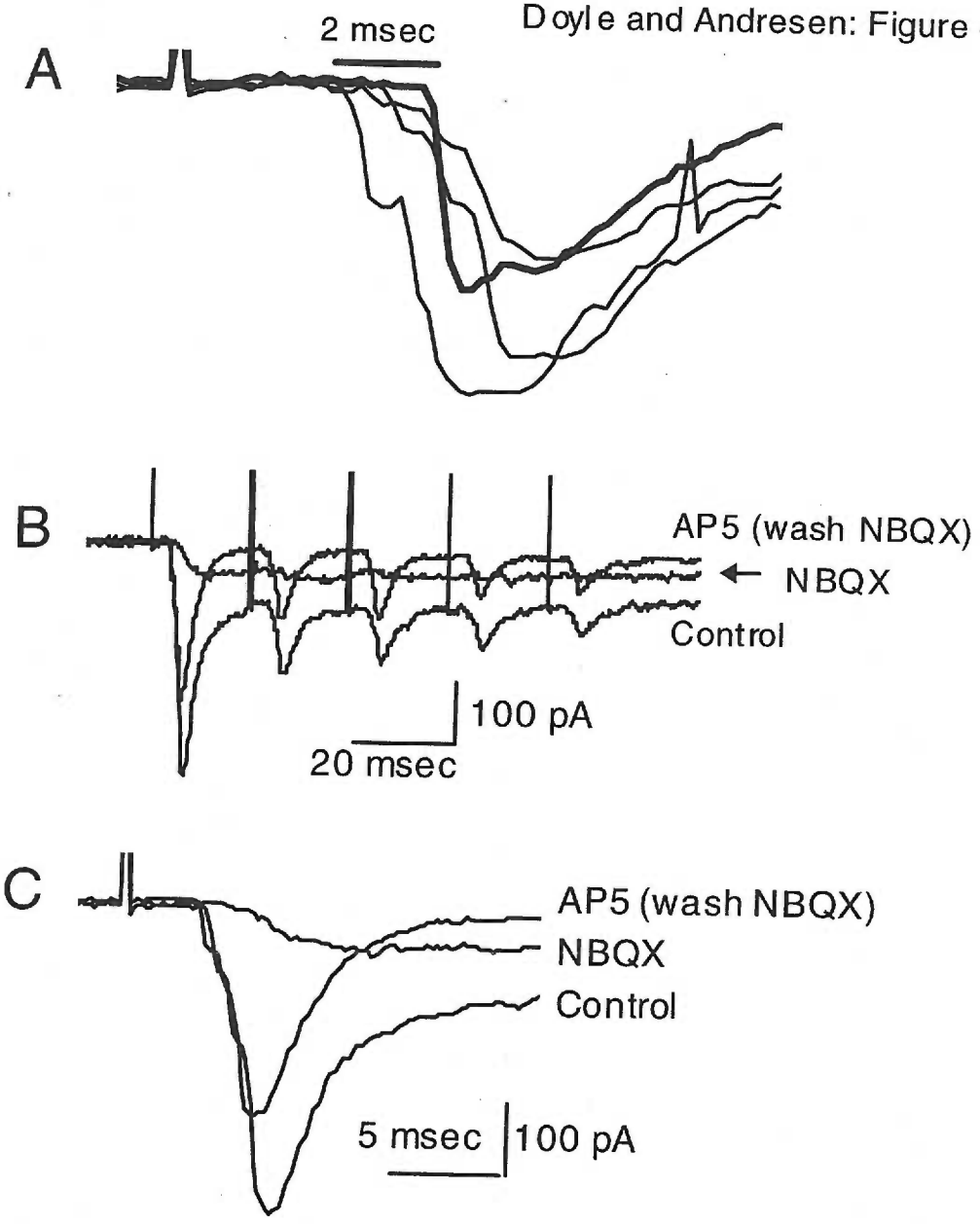

Many PSCs with the greatest jitter were inhibitory and some regularly failed in response to high frequency trains of stimuli (**Figure 2-5**). Interestingly, the long latency, high jitter IPSCs could be blocked with either the $GABA_A$-receptor antagonist bicuculline or the excitatory non-NMDA-receptor antagonist NBQX (**Figure 2-5 b,c**). This direct pharmacological evidence is consistent with a polysynaptic connecting path from the ST. For these types of PSCs, one step in the path from ST was mediated by non-NMDA glutamate receptors and this event was responsible for evoking the recorded $GABA_A$ IPSC. Because of their relatively high temporal variability, long latencies, and common failures, these polysynaptic responses were the least reliable.

Doyle and Andresen: Figure 5

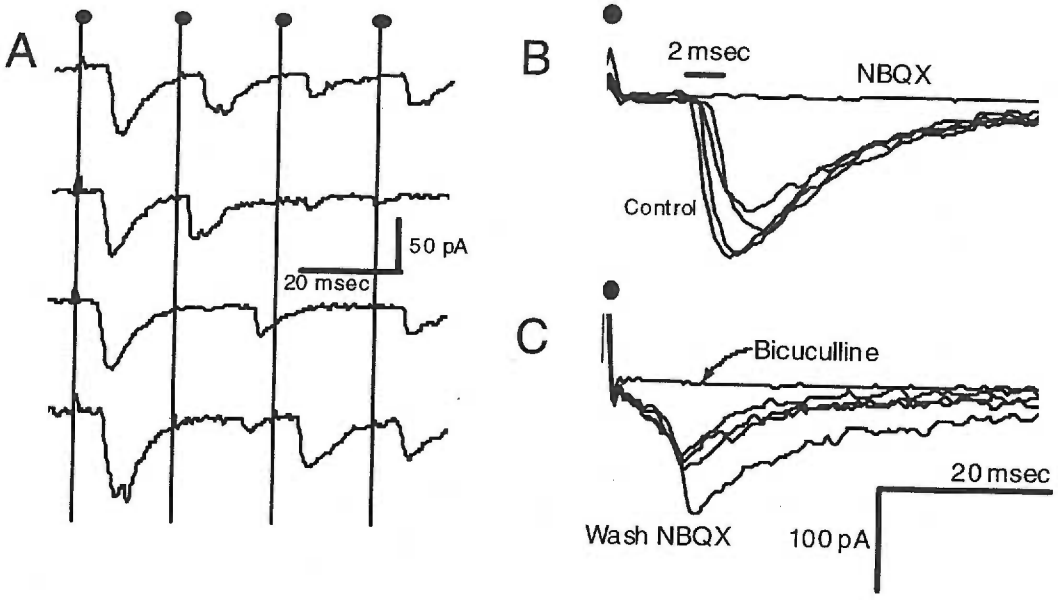

Our pool of 49 NTS synaptic responses included both EPSCs and IPSCs. Across this sample, synaptic jitter generally increased as the absolute latency increased with a strong and significant positive correlation (R=0.573, **Figure 2-6A**). Given the nature of the characterization of individual synaptic responses described above, this pool represents a mixture of second and higher order responses. Subregions of this jitter relationship may reflect differences in this mixture of mono- and polysynaptic response pathways. At the very shortest latencies (<2.8 msec), values fell within a quite restricted range of jitter values with no jitter values greater than 100 µsec (**Figure 2-6A**). Beyond this short latency range, jitter values ranged widely. Note that in the range of 3-9 msec, jitter could be as low as the lowest values found at the shortest latencies or over 700 µsec. In the simplest interpretation, some long latency events were highly reliable and likely were mediated by simple, monosynaptic pathways despite their late arrival after ST-activation. The high jitter synaptic group included the pharmacologically, disynaptic $GABA_A$ IPSCs described above. Beginning at approximately double the shortest latency that we recorded, intermediate latency EPSCs (>2.8 msec) had jitters ranging from among the lowest of the entire sample to substantial (>100 µsec). These intermediate latencies could not be unequivocally classified as mono- or polysynaptic based on their latency or jitter characteristics to ST burST-stimulation.

Figure 2-6 **A.** Summary relationship between jitter and the absolute latency. Jitter was positively and significantly correlated to increasing latency (correlation coefficient = 0.573). Points represent values from 49 separate medial NTS synaptic responses. Jitter was expressed as the standard deviation of the absolute latency. Dotted line is a least squares linear regression fit to the data ($y=52.6X-55.9$; $R=0.577$; $n=49$; $p<0.0001$). At latencies >3.0 msec, many synaptic responses displayed very high jitter or very low jitter so that values fell far from the regression fit. Circled points indicate neurons that were anatomically identified as being second-order to sensory contacts with DiA labeling. Data points derived from related figures are indicated for several individual values by arrows. Ψ indicates average jitter point for EPSC with expanded display in Part B.

B. Individual histograms showing the distribution of individual latency values to a series of ST shocks for two individual neurons with similar overall latency (about 5 msec) but very different synaptic jitter. Ψ and filled bars display latency values for an EPSC from a DiA ADN labeled, anatomically second-order NTS neuron. Note the narrow range of values for this monosynaptic response. In contrast, the open bars display the range of latency values for the pharmacologically polysynaptic response of the neuron from Figure 5. In such cases, the range of latency values is quite large (nearly 1.5 msec) and the distribution less symmetrical.

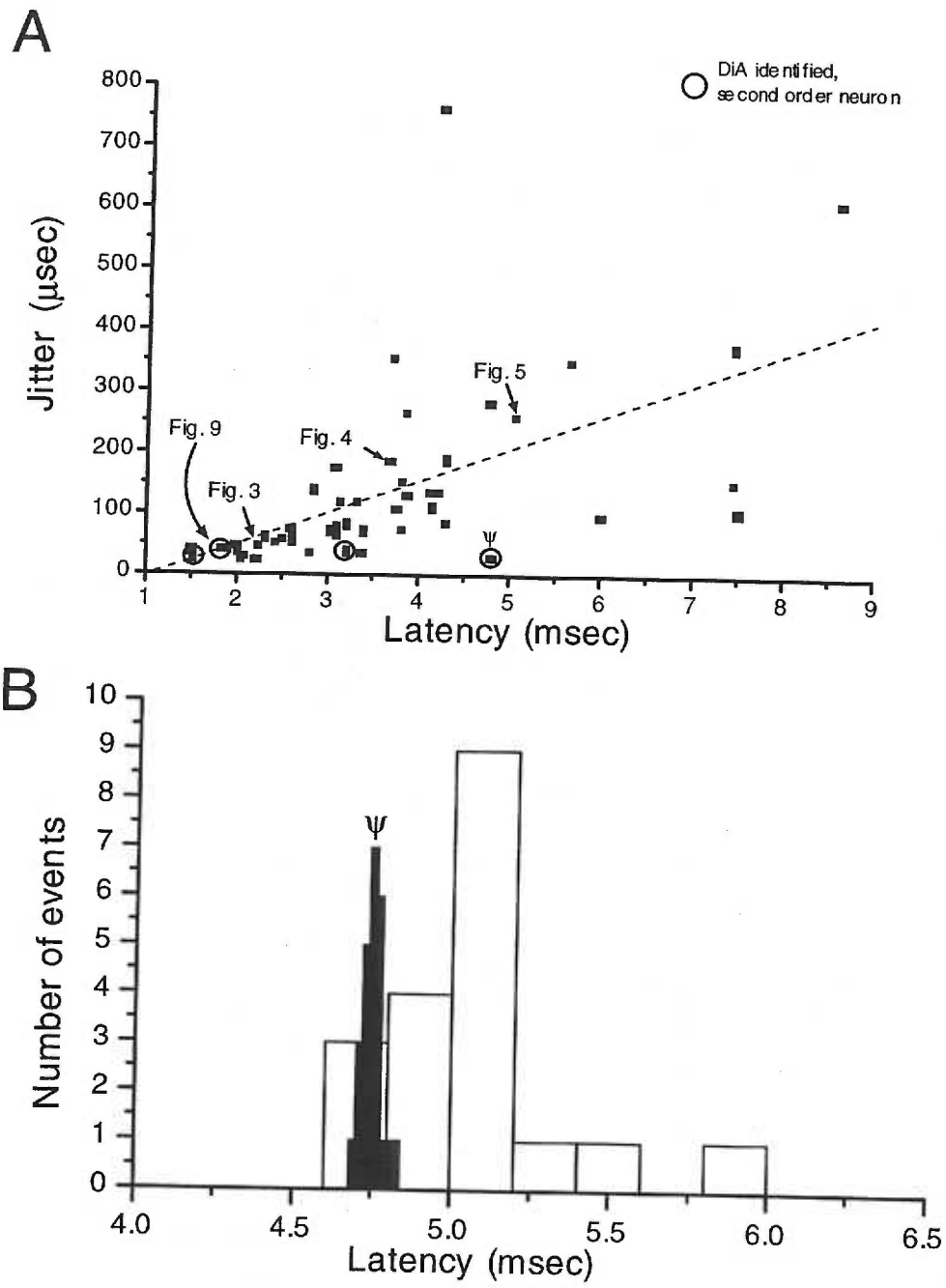
A
DiA identified,
second order neuron
Jitter (µsec)
800
700
600
500
400
300
200
100
0
Fig. 9
Fig. 3
Fig. 4
Fig. 5
ψ
1
2
3
4
5
6
7
8
9
Latency (msec)
B
Number of events
10
9
8
7
6
5
4
3
2
1
0
ψ
4.0
4.5
5.0
5.5
6.0
6.5
Latency (msec)

Conventionally, polysynaptic events have been distinguished by their inability to sustain synaptic responses to two, closely timed stimuli. This is based on the premise that increasing the number of synapses increases the likelihood that an element will fail in the pathway required for transmission. If failures can distinguish mono- from polysynaptic responses, then the frequency of failures to bursts of stimulation should be directly correlated to events with the shortest latencies and the smallest jitters. Our data do not support this concept. Responses with high failure rates (**Figure 2-7a**) occurred over such a broad range of latencies that no relation was detected by regression analysis ($p=0.540$). Likewise, the magnitude of synaptic jitter (**Figure 2-7b**) was unrelated to failure rate ($p=0.139$). Also, responses that were clearly disynaptic (e.g. **Figure 2-4**) could have zero failures at high frequencies of activation. Thus, the absence of overt failures poorly predicts synaptic order. In this preparation, monosynaptic PSCs appear to have jitter of less than 100 µsec. As a group (n=27) such EPSCs had an average latency of 2.8±1.0 msec with a jitter of 54±21 µsec and an average failure rate of 5.9±11.5% (e.g. Figure 3). These electrophysiologically based reliability criteria for monosynaptic events are consistent with the pharmacological data. High jitter (>100 µsec) synaptic PSCs (n=22) had an average latency of 4.6±1.6 msec, an average jitter of 237.4±170.1 µsec and average failure rate of 6.8±7.9%. High jitter (>100 µsec) EPSCs (**Figure 2-4**) and all IPSCs (**Figure 2-5**) were considered polysynaptic (see below). To test further the relationship between jitter and synaptic pathway order, we recorded ST evoked EPSCs from NTS neurons with anatomically verified, direct connections to ST sensory afferents.

Figure 2-7 Summary of relationships between failure rates (responses missing expressed as % of all stimuli) of individual synaptic responses and either the absolute latency (**panel A**) or the jitter (**panel B**). The failure rate was independent of the absolute latency or the magnitude of synaptic jitter. Dotted lines are least squares linear regression fits to the respective datasets (panel A, latency: Y=0.55X+4.30; R=0.09; n=49; p=0.540; panel B, jitter: A=0.015X+4.32; R=-0.21; n=49; p=0.139). Circled points depict neurons with anatomically identified sensory contacts.

Doyle and Andresen: Figure 7

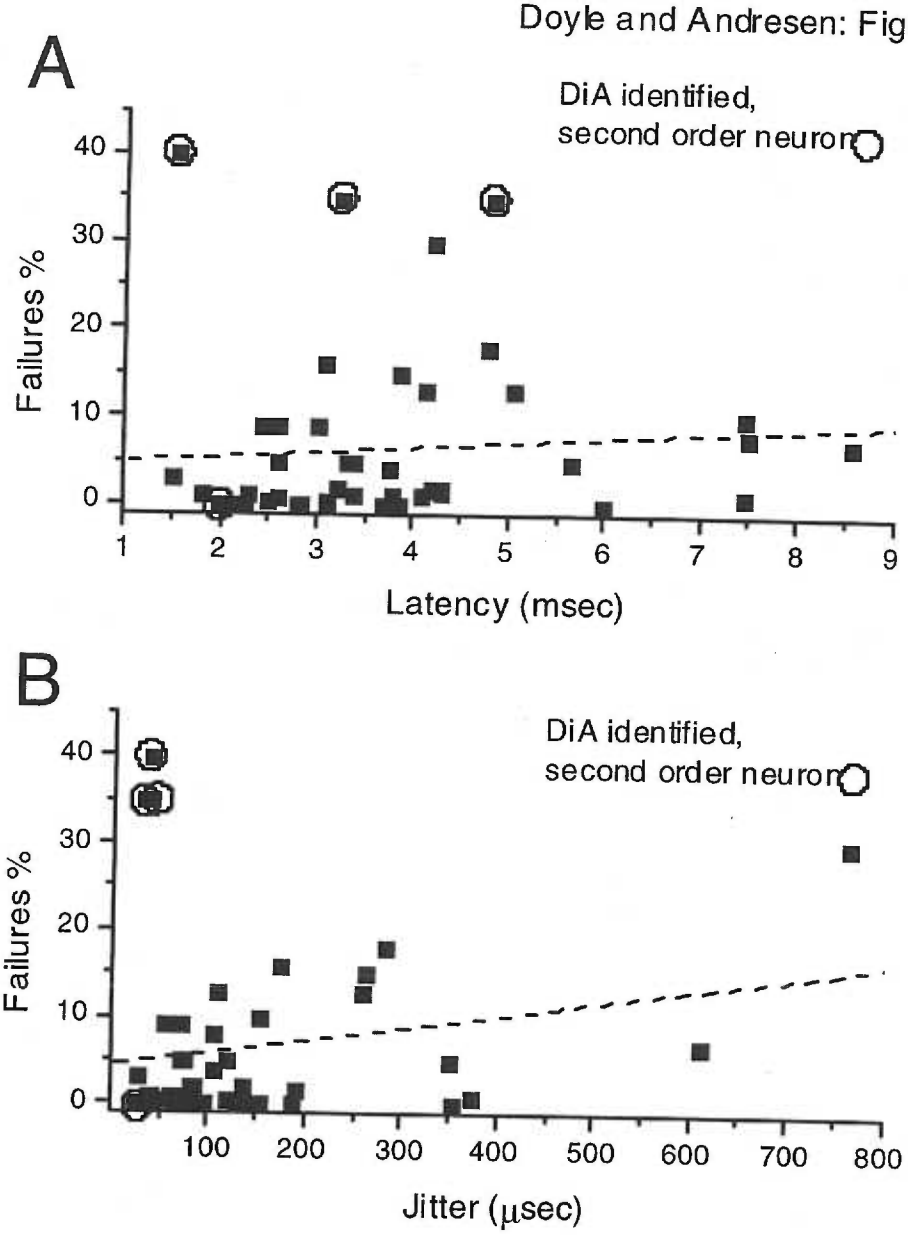

The aortic depressor nerve (ADN) in the rat contains primary afferent fibers that enter the brainstem travel through the ST and terminate in NTS. The ADN forms axo-somatic synapses with NTS second-order neurons (Mendelowitz et al. 1992). In a subset of experiments, we studied brainstems of animals with fluorescently tagged ADNs. We searched for and recorded from neurons with DiA labeled primary terminals within NTS (see Methods). Time integrated images revealed the presence of punctate fluorescently labeled terminals (**Figure 2-8**, green dots). Using IR illumination, real time, differential interference contrast (DIC) images of the underlying neuron structure were compared to the locations of fluorescent terminals. The real time IR DIC images were used to guide patch electrodes to the anatomically identified, second-order neurons and record synaptic responses. Train stimulation of the ST evoked fast EPSCs that rapidly depressed in these identified neurons (**Figure 2-9**). These EPSCs ranged in latency from 1.9 to 4.8 msec (**Figure 2-6**, circled points) and failure rates (**Figure 2-7**, circled points) ranged from no observable failures to 39%. Interestingly, jitter was remarkably invariant across these synaptic responses ranging from 31 to 61 □sec and, overall, the values fell along the minimum jitter range across our whole sample of NTS synaptic responses (**Figure 2-6**, circle points). NBQX completely blocked all these synaptic responses. In this study, we had characterized five bicuculline-sensitive, ST evoked IPSCs and concluded that these were clearly polysynaptic – both pharmacologically and according to their synaptic performance. We then compared these two groups – proposed monosynaptic and polysynaptic IPSC responses - for their relative synaptic performance parameters.

EPSCs from identified second-order neurons had shorter latencies and much lower jitters than the $GABA_A$ IPSCs (mean±SEM - latency 2.95±0.71 vs. 5.56±0.74 msec p = 0.027; jitter 42.3±6.5 vs. 416.3±94.4 µsec, p=0.013, n=4 and 6, respectively). Surprisingly however, the failure rates across these two groups were similar (27.8±9.0 vs. 9.7±4.4 % failures; n=4 and 6, p=0.08, respectively).

Figure 2-8 Example of location of fluorescent labeling from aortic baroreceptor afferent terminals on medial NTS neuron. Punctate fluorescent label was found primarily directly over the soma of NTS neurons. Overlay of a time integrated fluorescent DiA signal with a real time IR illuminated differential interference contrast (DIC) image allowed a patch electrode to be guided to the labeled neuron. Fluorescent ADN terminals formed green patches co-incident with cell body identifying a second-order NTS neuron within the slice.

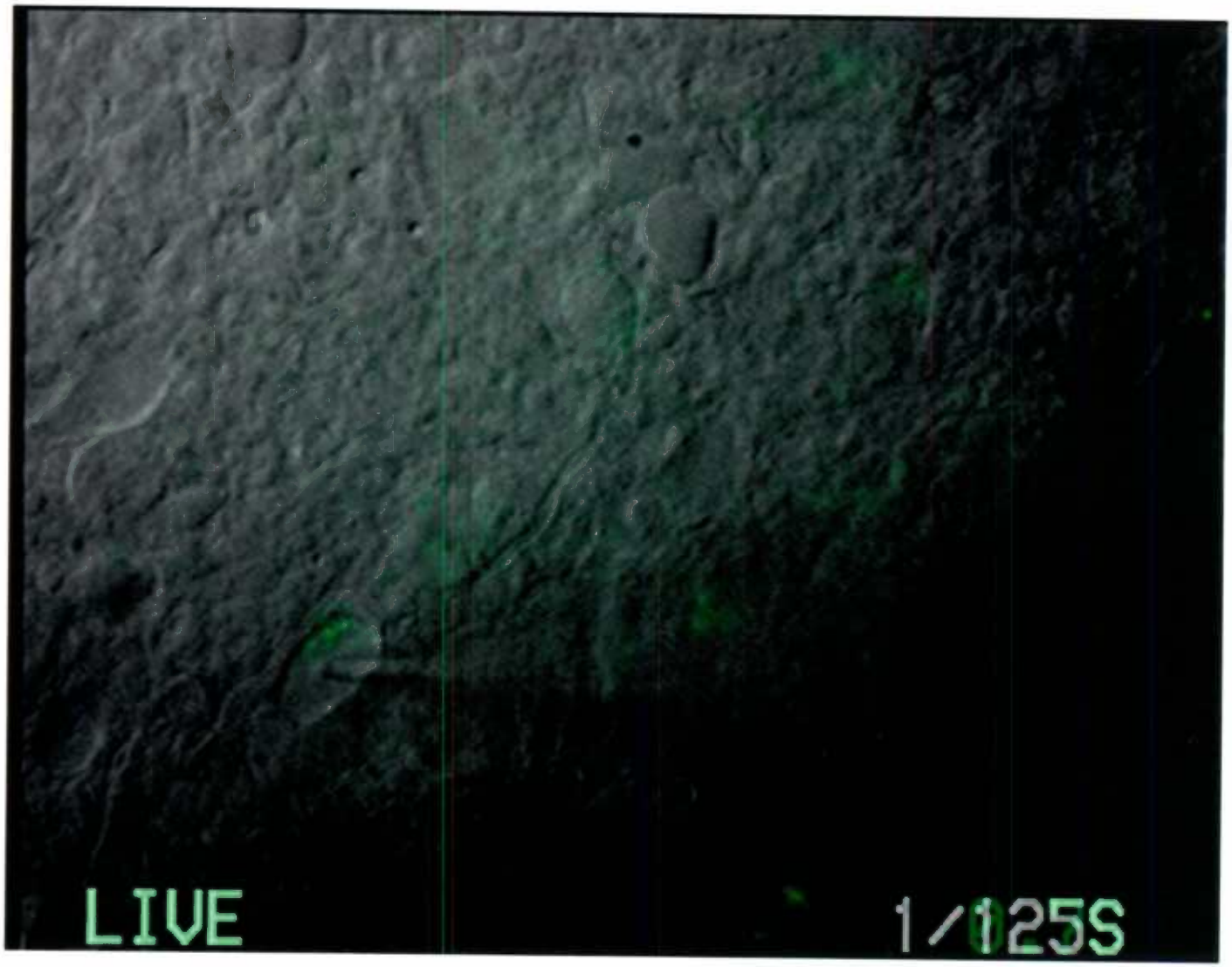
LIVE
1/125S

Figure 2-9 Synaptic responses to ST-stimulation of an anatomically identified neuron (see Figure 8 for image of recorded neuron). **A**: Single unaveraged traces of fast EPSCs evoked by ST when voltage clamped at -70 mV. Note the consistent and short latency (latency = 2.3 msec) and the low jitter (jitter = 61 µsec). Each ST shock evoked an EPSC (train of 5 pulses at 100 Hz, (•) = stimulus). No failures occurred in this example despite robust frequency dependent depression. **B**. Overlay of five successive EPSCs indicative of only small jitter in the latency across stimuli. Responses were completely blocked with the non-NMDA glutamate receptor antagonist NBQX. The NBQX trace is an average of 5 individual sweeps. Such low jitter glutamatergic EPSCs were found in all labeled neurons (see additional data in Figures 6 and 7). Thus, responses of anatomically identified second-order neurons suggest that while neurons monosynaptically activated by ST have low jitter, they can have remarkably high rates of failure and long latencies (see Figure 6).

Doyle and Andresen: Figure 9

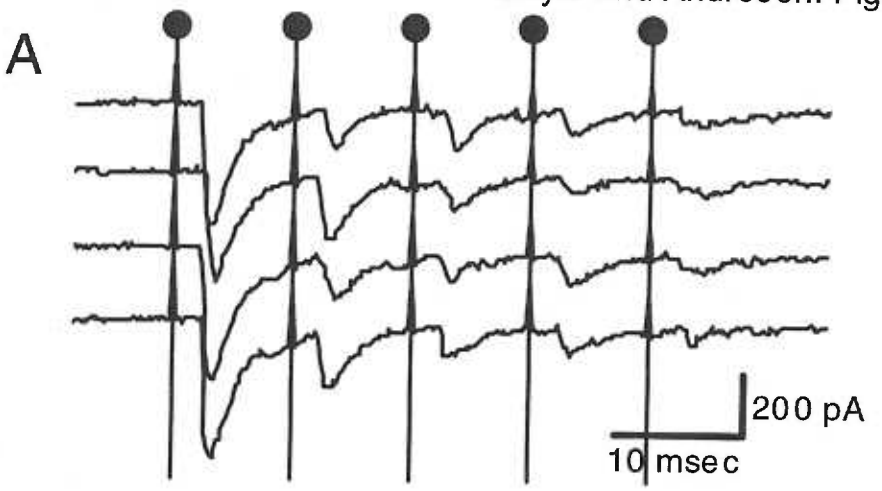

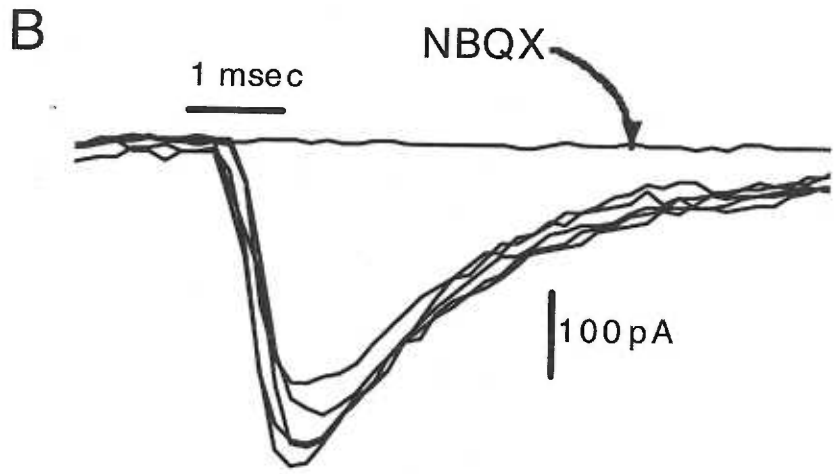

99312dlajtr

Our studies used three strategies to identify neurons in our slices: synaptic electrophysiology, antagonist pharmacology and dye labeling of second-order neurons. Comparing anatomically monosynaptic neurons to pharmacologically polysynaptic responses display characteristically different variation patterns to a series of ST shocks. The individual latency values for ST EPSCs in anatomically monosynaptic neurons were very narrowly and fairly symmetrically distributed around the mean latency value (**Figure 2-6B**). This was typical of low jitter, presumed monosynaptic EPSCs. In contrast, individual latency values for polysynaptic ST responses varied across a large range of latencies (several msecs) and the distributions could be quite asymmetrical (**Figure 2-6B**, open bars).

EPSC/IPSC sequences are common in NTS (Andresen and Yang 1990) and are often observed in response to ST-stimulation in this slice preparation (**Figure 2-10**). Such IPSCs follow the EPSC component (**Figure 2-10a**) and the IPSCs have an apparent latency of 4 to 6 msec from the ST stimulus. With this timing, a single shock to the ST evoked the IPSC beginning in the falling phase of the EPSC and as a result truncating the EPSC amplitude and time course (**Figure 2-10a**). Blocking the IPSC with bicuculline isolated the full characteristics of the EPSC (**Figure 2-10b**). In this example, the initial EPSC in the complex response was very reliable (1.52 msec latency; 28 μsec jitter) and had no observable failures at 200 Hz (Vm= -80 mV). However, during trains of ST shocks, at short interstimulus intervals, the long latency IPSC evoked by the first ST shock

coincided with the second, fast EPSC in the train (**Figure 2-10c**). This process continued through the train. Such a response appears as a failure of the EPSC and would be considered evidence for a polysynaptic pathway using the common criteria of paired pulses separated by 5 msec. In addition, note that even the polysynaptic IPSC in this example followed 200Hz stimulus trains (**Figure 2-10c,**arrows). Thus, simple two pulse paradigms separated by 5 msec were insufficient to consistently separate mono- from polysynaptic NTS responses.

Figure 2-10 In some medial NTS neurons, ST-stimulation evoked complex synaptic responses. **A.** ST-stimulation evoked a sequential EPSC/IPSC complex. The EPSC was of short latency (1.52 msec latency) and low jitter (28 μsec) consistent with reliability criteria for a monosynaptic response. No PSC failures were observed even at 200 Hz ST-stimulation. The long latency IPSC began before the full decay of the EPSC and therefore truncated its amplitude and time course due to the temporal overlap of the two synaptic events. The combined synaptic interactions (**panel A.**) were most evident at a holding potential of –40 mV that was displaced from the reversal potential for Cl. **B.** In the presence of the $GABA_A$ receptor antagonist bicuculline (100 μM), the full time course of the EPSC was evident at -70 mV. **C.** In control conditions near normal resting membrane potential (-60 mV), the long latency IPSC collided with subsequent evoked EPSCs in the train. Arrows have been placed at intervals of predicted onset of the IPSCs based on panel A. The result obliterated the net EPSC and mimicked a synaptic failure (no evident EPSC). In this example, the polysynaptic IPSC followed successive stimuli at 200 Hz ST-stimulation. Each trace is an average of 5 individual sweeps.

Doyle and Andresen: Figure 10

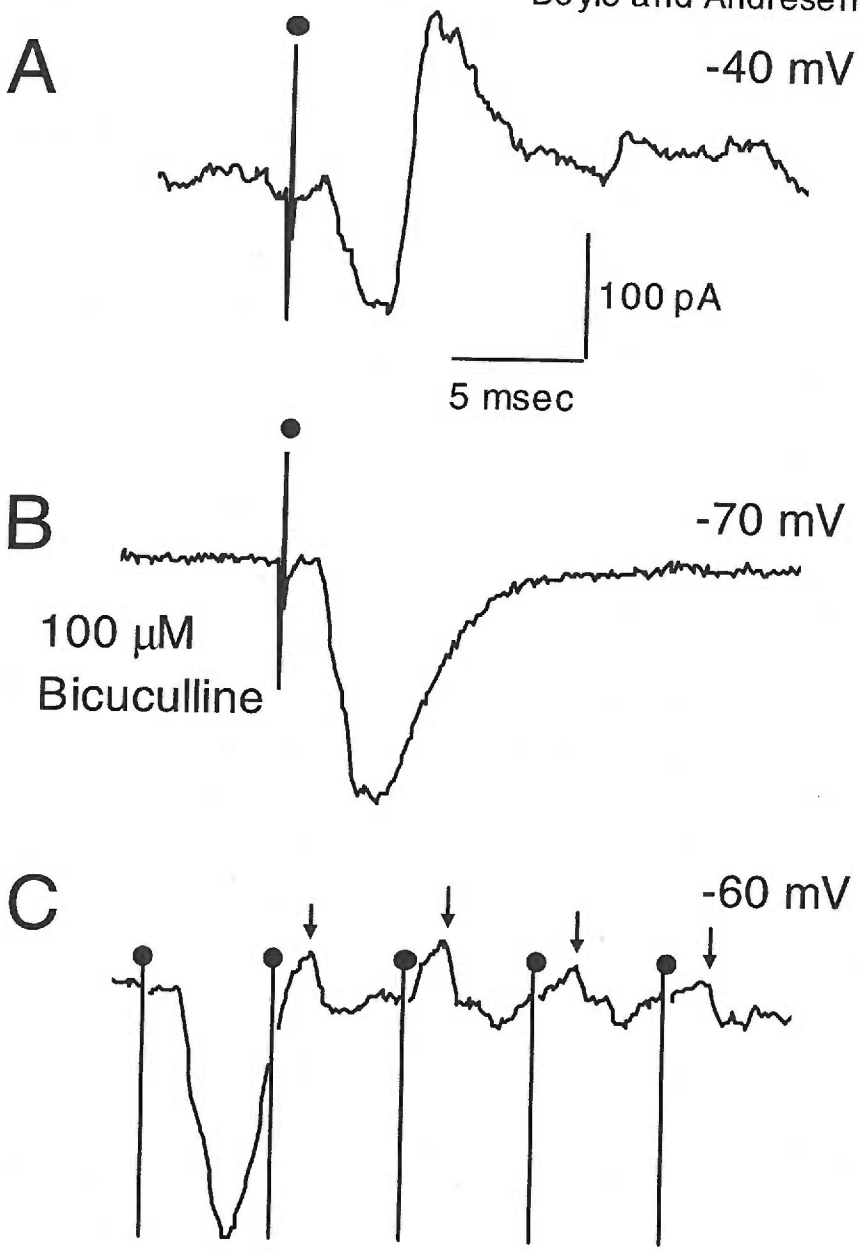

Discussion

To understand the mechanisms of information processing within a brain region, the nature of the pathway followed, i.e. the synaptic order, is critically important. In our study of medial NTS neurons, we sought to distinguish by electrophysiological means the responses mediated through monosynaptic pathways from those arising from polysynaptic pathways. We recorded synaptic currents evoked by ST-activation and used three measures of synaptic reliability including latency, jitter, and failure rate to determine whether these neurons received monosynaptic or higher order inputs from ST. We made the conventional assumption that as synaptic order increased, latencies would become longer for more complex, polysynaptic pathways. In addition, we assumed that the reproducibility of the precise timing of the synaptic responses would also decline with an increasingly complex pathway and result in an increase in synaptic jitter. Thirdly, we anticipated that monosynaptic responses would rarely fail, while more complex pathways (third order and higher) would fail more frequently.

Our fundamental measure of synaptic performance was latency. In medial NTS, the latency between the stimulus and the onset of the PSC varied considerably from neuron to neuron. The excitation pathway from stimulus to response involves multiple steps (Sabatini and Regehr 1999) and, among the mechanisms contributing to latency of the measured PSCs, time is required for: 1.

activation of the afferent nerve fiber, 2. conduction to the terminal site, 3. synaptic transmitter release, and 4. development of the postsynaptic response. Thus, in the simplest case, a monosynaptic response requires a single iteration of each of these processes and should require completion in minimum time for the shortest latencies. In the case of polysynaptic responses, all of these processes are repeated at other, higher order neurons in the pathway and should thus proportionately add to the observed absolute latency and should make such complex pathways inherently more variable. Thus, the PSCs arising from ST-activation through monosynaptic and polysynaptic pathways should display different frequency dependent characteristics related to pathway complexity.

To test the relation between latency and synaptic performance in NTS, we utilized a horizontal slice preparation of the brain stem. This slice orientation exposed the rostral-caudal course of the ST input pathway and an electrode was placed under visual guidance directly on ST relatively distant (1-3 mm) from the recording site in medial NTS. Such remote activation of the afferent pathway minimized confounding local activation of interneurons. Finally for comparison, we used a newly developed technique to record selectively from a group of anatomically identified second-order neurons. These neurons were identified by anterogradely transported DiA as having anatomically monosynaptic contacts from aortic baroreceptor afferents. Such identified neurons were considered positively identified, second-order NTS neurons of the baroreflex sensory pathway (Loewy 1990). Only one of our conventional assumptions was consistently upheld across

the data: jitter was minimal (<61 μsec) in all ST responses of anatomically identified second-order neurons and thus we conclude that variation in the synaptic latency from stimulus to stimulus within neurons is the best measure of pathway complexity. In contrast, the absolute latency values as well as the rates of failure ranged widely across all recorded neurons and were uncorrelated to the degree of jitter including that of neurons anatomically identified as second-order. Such results raise serious concerns about strategies based on dividing NTS neurons into putative mono- and polysynaptic groups by absolute latency alone, e.g. (Kasparov and Paton 1999; Andresen and Yang 1990).

Our electrophysiological analyses strongly depended on our measure of latency. Low resistance recording electrodes helped reduce electrical recording noise and voltage clamp reduced membrane potential influences. To improve the latency and jitter measurement, the derivative of individual data traces was used to improve the resolution of the rising edge in indicating the initiation point of the synaptic current. By relying on the leading edge of the synaptic current, our approach minimized potential influences of variations in amplitude or kinetic differences across individual synaptic traces that might add the variation if alternative aspects of the waveform such as 10% peak amplitude point were used.

The latency of monosynaptic PSCs includes synaptic delay and conduction time. Pre-synaptic processes involved in transmitter release and diffusion are estimated to be as short as 90 µsec at other fast mammalian synapses (Sabatini and Regehr 1999; Sabatini and Regehr 1996). In NTS, the latency between extracellularly recorded terminal action potentials and focal synaptic potentials was about 600 µsec (Berger and Averill 1983; Champagnat et al. 1985). These values for synaptic delays are quite short compared to our measured synaptic latencies. Contributing factors that might differ along pathways to medial NTS neurons may include myelination of varying degrees together with the loss of myelin that occurs as afferent fibers leave the ST (Kalia and Richter 1988). Indirect paths with multiple branch points could greatly slow the conduction time of the evoked action potential but these are poorly described for NTS. Dividing the latency by the distance between the stimulation and recording electrodes (roughly averaging 2 mm), a crude index of conduction was less than 2 m/sec – a conduction rate that would correspond to an unmyelinated axon in the peripheral nervous system. A true central conduction velocity along the presynaptic axon would be greater if these were corrected by the conduction delay time. Despite the short portion of the afferent paths preserved in our brain slice preparation, the range of absolute latencies was several fold even among anatomically identified second-order NTS neurons. Together, the data suggest that a major portion of the synaptic latency may reside in substantial differences in the afferent pathway character and length

for monosynaptic responses.

The location and density of synaptic innervation varies across regions of the central nervous system and importantly impacts synaptic integration (Thomson 2000). The presence of synaptic terminals from ADN on the soma and proximal dendrites of the second-order NTS neuron (Mendelowitz et al. 1992;Chan et al. 2000) are likely responsible for the very powerful sensory synaptic responses. Additional DiA staining might be located more distally but was undetectable with our approach. Nonetheless, the striking prominence of afferent baroreceptor terminals at the soma suggests that these synaptic inputs are likely to dominate synaptic integration near the axon hillock at the soma. Increases in ST stimulus current intensity evoked a non-graded, all-or-nothing synaptic current in our horizontal slice preparation (Andresen and Yang 1995). The tip face of the concentric stimulating electrode is quite large (50 μm diameter inner core) compared to the dimensions of either single afferent axons and, since it visibly covers a major portion of the ST, the tip should be in close proximity to multiple ST axons at the location of contact. Axon diversity in conduction velocity and myelination is pronounced in the vagus and ADN source nerve trunks (Andresen and Kunze 1994). We interpret this inability to grade either the amplitude or the number of synaptic events as evidence that, in general, single ST axons contact the recorded NTS neurons so that monosynaptic responses might be considered "unitary" (Titz and Keller 1997). This electrophysiological finding together with the

distribution of fluorescent-labeled ADN terminals into visually multiple clusters seems to indicate multiple innervation by single axons onto single neurons. This might explain the complexity of some apparently monosynaptic EPSC waveforms that appear to have clear multiple inflections or, in some cases, fully separated synaptic events that others and we have observed (Miles 1986) and yet cannot be independently recruited with stimulus intensity changes. In addition, if this conclusion is correct, it suggests that individual NTS neurons may directly receive only relatively discrete sensory inputs, i.e. afferent convergence at second-order medial NTS neurons may be rare.

This axosomatic input pattern is common at other sensory regions within the brain stem and contrasts with the spatial distribution and low unitary synaptic strength typical of many cortical regions (Conti and Weinberg 1999). Such brain stem synapses are at the initial stage of sensory processing and appear to be specialized for high efficacy with single action potentials releasing multiple vesicles (Conti and Weinberg 1999). This contrasts to the axospinous synapse pattern commonly found in cortical structures where the probability of release may be more restricted (Conti and Weinberg 1999;Thomson 2000). The brain stem sensory synaptic pattern commonly exhibits substantial frequency dependent depression of the degree that we observed in our NTS neurons and such release characteristics would be consistent with the surprisingly low failure rates within NTS (Thomson 2000). The result for throughput within NTS is a large synaptic safety factor especially for the initial EPSC (Andresen and Yang 1995).

Several factors, however, affect the observed amplitudes of synaptic responses and determine whether responses are propagated further within NTS. We observed both monosynaptic and polysynaptic currents in response to ST-activation in single or separate neurons. In our studies, some polysynaptic responses faithfully tracked input stimulation throughout even high frequency (200Hz) trains. Some neurons received monosynaptic EPSCs followed by IPSCs with a longer latency (4 to 6 msec) suggestive of a di-synaptic path for the IPSC. In such train responses, the late polysynaptic IPSC arrived in time to interrupt the subsequent EPSCs in these trains. Stimulating in the ST in horizontal slices, we never observed IPSCs that could not be blocked by non-NMDA glutamate receptor antagonists. This observation suggests that ST stimuli do not activate descending inhibitory fibers to NTS such as those from parabrachial nucleus (Felder and Mifflin 1988;Mifflin and Felder 1990). Combination EPSC/IPSC responses to sensory axon activation are commonly reported in NTS both in vivo as well as in vitro (Andresen and Mendelowitz 1996;Felder 1986; Feldman and Felder 1991; Brooks et al. 1992; Aylwin et al. 1997; Champagnat et al. 1985). Depending on the sensory input timing, an EPSC may be completely shunted by a following IPSC. These common, rapidly recurrent inhibitory inputs may thus confound detection of monosynaptic excitatory events especially in extracellular recordings since such local circuitry would powerfully mask afferent input responses.

The functional ramifications of frequency dependent depression in NTS are

substantial. Relatively modest stimulus frequencies substantially depress ST evoked synaptic responses (Andresen and Yang 1995; Champagnat et al. 1986). In some cases, depression to high frequencies (200 Hz) in NTS was great enough to induce failures within our short trains of stimuli by the third or fourth stimulus despite the fact that such neurons met anatomical and/or very low jitter criteria for a monosynaptic pathway. Frequencies that maximally release neurotransmitter stores could tend toward failure by depletion or strong drive to recurrent inhibitory neurons. This may explain the prominent failure rates in several of our dye identified second-order neurons. Such failures challenge the operating definition of monosynaptic events as distinguished by their ability to follow paired shocks separated by 5 msec (Miles 1986; Aylwin et al. 1997; Yoshimura and Jessell 1989; Gil et al. 1999; Zhang and Mifflin 2000; Deuchars et al. 2000). Our results suggest a potential pitfall of this paired pulse protocol, particularly in NTS. The likelihood is substantial that monosynaptic sensory NTS responses may be mistakenly classified as polysynaptic due to apparent failures that actually arise from either monosynaptic depression or disynaptic recurrent inhibitory interactions.

The chain of events required for synaptic transmission via a monosynaptic pathway must be repeated for polysynaptic circuits following generation of an action potential in the postsynaptic neurons. Any intrinsic variation in the timing of these mechanisms should increase the temporal variability (jitter) of higher order synaptic latencies. The triggering of the action potential by postsynaptic current may be a major source of variation at the 50-μsec-time scale and reflect variation

in the action potential threshold. Action potential threshold and synaptic amplitude are actively modulated by a variety of mechanisms including neurotransmitter actions. These add sources of variability to polysynaptic pathways and should substantially increase their response jitter. Conduction time in a single neuron is likely to be relatively invariant and thus should contribute little to variation in synaptic latency assessed within neurons by jitter. Also, unlike failures, inhibitory circuits should less affect jitter of PSCs evoked by infrequent stimuli. As predicted, jitter was greater in pharmacologically verified polysynaptic responses and low jitter EPSCs were pharmacologically distinct from high jitter EPSCs or IPSCs. Most importantly, the jitter of ST-evoked EPSCs in identified second-order neurons was very low despite a wide range of latencies and failure rates. As such, jitter appears most sensitive to the processes thought to contribute to intrinsic differences in synaptic performance with increasing pathway complexity and thus is the best indicative measure of synaptic order.

Functional Perspective Emerging evidence from brain stem sensory pathways suggest that these circuits may follow somewhat different principles of integration which determine synaptic performance compared to cortical models (Conti and Weinberg 1999;Thomson 2000). For example in auditory portions of the brain stem, sensory synapses are large and concentration on the soma and transmitter release probability at the calyx of Held is quite high and can approach 0.9 (Von Gersdorff et al. 1997). This contrasts to typical cortical models of integration in which synapses tend to be dendritic with relatively small individual

contributions and lower release probability; e.g. at hippocampal spiny interneurons release probability drops to as low as 0.01(Thomson et al. 1995). Depression and transmitter depletion are most often dominant performance characteristics of high release synapses (Thomson 2000). The NTS sensory synapse appears to follow the high release, somatic delivery model (Andresen and Yang 1995;Schild et al. 1995). The axosomatic location of baroreceptor sensory synapses (Mendelowitz et al. 1992) which allowed us to identify second-order neurons in NTS must impact the integrative properties of the sensory-NTS pathway differently than the dendritically weighted patterns found in cortical structures. This axosomatic model for NTS may represent a strategy for spatio-temporal integration which incorporates multiple specializations contributing to the high synaptic efficacy found at other brainstem sensory synapses (Trussell 1999). Functionally, this high probability of transmitter release may confer the high degree of rate dependent depression observed at these NTS sensory synapses. Functionally for baroreceptor afferents, this rate sensitive property could strongly contribute to the bidirectional rate sensitivity found with reflex responses to baroreceptor activation (Franz 1969;Jung and Katona 1990). Baroreceptors discharge substantially even under resting blood pressure conditions and in the discharge frequency range which produces substantial synaptic depression (Andresen and Kunze 1994). When blood pressure drops, the accompanying decrease in baroreceptor afferent discharge and thus in synaptic activation should release an ongoing synaptic depression and this process may contribute to the well known disproportionate reflex responses for increases compared to decreases in blood pressure. Such

performance characteristics may make modulation of depression by presynaptic mechanisms a particularly powerful site for overall autonomic reflex modulation by accessory, non-glutamatergic transmitters so common in NTS (Andresen and Kunze 1994).

Chapter 3

Vanilloid and P2X receptors selectively modulate pre-synaptic transmission of cranial visceral afferents

Mark W. Doyle, Jeong-Seop Rhee*, Shutaro Katsurabayashi*,
Norio Akaike* and Michael C. Andresen

Department of Physiology and Pharmacology
Oregon Health Sciences University
Portland, Oregon USA 97201-3098

*Department of Physiology
Faculty of Medicine
Kyushu University

Abstract

Vanilloid (VR1) and purinergic (P2X) receptor expression are commonly associated with unmyelinated spinal sensory neurons including nociceptors. Both have recently been reported in cranial visceral sensory neurons of nodose ganglion and at sensory synaptic terminations at the nucleus tractus solitarius (NTS). To test for functional VR1 and P2X receptors on afferent synapses, we recorded synaptic currents in medial NTS neurons in rat horizontal brainslices in response to electrical stimulation of the solitary tract (ST). ST shocks evoked excitatory synaptic currents (EPSCs) with short latency (mean ± SEM, 2.56±0.13 msec, n=20) and minimal jitter (55.8±23.1 μsec). ST EPSCs were completely blocked by the non-NMDA antagonist NBQX even in zero Mg^{++}. The VR1 selective agonist capsaicin (100 nM CAP) evoked an inward current and increased spontaneous synaptic events, both of which were prevented by NBQX. CAP current declined during prolonged exposure and ST evoked EPSCs were blocked after five minutes in CAP. The results are consistent with the presence of VR1 on presynaptic sensory terminals. Central terminals of aortic baroreceptors were labeled by placing DiA on the cervical aortic depressor nerve. In DiA labeled brainslices, anatomically second-order NTS neurons with fluorescent terminals on their cell bodies were identified and recorded with visualized patch recording. Identified neurons exhibited short latency, low jitter ST EPSCs that were completely blocked by NBQX or prolonged exposure to CAP. α, β methylene ATP

(αβ metATP), a selective agonist for P2X1 and P2X3 receptors evoked complex synaptic excitatory responses in identified neurons. To better discriminate pre- from postsynaptic mechanisms, individual neurons were mechanically dispersed from medial NTS without enzymes and attached synaptic boutons preserved. In the presence of TTX, spontaneous release of glutamate, glycine and GABA evoked miniature synaptic currents (mPSCs). Dispersed NTS neurons showed mixtures of mPSCs that were pharmacologically distinguished through selective antagonists as glutamatergic, GABAergic or glycinergic. αβ metATP evoked bursts of glutamatergic mEPSCs. Neither glycinergic nor GABAergic mIPSCs were altered. TNP-ATP (2', 3'-O-trinitrophenyl-ATP) reversibly blocked the αβ metATP effects. Likewise, CAP increased the frequency of mEPSCs in such neurons without altering their amplitudes. We conclude that presynaptic P2X and VR1 receptors selectively facilitate the release of glutamate onto medial NTS neurons. Thus, the VR1/P2X pairing is common across both spinal and cranial sensory neurons. These results raise the possibility that cranial visceral afferents may have an unrecognized capacity to sense organ tissue damage and trigger homeostatic regulatory responses that supplement pain perception via spinal visceral pathways.

Introduction

Information about the viscera enters the central nervous system (CNS) both through the spinal cord and through the brainstem. These two sources of sensory input give rise to a wide range of behaviors and reflexes. Although many aspects of the neurophysiological properties of cranial sensory neurons appear analogous to spinal sensory neurons, it is not clear whether common cellular and molecular mechanisms prevail (Lawson 1992). Much less is known about synaptic mechanisms arising from cranial visceral afferents than their spinal counterparts. Cranial afferents enter the brainstem to form the solitary tract (ST) before terminating at the nucleus tractus solitarius (NTS) (Loewy 1990). NTS terminations of cranial visceral afferents from the cardiovascular, respiratory and gastrointestinal systems constitute the first stage of neural circuits for regulation of these organ systems. As with dorsal root ganglion (DRG) neurons (Gu et al. 1996;Lawson 1992;Gu and MacDermott 1997), central terminals of ST afferents release glutamate (Andresen and Yang 1990).

One of the most prominent parallels between cranial or spinal afferents is the subclassification based on axon myelination – unmyelinated C-type and myelinated A-type afferents. In the spinal cord, some somatic and visceral afferent dorsal root ganglia (DRG) neurons with unmyelinated axons are associated with pain pathways. Recent attention in the pain literature has focused on the possibility that expression of a collection of several particular ion channels

might be nociceptor-specific. Thus, this ion channel group might provide the molecular mechanisms by which these nociceptors transduce tissue damage into sensory excitation (Caterina et al. 2000;Caterina and Julius 1999; Mantyh and Hunt 1998;McCleskey and Gold 1999;Snider and McMahon 1998;Wood 2000). Included in this group are vanilloid VR-1 receptors (Caterina et al. 1997) along with TTX-resistant sodium channels, and purinergic P2X3 receptors, (Cook and McCleskey 2000; Chen et al. 1998) all of which are found in DRG sensory neurons.

Nodose neurons express broad similarities of receptors and ion channels to this nociceptor-associated group of neurons. VR-1 (Helliwell et al. 1998;Tominaga et al. 1998; Mezey et al. 2000) and various purinergic receptor subunits including P2X3 (Thomas et al. 1998; Burnstock 2000) are expressed at cell bodies of the cranial visceral sensory neurons in the nodose ganglion and also appear to be anatomically present within the central synaptic fields of these sensory neurons in NTS (Guo et al. 1999). Here, we examined cranial afferent synaptic transmission at NTS. Our results demonstrate that both VR-1 and P2X receptors can selectively modulate glutamate release by highly specific presynaptic mechanisms. Overall, remarkable similarity exists between spinal vanilloid and purinergic receptor mechanisms and brainstem autonomic homeostatic regulation.

Materials and Methods

NTS slices Male Sprague-Dawley rats (150-350g, Charles River) were anesthetized with ether and rapidly killed by cervical dislocation. The hindbrain was removed and placed for one minute in cold (0-2° C) artificial cerebral spinal fluid composed of (mM): 125 NaCl, 3 KCl, 1.2 KH_2PO_4, 1.2 $MgSO_4$, 25 $NaHCO_3$, 10 dextrose, 2 $CaCl_2$, and bubbled with 95%O_2 / 5%CO_2. The medulla was trimmed to a 1 cm rostral-caudal block centered on the obex. A wedge of tissue was removed from the ventral surface so that 250 µm slices cut with a sapphire knife (Delaware Diamond Knives) mounted in a vibrating microtome (Leica VT-1000) contained the left ST in the same plane as the left NTS. Slices were submerged in a perfusion chamber at 34-37 °C; pH 7.4.

Visualized patch recordings. Neurons were visualized using a Zeiss Axioskop microscope equipped with fluorescence, differential interference contrast (DIC) optics (40x water immersion lens) and an infrared (IR) sensitive camera. Patch electrodes were guided using IR DIC microscopy to neurons that were voltage clamped in the whole cell configuration (Axopatch 200A). Recording electrodes (1.8 to 3.5 Mohm) were filled with an intracellular solution containing (in mM): 10 NaCl, 130 K Gluconate, 11 EGTA, 1 $CaCl_2$, 2 $MgCl_2$, 10 HEPES; pH 7.3; 295 mOsm. In some experiments (noted in the text), 130 K Gluconate in the internal

solution was replaced with 125 KCl (high internal Cl solution) in order to displace the chloride reversal potential away from the resting membrane potential. Data were filtered at 5 kHz and sampled at 10-20 kHz using p-Clamp7 software (Axon Instruments). Neurons were accepted for recording if they had an initial seal resistance greater than 1 GΩ and over the initial 10 minutes required no more than 100 pA to hold the neuron at -70 mV.

Stimuli were delivered by placing a 200-μM diameter concentric bipolar stimulating electrode (F. Haer) on the visible ST 1-3 mm from the site of the recorded neuron soma. Bursts of 5 ST stimuli every 4 or 5 seconds (stimulation duration 0.1 ms) at frequencies of 50, 100, or 200 Hz were generated with a Master-8 isolated programmable stimulator (A.M.P.I. Jerusalem, Israel). Neurons were rejected from further study if the evoked synaptic currents initiated fast sodium current at clamped potentials more negative than -40 mV indicating inadequate voltage control. All drugs were dissolved in 100 μL DMSO, diluted with external solution and bath applied. All studies reported here used maximally effective concentrations that were established in initial dose-response studies in NTS neurons for both agonists and antagonists. NBQX and bicuculine methobromide were purchased from Tocris-Cookson (Ballwin, MO) and all other drugs were purchased from Sigma (St. Louis, MO). Application of the highest concentration of vehicle used for dissolving drugs had no effect on neuron properties or synaptic responses (data not shown).

Labeling of the aortic depressor nerve. The aortic depressor nerve (ADN) is a peripheral sensory nerve that carries only arterial baroreceptor axons (Sapru et al. 1981). In 20 day old, pentobarbital anesthetized (50 mg/ kg) rats, the ADN was located and gently separated from surrounding tissue peripheral to where it joins the superior laryngeal nerve and enters the nodose ganglion(Mendelowitz et al. 1992). The nerve trunk was then placed within a pre-formed molded shell of dental impression compound (Coltene, Mahwah, NJ). The lipophilic fluorescent dye, DiA (Molecular Probes, Eugene, OR), was placed on ADN making sure that dye did not contact adjacent nerves and structures. To prevent dye migration, the ADN was then sealed in place by application of additional dental impression compound and allowed to cure in place. The anterograde label was allowed to travel for 2-3 months before sacrifice. Previous studies indicate that this procedure fills synaptic terminals belonging to aortic arch baroreceptors and these terminals are concentrated over cell bodies in medial portions of caudal NTS (Mendelowitz et al. 1992). The size and location of these dye labeled terminals are consistent with sensory terminals observed on these NTS neurons at the electron microscopic level (Drewe et al. 1988). For electrophysiological experiments, fluorescent ADN terminals within NTS were located visually with brief excitation wavelength exposures and then captured digitally using time integration intervals of 2 to 5 seconds. Fluorescent terminal images were then overlaid with real time IR DIC images using an ARGUS 20 image processor (Hammamatsu Bridgewater, NJ) to establish co-localization of fluorescence with the underlying neuron profile. The presence of fluorescent ADN sensory terminals coincident

with the neuron soma identified second-order neurons within NTS with anatomically monosynaptic connections and the synaptic responses to ST-activation were then studied in these neurons under voltage clamp. Sections containing the dorsal motor nucleus of vagus (DMN) were also examined as a control for dye contamination. The presence of intracellular, therefore retrograde, neuron labeling in DMN by DiA indicated that dye had migrated from the ADN site and contaminated the vagus nerve following implantation. NTS slices from these animals with numerous dye-positive DMN neurons were rejected from further study. Neurons with DiA positive terminal staining were considered anatomically second-order baroreceptor NTS neurons.

Derived synaptic parameters (latency, jitter and failure rate) were compared across groups using two sample t-tests (Snedecor and Cochran 1980) and groups were considered significantly different at p-values less than 0.05. In addition, correlations were tested as described in the Results using linear models with least squares fitting (Origin 6.1, OriginLab Corp.).

Mechanically dissociated neurons We dispersed medial NTS neurons in order to better isolate the pre- and post-synaptic mechanisms of vanilloid and purinergic receptor actions. For these studies, 10-14 day old Wistar rats (Kyudo, Japan) were decapitated under pentobarbital anesthesia. The brain was quickly removed and sliced to 400μm sections (DTK-1000, Dosaka, Kyoto, Japan). The brain slices were incubated with 95% O_2 and 5% CO_2 at room temperature (22-25 $^{\circ}C$) for at

least 1 hour. Slices were transferred into a culture dish and medial portions of the caudal NTS were identified under a stereomicroscope (SMZ-1, Nikon, Tokyo, Japan). A fire-polished glass pipette was placed lightly onto the surface of the slice at medial NTS. Pipettes were vibrated at 3-5Hz with 0.3-0.5 mm amplitude for about 2 min for optimal NTS dissociations (Rhee et al. 2000;Vorobjev 1991). Dispersed NTS neurons floated away and adhered to the bottom of the dish within 10 min (Koyama et al. 1999).

Such enzyme-free dissociations produced neurons that retained some of their original morphological features including the proximal dendritic processes. Miniature spontaneous synaptic currents were measured using nystatin perforated-patch electrodes under voltage-clamp (V_H = -60 mV; CEZ-2300, Nihon Kohden, Tokyo, Japan). Patch pipettes were pulled in two stages (PB-7, Narishige) from borosilicate capillary glass (1.5 mm o.d., 0.9 mm i.d.; G-1.5, Narishige, Tokyo, Japan). Electrodes were filled with internal solution (mM): 20 N-methyl-D-glucamine methanesulfonate, 20 Cs methanesulfonate, 5 $MgCl_2$, 100 CsCl, 10 HEPES; pH 7.2; 295 mOsm (5-7 MΩ). Nystatin was dissolved in acidified methanol at 10 mg/ml. All of these dispersed neuron experiments were performed at room temperature. Neurons were visualized under phase-contrast on an inverted microscope (Diaphot, Nikon). Measurements were monitored on both an oscilloscope and a pen recorder (Recti-Horiz 8K, Nippondenki San-ei, Tokyo, Japan). Data were stored on videotapes via pulse-coded modulation (PCM-501 ES, Sony). Membrane currents were filtered at 1 kHz (E-3201A Dicade Filter, NF

Electronic Instruments, Tokyo, Japan) and data were digitized at 4kHz using pClamp 8 and then analyzed using Mini Analysis software (Synaptosoft, Inc.). Miniature EPSCs and IPSCs were generally separated pharmacologically with selective antagonists (see Results). Miniature synaptic currents were detected by their uniformly fast rise times (≈ 1 msec). In some cases, it was possible to simultaneously record EPSCs and IPSCs together and kinetically separate events based on fitting time constant(s) of the current relaxations. GABA and glycine mediated IPSCs had two components to these relaxations and were clearly slower and more prolonged (see Results). Cumulative distributions of miniature synaptic current events were constructed and then compared using the Kolmogorov-Smirnov test for significant differences. In the case of mEPSCs, here we report only data from those neurons that responded to VR-1 and/or purinergic agonist. A statistically significant difference was assumed for p-values < 0.05. Numerical values are provided as mean ± standard error of the mean. Differences in mean amplitude and frequency were tested by paired two-tailed t-tests.

Monosynaptic Solitary Tract Responses. NTS is a diverse nucleus with dozens of potential neurotransmitters and widespread reciprocal connections with diverse brainstem and supramedullary nuclei (Andresen and Kunze 1994). In order to focus our tests for VR1 actions on brainstem sensory synapses, we isolated ST axons together with their terminations within NTS in horizontal brainstem slices from rat (Andresen and Yang 1990). This slice configuration (**Figure 3-1A**) permitted direct visualization of ST in the brainstem slices. We placed a concentric bipolar stimulating electrode on ST sensory afferent axons 1-3 mm away from the recorded NTS neurons. Recordings were focused on an area within NTS well known to receive dense sensory innervation from aortic baroreceptors (Mendelowitz et al. 1992), located just medial to the ST and within 200 µm rostral or caudal from the obex. Electrical shocks to ST evoked postsynaptic currents (PSC) with a range of temporal dynamics including those characteristic of both mono- and polysynaptic pathways (Doyle and Andresen 2001). The shortest latency PSCs were always excitatory (**Figure 3-1B**). Bursts of high frequency stimuli (100-200 Hz) consistently evoked EPSCs with minimal latency variation within neurons despite rapid and substantial frequency-dependent amplitude depression.

Figure 3-1 A. Orientation of the rat brain stem slices in the horizontal plane. Concentric bipolar stimulating electrode was placed on the solitary tract (ST) several mm from the recording region in NTS. **B.** ST-activation evoked monosynaptic EPSCs. Medial NTS neuron voltage clamped at -70 mV. In control, each ST shock (train of 5 pulses at 100 Hz) evoked a monosynaptic EPSC with high reliability (latency = 1.9 ms; jitter =38 μsec and no observable failures). Latency averaged over 50 trials. Synaptic jitter was expressed as the standard deviation of these trial latencies. Successive shocks evoked a frequency dependent depression of EPSC amplitude. 50 μM NBQX completely blocked EPSCs. Note that these recordings are from the neuron in Figure 3D inset with fluorescently labeled baroreceptor sensory terminals. **C.** ST evoked monosynaptic responses in nominally Mg^{++} -free solution. NBQX completely blocked this EPSC (latency =2.3 ms: jitter=46 μsec; no observable failures at 200 Hz ST-stimulation).

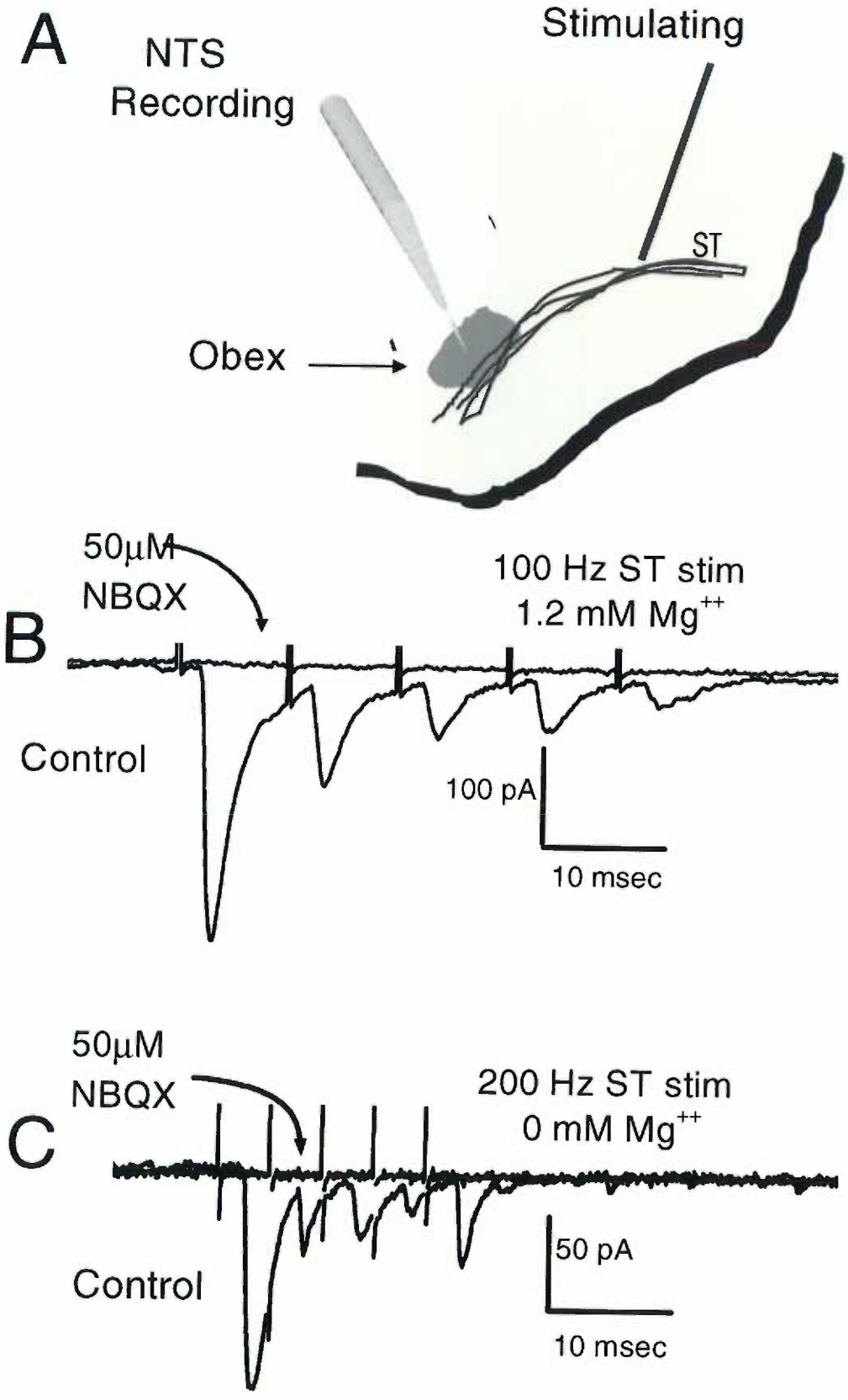
A
NTS
Recording
Stimulating
ST
Obex
B
50μM
NBQX
100 Hz ST stim
1.2 mM Mg++
Control
100 pA
10 msec
C
50μM
NBQX
200 Hz ST stim
0 mM Mg++
Control
50 pA
10 msec

We judged ST responses as monosynaptic based on a combination of three measures of synaptic reliability: 1) absolute latency; 2) synaptic jitter, the shock-to-shock variability in latency for a given neuron and; 3) the prevalence of synaptic failures at high stimulus frequencies. Such EPSCs had short (averaging 2.56±0.13 msec, n=20), nearly invariant latencies (jitter averaging 55.8±23.1 μsec; n=20) and few observable PSC failures.

The non-NMDA glutamate receptor antagonist NBQX completely blocked these monosynaptic responses (**Figure 3-1B,C**). At membrane potentials near rest, possible contributions to the synaptic current from NMDA receptors might be blocked by extracellular Mg^{++} (Nowak et al. 1984). To test this possibility, we also examined synaptic responses at depolarized potentials and with nominally zero bath Mg^{++}. NBQX fully blocked short latency EPSCs (n=12) even when recorded at quite depolarized potentials (+10mV, data not shown) with or without extracellular Mg^{++} (Figure 1C). Likewise, the NMDA receptor specific antagonist AP-5 failed to alter such EPSCs (n=9; data not shown and (Andresen and Yang 1990)). Unlike sensory transmission in the spinal dorsal horn where NMDA receptors contribute substantially (Cerne and Randic 1992; Sandkuhler et al. 1997), fast cranial visceral sensory transmission in NTS appears to rely primarily on non-NMDA glutamatergic receptors. It is possible that in our preparation electrical stimulation is only activating lightly mylenated, A- fiber sensory afferents

within the ST. A-fiber axons are more easily activated by electrical stimulation than the unmyelinated C-fibers. Due to the wide variety of synaptic responses evoked in NTS we feel that both A- and C-fiber axons within the ST were activated.

ST Evoked Polysynaptic Responses. We observed many longer latency responses whose temporal and pharmacological characteristics were quite varied. We assumed that these longest latency PSCs evoked by ST-activation likely arose after delays along polysynaptic pathways that began with activation of ST axons. Many synaptic events with longer ST latencies (>3 msec) were inhibitory PSCs (IPSC) in NTS (**Figure 3-2**). These IPSCs were blocked by the GABAa antagonist, bicuculline, and had reversal potentials close to the estimated chloride reversal potential. Similar IPSCs were reported from in vivo preparations in response to peripheral activation of cranial afferent nerve trunks (Mifflin and Felder 1990) and were polysynaptic. As a group, ST synaptic responses with latencies greater than 3 msec (mean latency= 5.15±1.35 msec; n=10) had nearly a four-fold greater synaptic jitter than the monosynaptic group (mean jitter= 204.6±106.8 μsec; n=10). In addition, numerous synaptic failures emerged in 6 out of these 10 neurons to short bursts of ST stimuli at 100 Hz (**Figure 3-2A, arrow**). Note that such long latency IPSCs could be blocked by either bicuculline (**Figure 3-2C**) and/or by NBQX (**Figure 3-2B**). This dual pharmacological pattern is consistent with a local circuit response (**Figure 3-2D**) in which ST-stimulation activated excitatory glutamatergic sensory afferent synapse onto second-order NTS neurons

which then lead serially to activation of the recorded GABAergic IPSCs – thus, minimally, a di-synaptic pathway.

Figure 3-2 A. Polysynaptic responses evoked by ST-stimulation had long latencies with high variability (latency = 5.3 msec; jitter = 260 μsec). This IPSC appears to be di-synaptic since it was blocked by either the non-NMDA antagonist NBQX (**B**) or the GABAa receptor antagonist bicuculline (**C**). This IPSC was reversed under our experimental conditions (Vm = -80mV, E_{Cl} = -20mV). Note the clear failure of synaptic transmission (**A**, arrow) during 50 Hz ST-stimulation. **D.** This local circuit must consist of an initial glutamatergic EPSC evoked by ST-stimulation (Mitsikostas et al. 1999). Activation of second-order neurons then would evoke a GABAa IPSC (bicuculline block) in the recorded neuron.

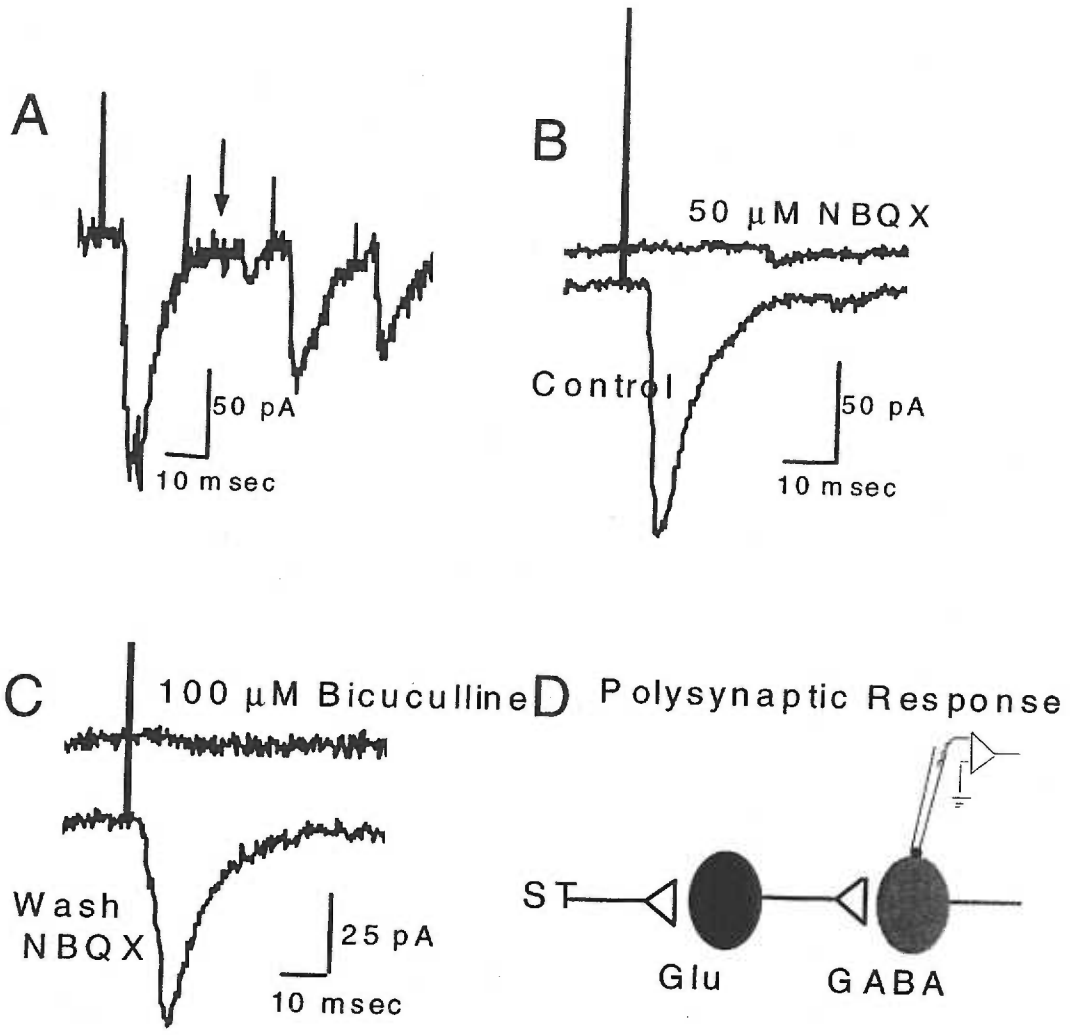
A
50 pA
10 msec
B
50 µM NBQX
Control
50 pA
10 msec
C
100 µM Bicuculline
Wash
NBQX
25 pA
10 msec
D
Polysynaptic Response
ST
Glu
GABA

Vanilloid Synaptic Modulation of ST Synaptic Responses. Recently anatomical evidence has localized VR-1 to the afferent limb of cranial pathways to autonomic regions of the brainstem. High affinity binding sites for two prominent VR-1 selective agonists, capsaicin (CAP) and resiniferotoxin, as well as immunocytochemical VR-1 labeling are prominent within caudal NTS (Mezey et al. 2000; Szallasi and Blumberg 1999). Since VR-1 is strongly associated with sensory neurons and VR-1 mRNA is present in nodose ganglion cell bodies (Michael and Priestley 1999), the NTS localization might represent VR-1 within presynaptic endings of cranial sensory neurons. In the aortic depressor nerve (ADN), CAP selectively blocked conduction of unmyelinated axons without blocking conduction in lightly myelinated fibers (Fan and Andresen 1998). Here, we tested whether CAP could selectively alter sensory synaptic transmission within NTS.

In neurons with EPSCs that met our reliability criteria for the monosynaptic ST profile, superfusion of brainstem slices with 100 nM CAP evoked two characteristic responses, both of which were transient in nature (**Figure 3-3**). First, CAP evoked a net inward current (Icap, **Figure 3-3A**) that rapidly developed to a peak (156 +/- 37 pA, n=8) over 15-30 seconds but then declined even in continued presence of CAP. Second, CAP evoked a rapid increase in spontaneous synaptic activity that developed simultaneously with Icap (**Figure 3-3B**, middle panel). As Icap

developed the observed amplitudes of ST evoked EPSCs became difficult to distinguish from the spontaneous synaptic events and after 1-2 minutes the evoked ST EPSC amplitudes decreased (**Figure 3-3A**). ST evoked EPSCs disappeared entirely and remained blocked after Icap had subsided in the continued presence of CAP (**Figure 3-3B**, right panel). Prolonged washing (>40 min) only very gradually reversed CAP blockade of ST synaptic transmission (**Figure 3-3D**, inset trace). Our results suggest that CAP evokes a large transient transmitter release.

Identified Second-order NTS Neurons. Among the wide spectrum of cranial visceral afferents (Andresen and Kunze 1994), arterial baroreceptors provide a unique opportunity to identify modality-specific neurons within NTS. Baroreceptors are mechanoreceptors signaling arterial blood pressure and their afferent axons comprise the aortic depressor nerve, ADN. The majority of ADN axons are unmyelinated and thus analogous in conduction velocity and many cellular properties to spinal C-fiber sensory neurons (Andresen et al. 1978; Kunze and Andresen 1991). To anatomically identify second-order NTS neurons, we prelabeled ADN with the anterograde tracer DiA. We then prepared brainslices from these animals, recorded selectively by patching such dye-positive neurons and tested whether capsaicin modulated synaptic transmission in these baroreceptive NTS neurons.

Fluorescent ADN terminal fields were visualized overlying NTS neurons (**Figure 3-3C, D** insets) and these neurons were selected for study. Using image overlays of

fluorescent baroreceptor label, we directed patch pipettes under IR DIC microscopy to record from these identified post-synaptic NTS neurons (**Figure 3-3C**, inset). Neurons deep within the slice often required lengthy times for integration of the fluorescent signal which yielded relatively diffuse patches of label (**Figure 3-3**). However, neurons less than 50 μm from the upper surface of the slice often showed discrete patterns of beads of fluorescence (**Figure 3-4C**). In all cases, fluorescence was confined primarily to the portions of the neuron soma or very proximal processes.

Figure 3-3 Capsaicin (CAP) actions on medial NTS neurons with monosynaptic EPSCs to ST-stimulation. **A.** Currents holding at -70 mV were small and steady during control. Application of 100nM CAP (bar) evoked a transient inward current, Icap, which subsided within 3 min. Measurements taken every 4 sec. **B.** Expanded time segments from **A** show that the train of EPSCs evoked by 5 ST shocks (•) were diminished at the peak of Icap (middle) when spontaneous synaptic activity increased. After 5 minutes in 100 nM CAP, Icap subsided and ST-stimulation no longer evoked synaptic responses (lower right trace). **C.** CAP response recorded in an mNTS neuron with anatomically identified sensory input. Fluorescent DiA labeling of aortic baroreceptor afferents (blue) was found primarily on cell bodies and confirmed directly that these neurons received sensory contacts. The image of ADN terminals (blue) was superimposed on the IR DIC image of this medial NTS neuron (inset). The outline of the neuron in the DIC focal plane is apparent with the associated fluorescently labeled terminals. CAP (100 nM, bar) evoked a transient inward current (Icap). Icap peaked in 1-2 minutes and subsided to control within 5 min in the continuing presence of CAP. **D.** The non-NMDA antagonist NBQX (50 μM) prevented Icap in a baroreceptor contacted medial NTS neuron. ST-evoked EPSCs in this neuron (see traces in Figure1a) also met electrophysiological reliability criteria as monosynaptic. NBQX blocked all ST evoked synaptic activity and prevented Icap in response to 100 nM CAP. Synaptic responses (lower right inset) returned following 60 min of perfusion in CAP-free, normal solution.

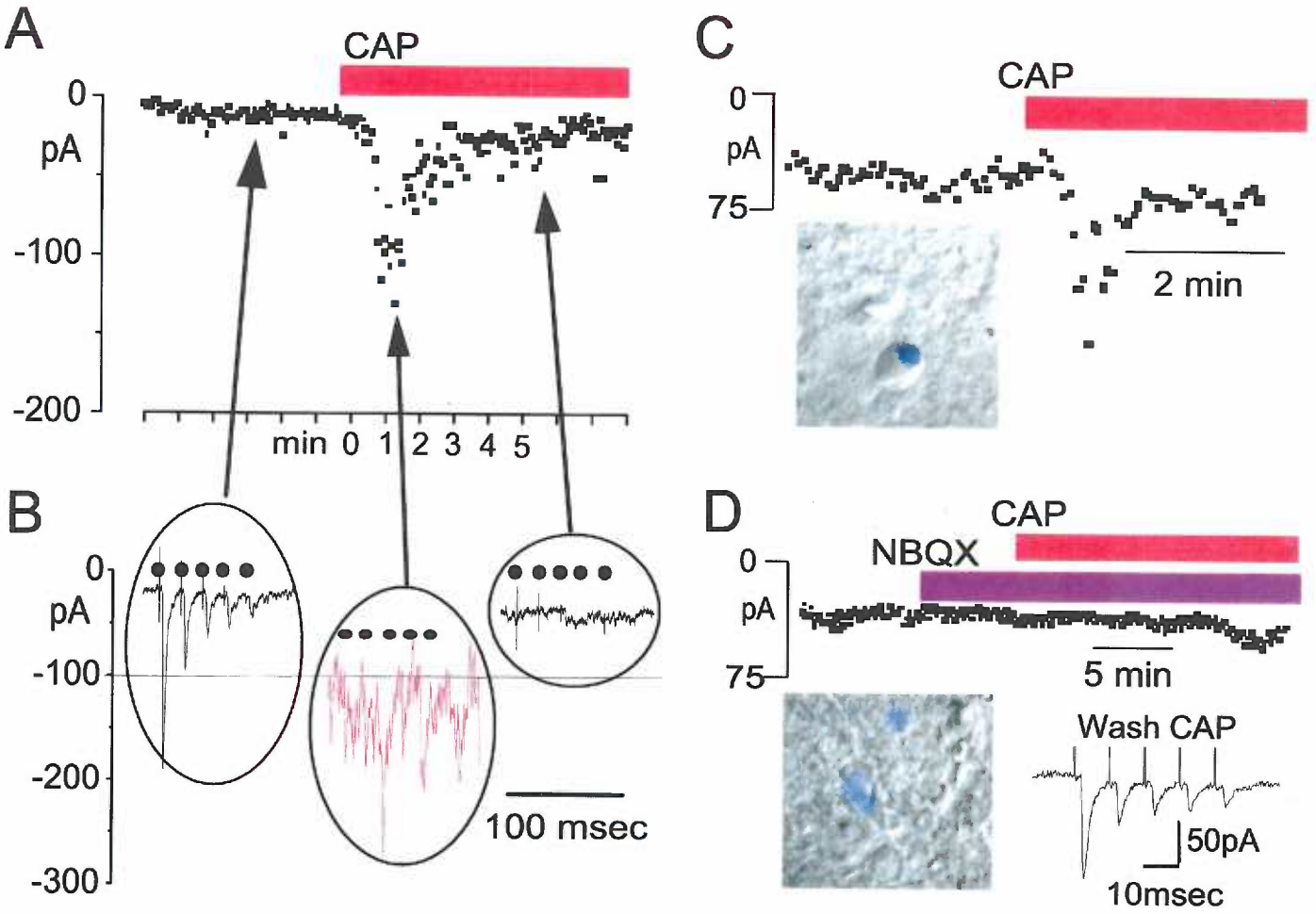
A
CAP
0
pA
-100
-200
min 0 1 2 3 4 5
B
0
pA
-100
-200
-300
100 msec
C
CAP
0
pA
75
2 min
D
CAP
NBQX
0
pA
75
5 min
Wash CAP
50pA
10msec

Typically, in neurons with tagged ADN terminals, ST-activation evoked a very short latency EPSC with minimal jitter and no failures even to bursts of ST shocks at stimulation frequencies as high as 100-200 Hz (**Figure 3-1B**). In such neurons (n=5), CAP induced a transient Icap comparable to other neurons receiving short latency ST evoked EPSCs (**Figure 3-3C**). Pre-treatment with NBQX blocked the monosynaptic ST EPSC (**Figure 3-1B**) and prevented Icap (**Figure 3-3D**). Thus, NTS neurons receiving ADN input showed ST responses similar to those characterized as monosynaptic to ST by electrophysiological criteria. The uniformity of results across labeled and unlabeled neurons suggests that sensory synaptic transmission in general in medial NTS is predominantly mediated by glutamate acting at non-NMDA receptors.

Presynaptic VR1 and P2X receptors modulate glutamate release. Although variable forms of multimeric P2X receptor gated channels have been recently described in nodose sensory neurons (Thomas et al. 1998), little is known about the function of such purinergic receptors. The P2X3 subunit in particular has been localized immunocytochemically to NTS processes (Llewellyn-Smith and Burnstock 1998) and was the predominant P2X subunit within the subpostremal region of NTS corresponding to our region of study (Yao et al. 2000). To test whether functional P2X receptors could modulate synaptic transmission in our

NTS slices, we recorded EPSCs with monosynaptic ST characteristics and applied α, β methylene ATP (αβ metATP), a relatively potent agonist for P2X1 and P2X3 receptors (North and Surprenant 2000). αβ metATP evoked complex changes in synaptic activity but did not alter the holding current. Spontaneous EPSCs increased in frequency (**Figure 3-4B**). Evoked EPSCs were recorded in NTS neurons identified as second-order baroreceptor neurons with DiA (**Figure 3-4c**). Jitter was characteristically low in control, however, during application of αβ metATP, EPSC failures in response to ST shocks and synaptic jitter increased. In addition, αβ metATP recruited ST-synchronized EPSCs at additional latencies suggesting activation of new, previously silent, synaptic pathways. Such complex response patterns to αβ metATP While such results appear consistent with a presynaptic action of αβ metATP on sensory axons, at least some of these new PSCs may have been recruited via indirect, polysynaptic pathways. Such mechanisms within the slice greatly complicate interpretation of the mechanisms of action of purinergic receptor activation. Thus, to better resolve the contributions of potential pre- and postsynaptic purinergic receptor actions, we turned to a simpler preparation. We dispersed neurons from medial NTS to study the properties of spontaneous miniature synaptic currents.

Figure 3-4 Application of αβ methylene ATP (100 μM, αβ metATP), increased the frequency of spontaneous as well as ST-evoked EPSCs in a medial NTS neuron recorded in a brainstem slice. Vertical artifacts mark ST stimuli delivered at 100 Hz for a burst of five pulses. DiA fluorescent terminals (digitally overlaid, panel C) ringed the soma visualized with IR-DIC in this slice. The presence of presynaptic label from aortic baroreceptors positively identified this neuron as a second-order NTS neuron. The shadow of the patch pipette enters from right to left in the micrograph.

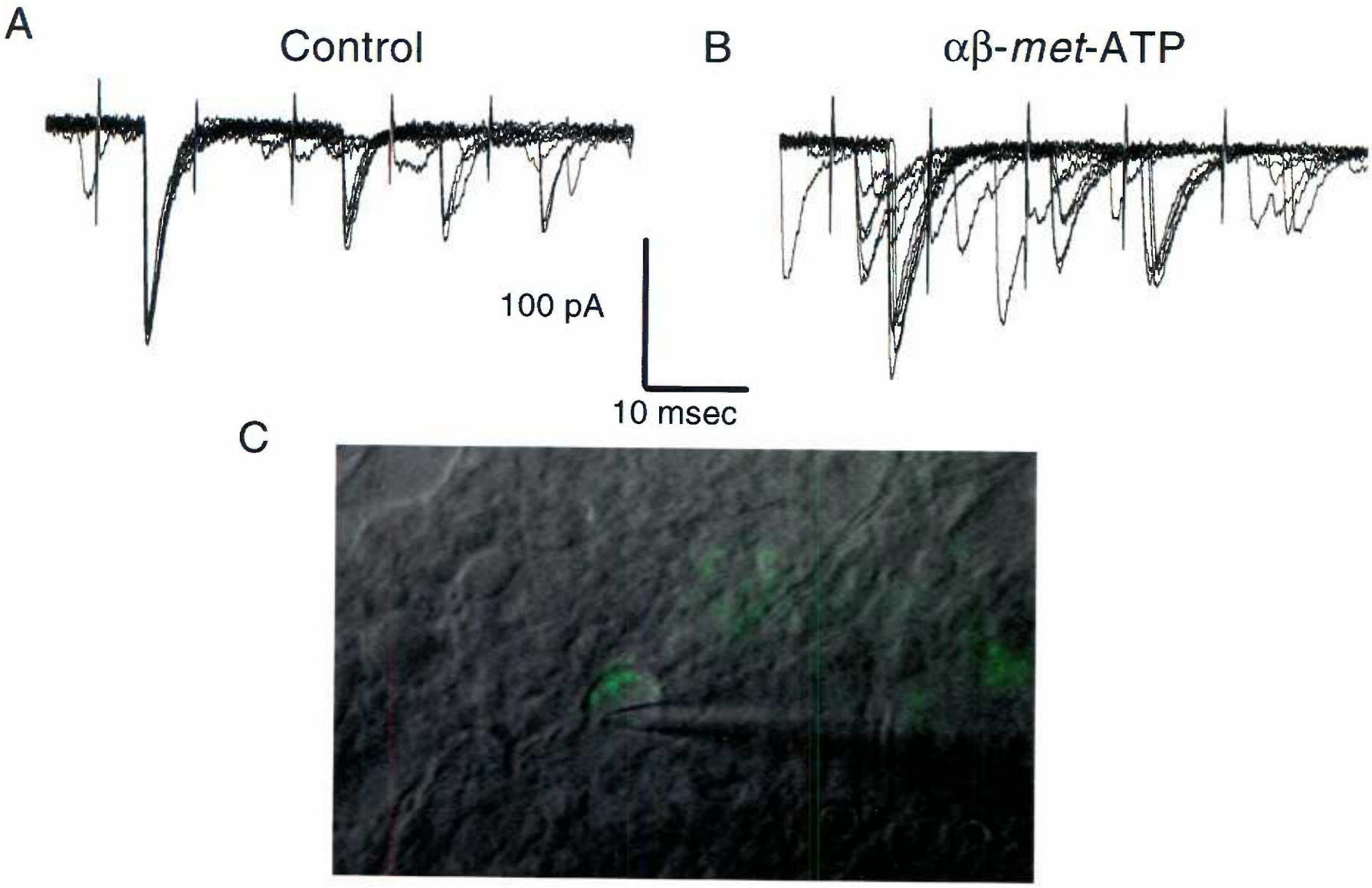
A
Control
B
αβ-*met*-ATP
100 pA
10 msec
C

By mechanically dispersing medial NTS neurons, we isolated neuron cell bodies with attached, functioning native synaptic terminals (Koyama et al. 1999). In the presence of TTX, we recorded spontaneous miniature postsynaptic events (mPSCs) to evaluate the pre-synaptic mechanisms modulating synaptic transmitter release (**Figure 3-5**). Similar to the mixed ST evoked synaptic responses observed in intact neurons in slices, dispersed NTS neurons often showed differing mixtures of mPSCs. Populations of spontaneous mPSCs were pharmacologically distinguished through selective antagonists as glutamatergic, GABAergic or glycinergic. These different responses could be additionally be identified kinetically since the IPSCs had prolonged decay phases compared to EPSCs (**Figure 3-5B**). In some cases, these different spontaneous mPSCs could be studied simultaneously within single neurons (**Figure 3-5A**).

Figure 3-5 Representative example of spontaneous miniature post-synaptic currents (mPSCs) recorded In 300 nM TTX in single, mechanically dispersed, medial NTS neurons (**A**). Two types of mPSCs were observed in this single medial NTS neuron (**B**). In the expanded records of **B**, mEPSCs (bold trace) had much more rapid kinetics and relaxation phases that were best fit with a single exponential decay. Most mIPSCs were much longer in duration and were best fit with two distinct exponential terms. mEPSCs were blocked by the non-NMDA antagonist CNQX and mIPSCs by bicuculline (3 μM) and/or strychnine (10 μM). In responsive neurons such as this one, αβ methylene ATP (100 μM, αβ met ATP) reversibly increased (bar, **A**) the mean frequency of the mEPSCs from 0.28 to 3.35 Hz but did not alter the mean frequency of mIPSCs (0.3, 0.39 and 0.4 Hz). Plots of cumulative distributions of the normalized inter-event intervals of mEPSCs for this experiment (**C, left**) were shifted to significantly (*, $p<0.05$) shorter intervals during αβ met ATP but returned to control following washing in normal solution. Cumulative distributions for mIPSCs (**C, right**) were unaffected by αβ met ATP. All neurons were held at V_H = -60mV. IPSCs were inward currents at these potentials due to the high internal Cl^- concentration in the pipette.

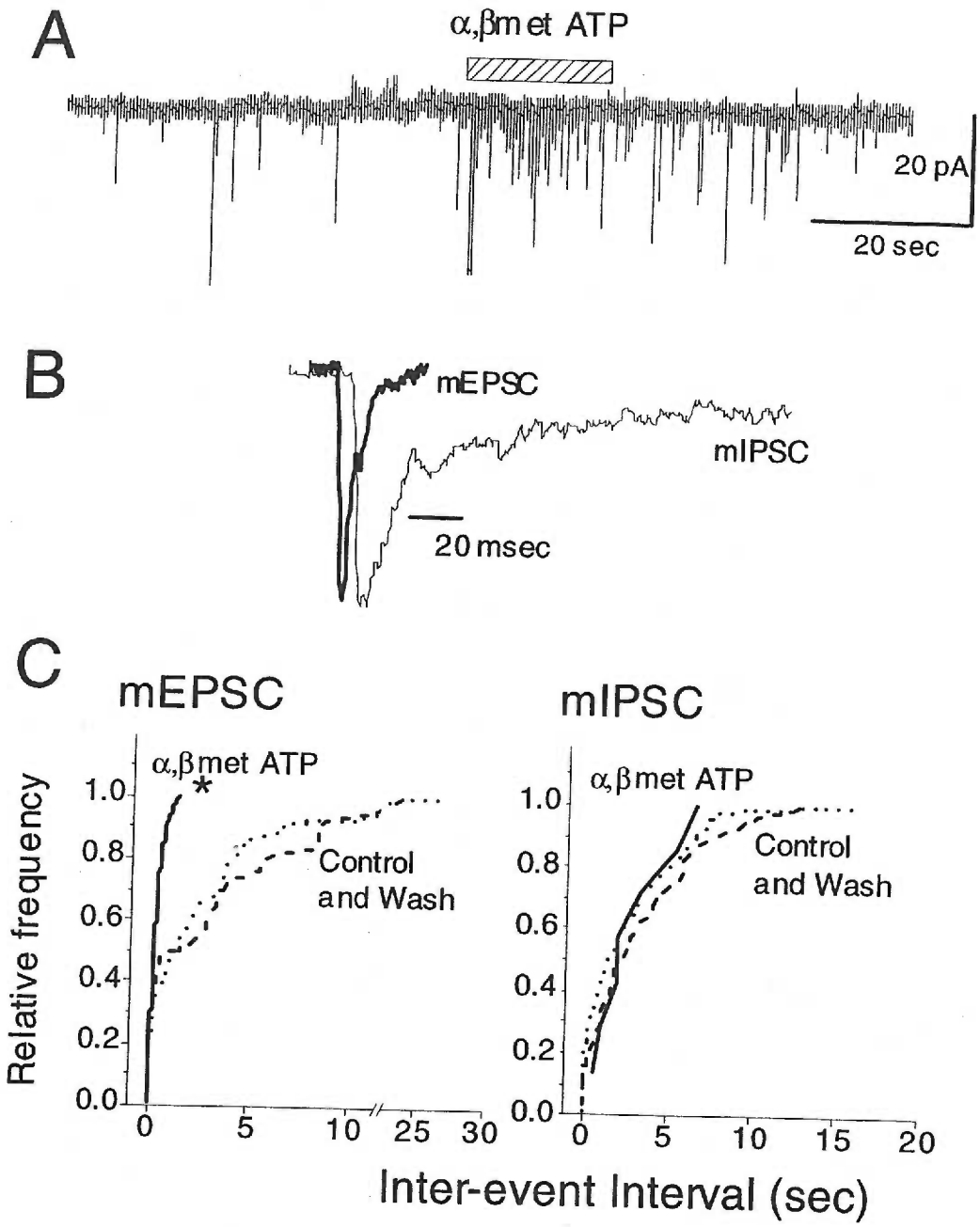
A
α,βmet ATP
20 pA
20 sec
B
mEPSC
mIPSC
20 msec
C
mEPSC
mIPSC
α,βmet ATP
Control
and Wash
Relative frequency
1.0
0.8
0.6
0.4
0.2
0.0
0
5
10
25
30
15
20
Inter-event Interval (sec)

In neurons with both glycinergic and glutamatergic spontaneous mPSCs (**Figure 3-5A**), brief application of αβ metATP evoked a burst of mPSCs that rapidly returned to control rates. Analysis of the distributions of the separate component mPSCs revealed that the frequency of glutamatergic spontaneous mEPSCs (**Figure 3-5C**) was increased without altering the glycinergic mIPSC frequency (**Figure 3-5C**). Pre-application of TNP-ATP (2', 3'-O-trinitrophenyl-ATP) reversibly blocked the αβ metATP effect on the frequency of glutamatergic mEPSCs (**Figure 3-6A**, upper panel, right, and middle panel left). Note that neither αβ metATP nor TNP-ATP evoked any sustained post-synaptic current. αβ metATP did not significantly alter the amplitude distributions and the mean event amplitudes for the glutamatergic (CNQX sensitive) and glycinergic (strychnine sensitive) mPSCs in this neuron (**Figure 3-5B**, lower panel). Note that αβ metATP–insensitive mEPSCs were also recorded in medial NTS neurons (data not shown). Together, these results suggest that many medial NTS neurons receive glutamatergic synaptic terminals that are selectively modulated by a purinergic pre-synaptic mechanism to increase the probability of glutamate release.

In other dispersed medial NTS neurons, CAP increased the frequency of mEPSCs without altering their amplitudes (**Figure 3-6B**). Such neurons were also sensitive to αβ metATP (**Figure 3-6B**). CAP did not alter the distribution of EPSC amplitudes or their mean in medial NTS neurons (**Figure 3-6B**, lower panel).

Again, our results are consistent with selective pre-synaptic mechanisms in which VR1 and P2X activation results in an increased probability of the release of glutamate. Thus, pre-synaptic P2X and VR1 receptors selectively facilitate the release of glutamate onto medial NTS neurons without apparent direct effects on the postsynaptic membrane.

Figure 3-6 In 300 nM TTX, mEPSCs were isolated pharmacologically in this dispersed, medial NTS neuron with 3 μM bicuculline. In a sequence of studies in this single neuron (**A**, **B**), the mean frequency of mEPSCs increased in response to αβ met ATP (0.12 vs. 3.48 Hz, **A**) and this response was blocked in the presence of 100 nM TNP-ATP (**A**, right). Washing restored the αβ met ATP response (**B**, left) and 100 nM CAP (**B**, right) then increased mEPSC frequency (0.12 vs. 5.8 Hz). In **C**, plots of cumulative distributions of the normalized inter-event intervals for this experiment demonstrate the shifts to shorter (*, $p<0.05$) mEPSC intervals (left). Amplitudes (lower right) show no significant changes from control for αβ-Met-ATP, αβ-Met-ATP+TNP-ATP and CAP. Mean frequency relative to control plotted as percent changes (right) was significantly (*, $p<0.05$) elevated by αβ-Met-ATP and CAP. All neurons were held at V_H = -60mV.

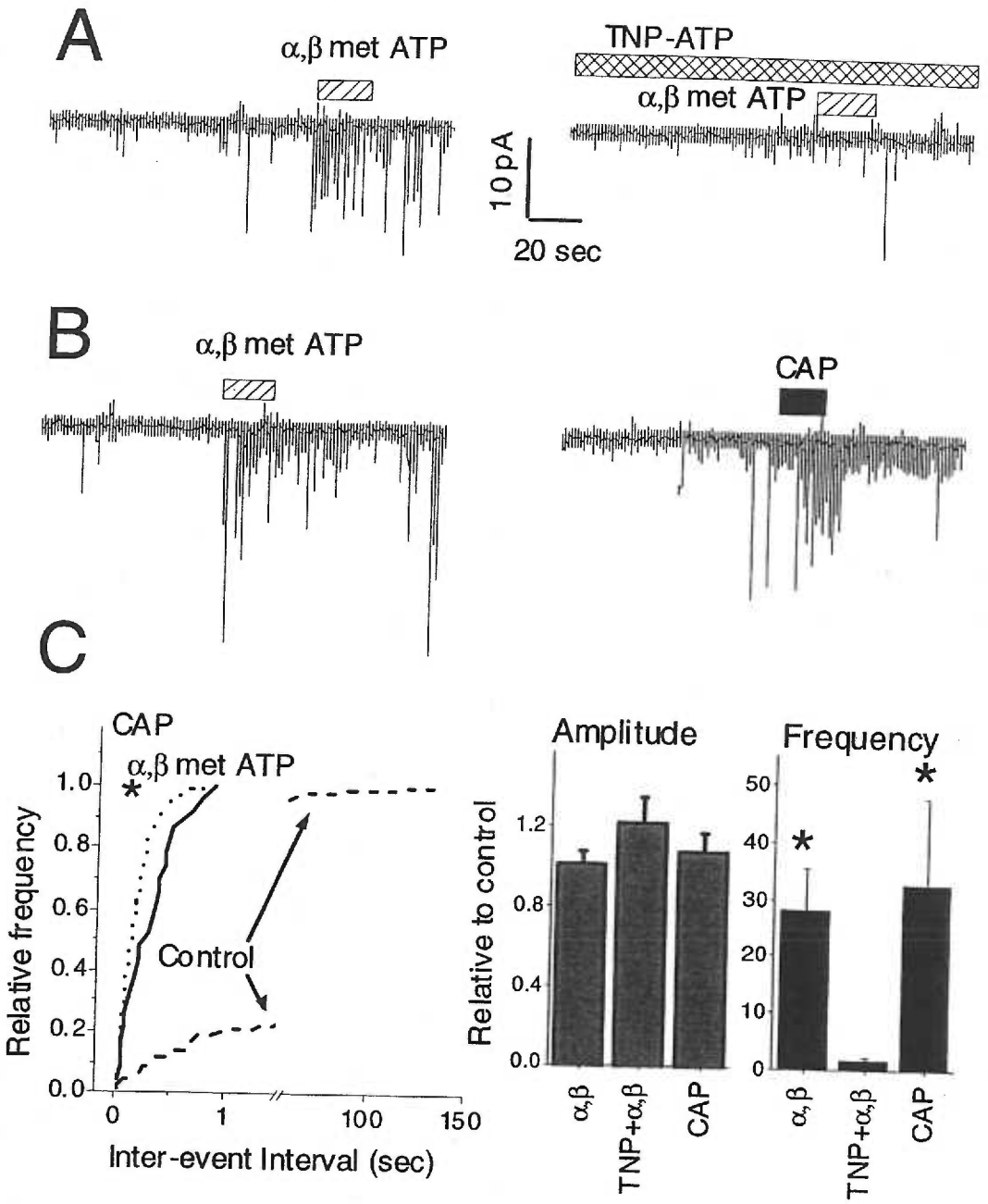
A
α,β met ATP
TNP-ATP
α,β met ATP
10 pA
20 sec
B
α,β met ATP
CAP
C
CAP
α,β met ATP
Control
Relative frequency
1.0
0.8
0.6
0.4
0.2
0.0
0
1
100
150
Inter-event Interval (sec)
Amplitude
Frequency
Relative to control
1.2
0.8
0.4
0.0
50
40
30
20
10
0
α,β
TNP+α,β
CAP
α,β
TNP+α,β
CAP

Discussion

The present studies demonstrate that presynaptic vanilloid and purinergic receptors modulate the release of glutamate at afferent synapses to NTS neurons. Our results are consistent with highly specific actions of such receptors on sensory terminals. Glutamatergic but neither glycinergic nor GABAergic transmission was altered. Glutamate is known to be the primary neurotransmitter of cranial visceral afferents (Andresen and Kunze 1994). Direct postsynaptic actions for either vanilloid or purinergic agonists were not detected. Both VR1 and P2X receptor mechanisms were found on NTS neurons that were anatomically identified as receiving fluorescently marked aortic baroreceptor terminals. Thus, both vanilloid and purinergic receptors are present at neurons involved in baroreflex autonomic pathways.

VR1 facilitates glutamate release in NTS VR1 expression is strongly associated with sensory neurons with slow conducting axons. In the present studies, activation of sensory axons within ST evoked short latency EPSCs that were exclusively mediated by non-NMDA receptors. The very low variance of synaptic jitter (<100 μsec) of such EPSCs appears to be a better index of monosynaptic connections to the ST than the value of the absolute latency itself. CAP activation of VR1 on such neurons released glutamate to activate non-NMDA receptors.

Interestingly, NMDA receptors were not activated by either ST-stimulation or by CAP in these second-order NTS neurons even in the absence of extracellular Mg^{++}. These results suggest that glutamate released from sensory terminals does not have access to NMDA receptors (Andresen and Yang 1990). Thus, unlike the spinal dorsal horn where NMDA receptors contribute substantially to sensory synaptic responses (Cerne and Randic 1992; Sandkuhler et al. 1997), fast cranial visceral sensory transmission in NTS relies primarily on non-NMDA glutamatergic receptors (Seagard et al. 1999; Zhang and Mifflin 1998a).

In the concentrations used, CAP had none of the so-called nonspecific effects attributed to CAP(Holzer 1991; Szallasi and Blumberg 1999). The identity of action and the occlusive interaction of CAP with electrically evoked synaptic currents indicate a common mechanism of glutamate release presumably by visceral sensory afferent terminals. The excitation induced by CAP in NTS likely also evoked indirect effects within the slice including activation of local circuits that feed back onto the second-order neuron. Thus, such indirectly activated synaptic activity may contribute to the observed current. The prolonged blockade of electrically evoked ST sensory transmission suggests that prolonged CAP produced either sustained presynaptic inactivation such as an inactivation of pre-synaptic voltage gated ion channels mediating neurotransmitter release and/or alternatively a depletion of readily releasable glutamate vesicles. Either mechanism might account for the disappearance of Icap during prolonged CAP

exposure and the long recovery time of ST evoked EPSCs after removal of CAP. In our isolated NTS neurons, CAP increased the frequency of spontaneous miniature synaptic glutamate responses. Consistent with CAP selectivity for sensory endings, CAP failed to modulate glycinergic miniature synaptic currents in these same isolated neurons. This transmitter selective modulation as well as the lack of other postsynaptic effects in these neurons supports CAP actions limited to presynaptic sensory afferent sites. Together, the slice and isolated NTS neuron results are consistent with VR1 localization at cranial visceral sensory presynaptic endings in a fashion comparable to spinal nociceptors.

P2X facilitates glutamate release in NTS ATP activates purinergic ligand-gated ion channels and the P2X3 subunits in particular are most heavily expressed in sensory neurons (Burnstock 2000). P2X3 is prominent in unmyelinated or lightly myelinated DRG neurons and linked to the nociceptor phenotype (Cook et al. 1998; Wood 2000). Recently however, structural studies have identified central P2X3 receptors within NTS (Guo et al. 1999; Llewellyn-Smith and Burnstock 1998) and, unlike the dorsal horn sites, these NTS terminals appeared to contain at the EM level both glutamate and peptide releasing vesicles (Llewellyn-Smith and Burnstock 1998). P2X3 mediated responses including calcium permeation were recently reported in nodose neurons (Thomas et al. 1998; Virginio et al. 1998).

Our present results demonstrate that, at the level of NTS, presynaptic

purinergic receptors modulate transmission of sensory inputs to brainstem pathways. A P2X1-P2X3 selective agonist and antagonists (North and Surprenant 2000) modulated only glutamatergic spontaneous miniature synaptic responses in our dispersed NTS neurons. The lack of postsynaptic effects and the selectivity for glutamatergic non-NMDA synaptic transmission over GABAergic or glycinergic synaptic mechanisms are consistent with a sensory afferent localization of the P2X receptor at these NTS neurons. Such pre-synaptic mechanisms are likely responsible for the depressor reflex responses to microinjection of αβ metATP into medial NTS and the impairment of baroreflex responses by P2X receptor antagonists (Scislo et al. 1998). Activation of ionotropic glutamate receptors is required for the αβ metATP effects within NTS (Scislo and O'Leary 2000). Given the evidence of P2X2 and P2X3 subunits in nodose sensory neurons (Vulchanova et al. 1997;Yao et al. 2000) and their presynaptic fields in NTS , it is highly likely that receptors including the P2X3 subunit are responsible. Again, the modulation of glutamate release by P2X3 receptors in NTS appears similar to that reported in the dorsal horn (Gu and MacDermott 1997). Our αβ metATP responses were well sustained for 20-30 seconds and showed no evidence of the rapid and complete desensitization of homomeric P2X3 receptors. This kinetic evidence argues for the likely participation of the non- or slowly desensitizing heteromeric P2X2/3 receptors described in nodose neurons (Virginio et al. 1998).

Cranial compared to spinal sensory integration. The molecular, cellular and

systems mechanisms engaged by somatic, primary sensory neurons of the spinal cord are known in considerable detail (Hudspeth and Tanaka 1998). Comparable detail for cranial visceral afferents is generally unavailable. Despite clear global similarities, cranial sensory neurons arising from the viscera are often considered different from spinal afferent DRG neurons (Saper 2000). Cranial visceral afferents certainly inform a very different complement of reflexes ranging from autonomic, hormonal to homeostatic central regulatory. Like spinal afferents, cranial afferents contain a large proportion of neurons with unmyelinated axons (Douglas and Ritchie 1962). These cranial sensory neurons share morphological and immunohistochemical features found in DRG neurons (Lawson 1992). Specific voltage and ligand operated ion channels are differentially identified with C-type spinal sensory neurons (Wood 2000) and similar patterns exist in the cranial afferent nodose neurons. Characteristically variable expression of TTX resistant Na^+ channels is found in DRG (Waxman et al. 1999) and nodose neurons (Schild and Kunze 1997). Peptide neurotransmitters are more closely associated with the C-type class of nodose neurons (Undem and Weinreich 1993). Thus, a common cellular vocabulary in the neurobiology of sensory neurons across a broad spectrum is expressed in cranial visceral afferents. Our present studies suggest that VR1 and P2X are powerful modulators of glutamate release from cranial visceral afferents. Interestingly, this pairing resembles that found in spinal pain transduction neurons (Caterina and Julius 1999; McCleskey and Gold 1999; Wood 2000) where P2X3 receptors are thought to have a specialized role in

nociceptors for sensing tissue damage (Wood 2000). Clearly, our results and those of others working in the brainstem suggest a broader context of purinergic actions.

Cranial afferent perspective of tissue damage transduction Conventional nociceptive pathways originate from afferents in somatic nerves as well as visceral afferents traveling in sympathetic nerves, both of which enter the dorsal horn (Foreman 1999; Willis, Jr. 1995) Visceral organs commonly have dual sensory innervation via both cranial and spinal pathways (Foreman 2000). All cranial visceral afferents project to NTS and tracing studies indicate that some spinal dorsal horn neurons also project to NTS (Menetrey and Basbaum 1987), although the nature and function of such a spinal-NTS pathway is uncertain (Saper 2000). Electrical activation of cranial visceral afferents of the vagus nerve variously increases or decreases pain thresholds depending on experimental circumstances (Foreman 2000; Janig et al. 2000; Randich et al. 1990) Some of the variable nature of this cranial visceral afferent interaction with pain pathways could well reflect differential involvement by specific afferent subpopulations perhaps from different organs that is masked by relatively nonspecific activation such as during electrical stimulation (Janig et al. 2000;Janig and Habler 2000).

Our studies clearly document the functional presence in NTS of VR1 and P2X receptors on individual neurons. Co- localization of VR-1 and p2X3 receptors

has been associated with nociceptors (Caterina and Julius 1999; Burnstock 2000). Most of our NTS neurons activated by ST electrical stimuli received unknown modalities of sensory input. In some of our studies, however, we identified inputs from arterial baroreceptors and such sensory neurons are clearly mechanotransducers whose reflex actions are focused on cardiovascular regulation (Kunze and Andresen 1991). This raises the possibility that the VR-1 /P2X3 pairing is associated with baroreflex function. In addition the presence of VR-1 and p2X3 receptors on baroreflex afferents may point to a broader role in monitoring tissue integrity.

Saper (Saper 2000) recently argued that perhaps the most fundamental sensory modality is the transduction of tissue integrity and that this is, above all, the most visceral of all sensory modalities. The traditional classification of cutaneous pain with somatic sensations that transduce representations of our interactions with the outside world may thus distract from an appreciation that transduction of tissue damage may well be the most universal sensory modality. Our findings certainly support this broad view at a cellular level and the idea that the VR1/P2X marker may be more general than pain transduction. The functional ramifications of the VR1/P2X complex within sensory afferent neurons not associated with pain are not clear. If function is analogous to DRG neurons in these cranial visceral afferents, then this receptor complex might convey a previously unappreciated modality of transduction by these neurons - tissue integrity.

Chapter 4

DISCUSSION

Nucleus Tractus Solitarius (NTS)

The modulation of the baroreceptor reflex and other homeostatic reflexes begins with the afferent inputs to NTS. All cardiovascular autonomic nervous system control is strongly influenced by the processing that takes place at the first NTS synapse. The sensory signal through NTS also provides information to other subsequent brainstem nuclei that contribute to multiple autonomic motor outputs. Sensory signals traveling through these autonomic centers are modulated by additional inputs that alter overall autonomic output (Andresen and Kunze 1994). Many of these modulatory inputs (e.g. hypothalamic) act at the level of NTS. Since the primary afferent input to NTS is common to the varied outputs of the autonomic nervous system, this first sensory synapse and the nature of the second-order NTS neuron is the first site for potential modulation of visceral reflex performance.

Synaptic mechanisms within NTS

It is likely that both presynaptic and postsynaptic mechanisms at the first synapse contribute to this modulation. One possible target for altering the strength of the first synapse is presynaptic modulation of the transmitter released evoked by each action potential in the central sensory terminal. Postsynaptically, the excitability of

the second-order neuron depends on the activity of postsynaptic ion channels and this can be strengthened or inhibited by neurotransmitter actions. The excitability of the second-order neurons is critical in translating impinging synaptic events into subsequent action potentials. Thus, hyperpolarizing the postsynaptic neuron would necessitate a larger EPSP to bring the second-order neurons' membrane potential to action potential threshold. Opening postsynaptic ion channels changes overall membrane conductance and may also decrease postsynaptic membrane excitability. Therefore, a larger synaptic current is required to change the membrane potential in the presence of a lower postsynaptic membrane resistance. Transmitters and modulators that activate or inhibit postsynaptic ion channels may alter throughput of sensory information by altering postsynaptic membrane excitability. Modulation of the primary synapse by various neurotransmitters and neuromodulators may contribute to the large variety of responses across neurons observed with ST-stimulation.

In my studies of NTS, I have been impressed by the spectrum of responses evoked in medial NTS neurons following activation of ST axons. The mechanisms underlying such response variation reflect several key aspects of the sensory processing in NTS itself. NTS, in general, is a highly heterogeneous nucleus with many subdivisions based part on regions of different sensory inputs as well as neuron morphology (Loewy 1990). In addition, higher order sources of inputs to NTS arise from neurons within brainstem and supramedullary areas and likely

have varied contributions. Even within the sensory class of inputs to NTS, major differences exist across afferents from visceral organs with respect to neurotransmitters as well as the second-order neurons themselves. Very little detail is known about the nature or impact of these differences on the fundamental processes of synaptic integration. Given the potential for heterogeneity, I developed experimental strategies to identify and study the primary sensory synapse and the second-order neuron.

Identification of the primary baroreceptor synapse

Surveying horizontally oriented slices of the brainstem, the cell bodies within NTS are gathered together in clusters and the clusters are separated by proportionally large areas of fibers (**Fig 4-1**). How these clusters of neurons are connected or interconnected to each other and the pattern of their innervation by inputs originating outside of NTS may clearly impact the function of the nucleus. Preliminary data suggests that some of these neurons are directly connected through gap junctions (personal communication with Mike Andresen and Tim Bailey). By fluorescently labeling the sensory endings, we anatomically identified a subset as second-order neurons that received aortic baroreceptor synapses. In general, labeled puncta apposed only some of the cell bodies in these clusters of neurons. This raises the possibility that only a minority of even adjacent neurons are directly connected to particular sensory afferents. This might reflect the overlap of sensory modalities suggested in other studies (Loewy 1990). However,

little is known about the efficiency of dye labeling (work in progress with Dr. Sue Aicher) so that other factors could contribute and such conclusions are tentative. This primary synapse was the target of my investigation. However, multiple types of synaptic events are often evoked in these identified cells and not all of these synaptic responses are monosynaptic. Thus, a major goal of my work was to identify the monosynaptic EPSC evoked from ST-stimulation and to distinguish it from polysynaptic PSCs evoked indirectly from ST-activation through a pathway with multiple serial synapses.

Pathway complexity and synaptic variability

Many visceral sensory afferents to NTS fire bursts of action potentials during activation. The changes in synaptic responses from one stimulus to the next provide temporal information that is directly dependent on synaptic order and define the dynamic characteristics of synaptic transmission along its pathway (Ferster, D., Spruston, N. 1995). Latency and amplitude are two key measures of synaptic responses. Complex pathways give rise to polysynaptic PSCs that have the added stimulus evoked response variability in latency from at least two synaptic processes. With pathways evoked by ST-activation, the pre-synaptic mechanisms at the sensory terminal are responsible for transmitter release and this mechanism is common to both mono- and polysynaptic events. In addition however, along the polysynaptic path, the excitatory PSP must be sufficiently strong to bring the postsynaptic membrane to threshold in order to initiate an action potential. The action potential is necessary in order to successfully transmit the signal through the pathway of serial synaptic connections and may be evoked at different times along the rise time of the EPSP.

Several mechanisms affect spike initiation in the post-synaptic neuron. The location of the post-synaptic receptor relative to the spike initiation zone of the axon can greatly influence the temporal character and strength of the PSP due to dendritic filtering (Jonas and Spruston 1994). This may be less of a factor in many medial NTS neurons given that dye labeled axo-somatic connections appear to be

characteristic of the primary sensory synapse. However, other synaptic configurations including dendritic connections are possible, and likely, especially along serial polysynaptic pathways. Dendritic filtering slows the rise time of the PSP. Spike initiation, thus, can be delayed if PSP depolarization is slowed. Rapid depolarizations are much more effective at the fast sodium currents underlying the action potential. Since an action potential may occur at different time points along an EPSP depending on its kinetics, this may importantly contribute to the increased jitter observed in downstream synaptic events (Andresen and Yang 1990). This transformation of excitatory synaptic input into spike initiation is further modulated by the activity of other postsynaptic channels that contribute to cell excitability and in turn can be modulated by membrane potential and the various neurotransmitters found in NTS. Dynamic modulation of the excitability of the NTS neurons may contribute as well added jitter in polysynaptic responses beyond that present in monosynaptic events. Jitter by virtue of its measure of synaptic response variability seems a superior indicator for assessing synaptic order.

Glutamate at the primary afferent synapse.

Many principal features of the monosynaptic responses in NTS to ST-activation parallel those of sensory processing in the dorsal horn of the spinal cord. Like the spinal cord, glutamate appears to be the primary neurotransmitter. Both myelinated and unmyelinated sensory terminals appear to release glutamate that act on ionotropic receptors postsynaptically (Sved and Curtis 1993). One key

difference may be the identity of those postsynaptic glutamate receptors, since unlike somatic sensory processing; glutamate in NTS appears to act almost exclusively at non-NMDA receptors for the basic synaptic event (Andresen and Yang 1990). The most compelling evidence for this is the lack of a postsynaptic response to glutamate release in the presence of selective non-NMDA receptor antagonists. This dominance of non-NMDA receptors was found in NTS even under conditions that exaggerated a potential contribution of NMDA receptors - the absence of extracellular magnesium and recording at depolarized potentials. NMDA receptor antagonists were ineffective on ST activated monosynaptic EPSCs. Furthermore, even chemical activation of sensory terminals with CAP failed to activate NMDA receptors. Together, these data in NTS suggest that glutamate released by sensory terminals does not have access to NMDA receptors on the postsynaptic second-order neurons. Clearly, additional sites of action for glutamate were not assessed in my studies and these could include important actions by metabotropic glutamate receptors and/or modulation of release from other synapses on these second-order postsynaptic neurons.

Labeling the primary afferent terminal.

Labeling the aortic depressor nerve terminals provided two important advances in the brain slice approach. First, the labeling technique allowed me to visually identify and record from second-order sensory neurons. Because these neurons possessed monosynaptic sensory terminals, EPSCs evoked by ST-stimulation in

such neurons are likely to be monosynaptic. As presented in the manuscripts, the jitter and the pharmacological profiles of the EPSCs evoked in such anatomically identified second-order neurons were comparable to monosynaptic events classified by electrophysiological analysis alone. Second, the label identified NTS neurons that participate in the baroreflex. The similarities in synaptic responses of second-order baroreceptor neurons compared to those of unlabeled electrophysiologically monosynaptic neurons suggest that the basic glutamate mechanism of synaptic transmission may be fairly uniform across modalities of sensory synapses. Thus, some of the differentiation across sensory modalities may reflect differences in the second-order neurons or perhaps the participation of other co-released neurotransmitters (Andresen and Kunze 1994).

Despite all the effort devoted to developing this method for identifying aortic baroreceptor inputs into NTS, important questions remain regarding ADN labeling. Perhaps the most important unknown is the uncertainty of whether the labeled endings we see are responsible for the synaptic responses that are evoked by stimulation. As such, it is possible that the evoked EPSCs are not baroreceptor in origin or are not solely baroreceptor mediated. The ST is a mixed population of sensory axons (e.g. barosensory and chemosensory; Mifflin and Felder 1990) and our relatively large stimulation electrode clearly contacts a major portion of the tract. However, electrophysiological evidence suggests that each second-order neuron receives only a limited projection of the afferent fibers that are activated.

The large size of the EPSCs with robust frequency dependent depression and all or none threshold for synaptic activation are consistent with activation of individual fibers. Such recruitment has been used by others to suggest that these responses are characteristic of "unitary" synaptic events, i.e. responses elicited by activation of single afferent axons (Titz and Keller 1997). Another line of evidence relates to the finding of CAP sensitive unmyelinated axons and CAP resistant myelinated axons in the peripheral ADN (Fan and Andresen 1998). The fact that CAP can block all of the EPSC in many medial NTS neurons suggests a lack of convergence of afferent subtypes onto single neurons. Because we know that the labeled neurons receive baroreceptor input and that ST-stimulation activates fibers that contact individual neurons, it is most likely that the monosynaptic EPSCs evoked by ST-stimulation in labeled second-order neurons are baroreflex in origin.

Heterogeneity among second-order neurons

The similarities in glutamate transmission and frequency dependent depression of primary synaptic transmission across second-order NTS neurons are impressive. However, it is unlikely that all second-order neurons are completely homogenous or that the afferents themselves are mechanistically identical (Andresen and Kunze 1994). As Table 1 suggests, multiple transmitters are present within NTS and their cellular mechanisms have not been clearly identified. Some of these transmitters may have presynaptic functions selective to distinct populations of primary afferents. Certainly, VR-1 is localized to only a subset of the sensory

afferents (Caterina and Julius 1999). Further experimentation in our lab have recorded monosynaptic ST evoked EPSCs that are insensitive to CAP. The all or none sensitivity to CAP suggests that the second-order neurons receive A-fiber connections or C- fiber connections but not both. This lack of convergence of the sensory afferent subtypes may represent the first stage of pathway differentiation for afferent inputs even at the first stage of a reflex loop.

FUTURE DIRECTIONS

Identification of the first synapse of the baroreflex in the brainstem slice preparation provides a platform to investigate the cellular mechanisms involved in NTS processing of the sensory signal. Preliminary data from my research has suggested both presynaptic and postsynaptic mechanisms are involved. Pre-synaptically, afferents appear to express unique neurochemicals and receptors. Presynaptic receptors can be a means of modulating transmitter release. Post-synaptically, the specific neurochemicals alter second-order neuron excitability. The lab is now actively investigating several of these mechanisms.

Role of Potassium channels in second-order neurons

Activation of A- or C-type baroreceptors evokes quite distinctly different baroreflex responses (Fan and Andresen 1998). The differences in these pathways appear to extend beyond the sensory element itself to the second-order neuron. I found that potassium currents in different second-order medial NTS neurons can differed

in their kinetics suggesting that distinct potassium channel populations may be present across NTS neurons. I noticed that application of CAP to the slice changed these voltage dependent potassium currents in some neurons. This interesting observation has been extended to demonstrate that the major differences appear to divide second-order neurons between those with CAP sensitive and CAP-insensitive, ST EPSCs (Bailey et al. 2001). CAP sensitive neurons have a rapidly inactivating potassium current that matches the kinetics of the fast transient A type conductance, I_{kA}. This current is found to a much lesser extent in CAP resistant neurons (**FIG 4-2**). I_{kA} has been linked to delayed excitation and bursting patterns of NTS neurons. (Dekin and Getting 1987; Tell and Bradley 1994; Schild et al. 1993). As such, I_{kA} is a reasonable target for modulation of second-order neuron excitability.

Figure 4-2 Different potassium currents are present in NTS neurons where the evoked EPSC is blocked by CAP (CAP-sensitive neurons). Currents were recorded after a prepulse to –90 mV to remove any inactivation. CAP positive neurons have a voltage dependent fast inactivating current with similar kinetics to I_{Ka} (top traces). These currents were not present in CAP insensitive neurons (middle traces). The bottom panel is the schematic of the voltage clamp paradigm.

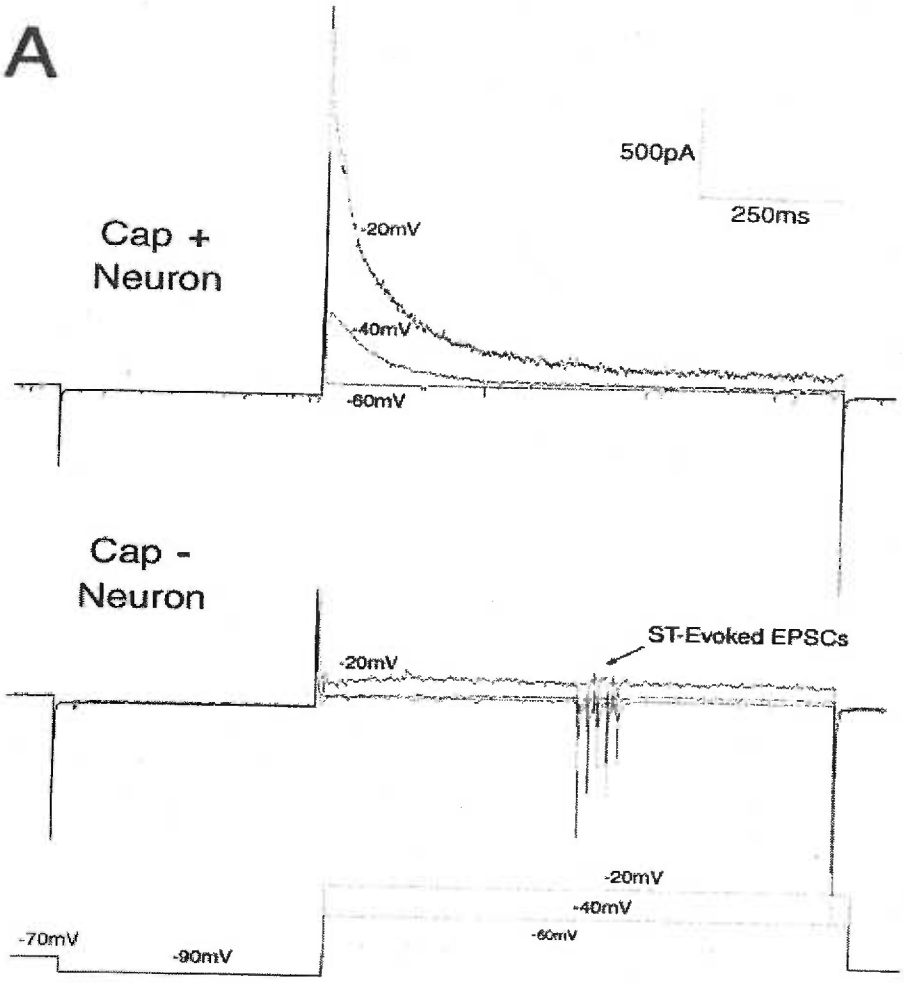
A
500pA
250ms
Cap +
Neuron
-20mV
-40mV
-60mV
Cap -
Neuron
ST-Evoked EPSCs
-20mV
-20mV
-40mV
-60mV
-70mV
-90mV

Indeed, activation of the sensory afferents with CAP decreases this early fast inactivating potassium conductance (**FIG 4-3**). Therefore, CAP-sensitive second-order neurons may have a unique potassium conductance that is modulated by a neurotransmitter that is released by CAP. Peptide release is a potential mechanism for potassium channel modulation (Takano et al. 1996; Takano et al. 1995) Candidate neuropeptides are many, but several studies have demonstrated that CAP releases substance P from sensory afferents (Donnerer and Lembeck 1983).

Figure 4-3 I_{kA} is decreased by application of CAP in NTS neurons where CAP blocks evoked EPSCs (CAP sensitive neurons). Currents were recorded after a prepulse to –90 mV to remove any inactivation. The bottom panel is the schematic of the voltage clamp paradigm.

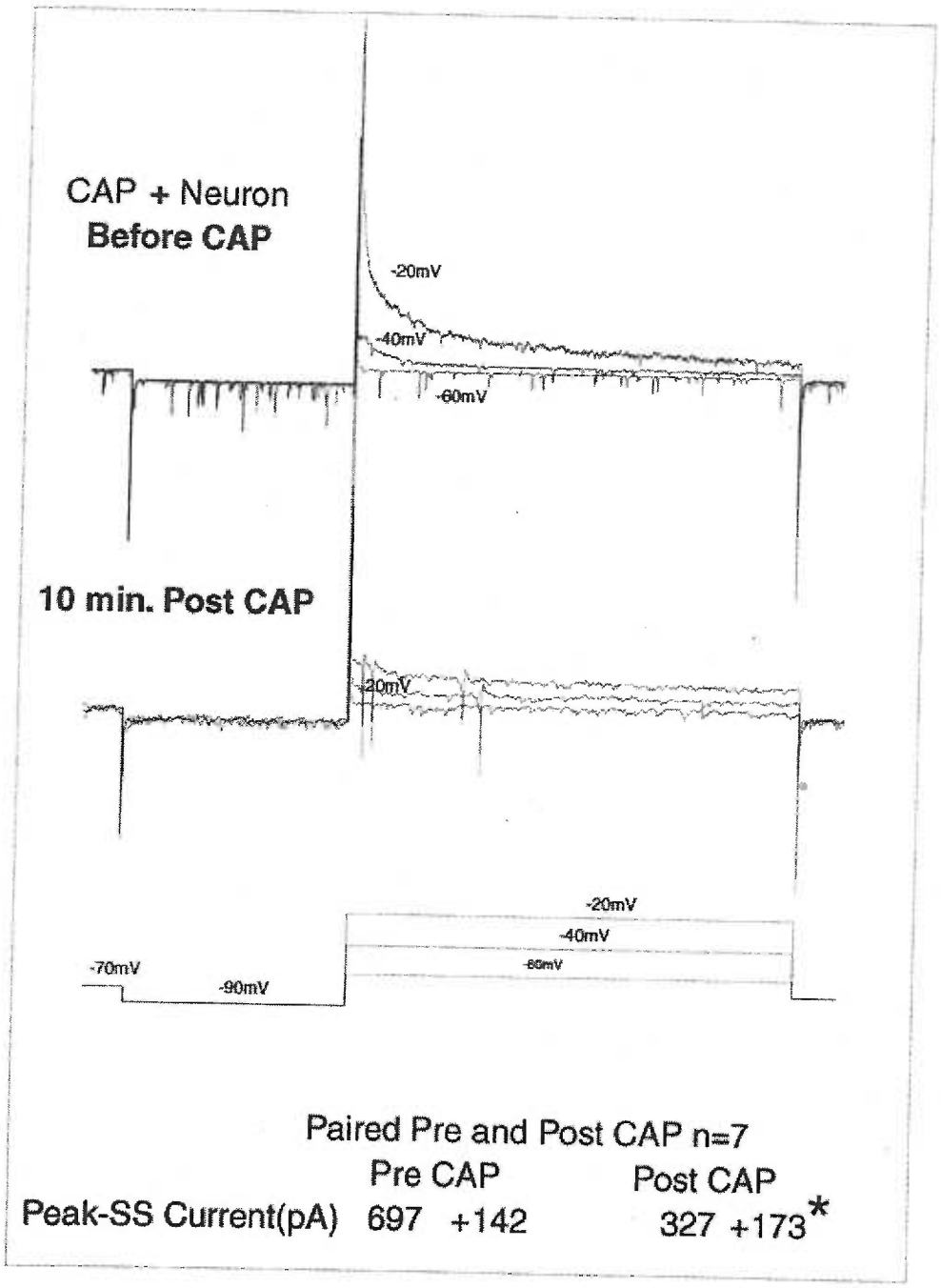

Paired Pre and Post CAP n=7

	Pre CAP	Post CAP
Peak-SS Current(pA)	697 +142	327 +173*

Role of neurotransmitters / neuromodulators:

Substance P.

Peptide actions within NTS are a longstanding issue given the extensive immunocytochemical and other data related to peptides within NTS (Lawrence and Jarrott 1996; Palkovits 1985). I have looked at substance P within NTS in a preliminary way but the results are complex. Substance P and other peptides are associated with CAP sensitive sensory afferents (Willis, Jr. and Coggeshall 1991a; Helke et al. 1981; Lorez et al. 1983) and alter cardiovascular responses when microinjected into NTS (Qu et al. 1996; Hall et al. 1993). In pilot experiments, I tested whether substance P binding and internalization of substance P receptors with CAP application in our brainstem slice. In the spinal cord, intense activation of peripheral sensory afferents induces varicosity formation within minutes (Mantyh et al. 1995). A similar response is visible within NTS. CAP application induces dendritic varicosities in neurons filled intracellularly with lucifer yellow. (**FIG 4-4**). In other experiments, we exposed slices to a fluorescent analogue of SP and captured serial images of NTS neurons over time. These time series of images suggest that the indicator substance P bound to NTS neurons and over time these became internalized. After exposure to this agonist for 5 minutes, the fluorescent substance P was removed and the slices washed in normal solution. Internalized receptors retained the fluorescent signal in varicosities similar to those induced by CAP (**FIG 4-5**). Note also that fluorescent SP was also retained in NTS cell bodies (**FIG 4-5**). Both of these structural changes in NTS neurons appeared to be

reversible over the course of 30-40 minutes. Such labeling patterns suggest receptor location on both the dendrites and cell bodies.

Figure 4-4 Exposure of the slice to CAP induces varicosity formation in NTS neuron dendrites. This neuron was filled with Lucifer yellow in order to visualize the neuronal processes. Varicosities formed in the dendrites (arrow lower panel) within a 5-minute exposure to CAP.

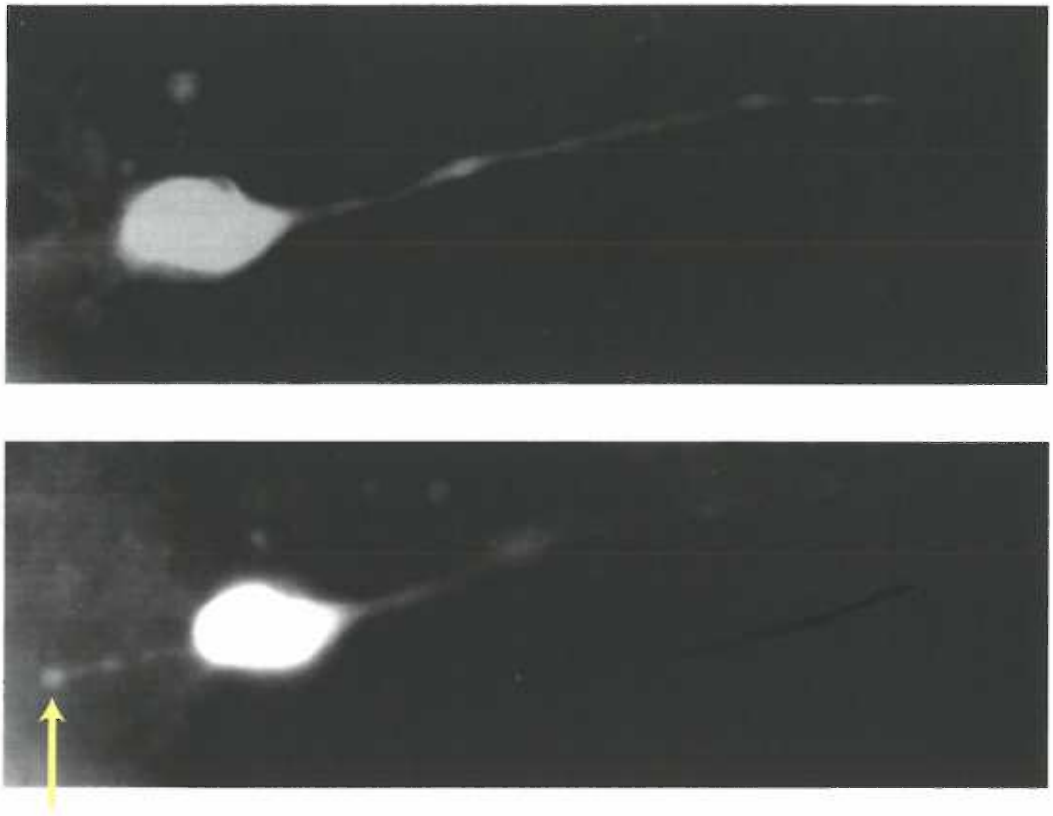

Figure 4-5 Incubation of the slice with fluorescent substance P labels both the soma and varicosities on neuronal processes (Arrow).

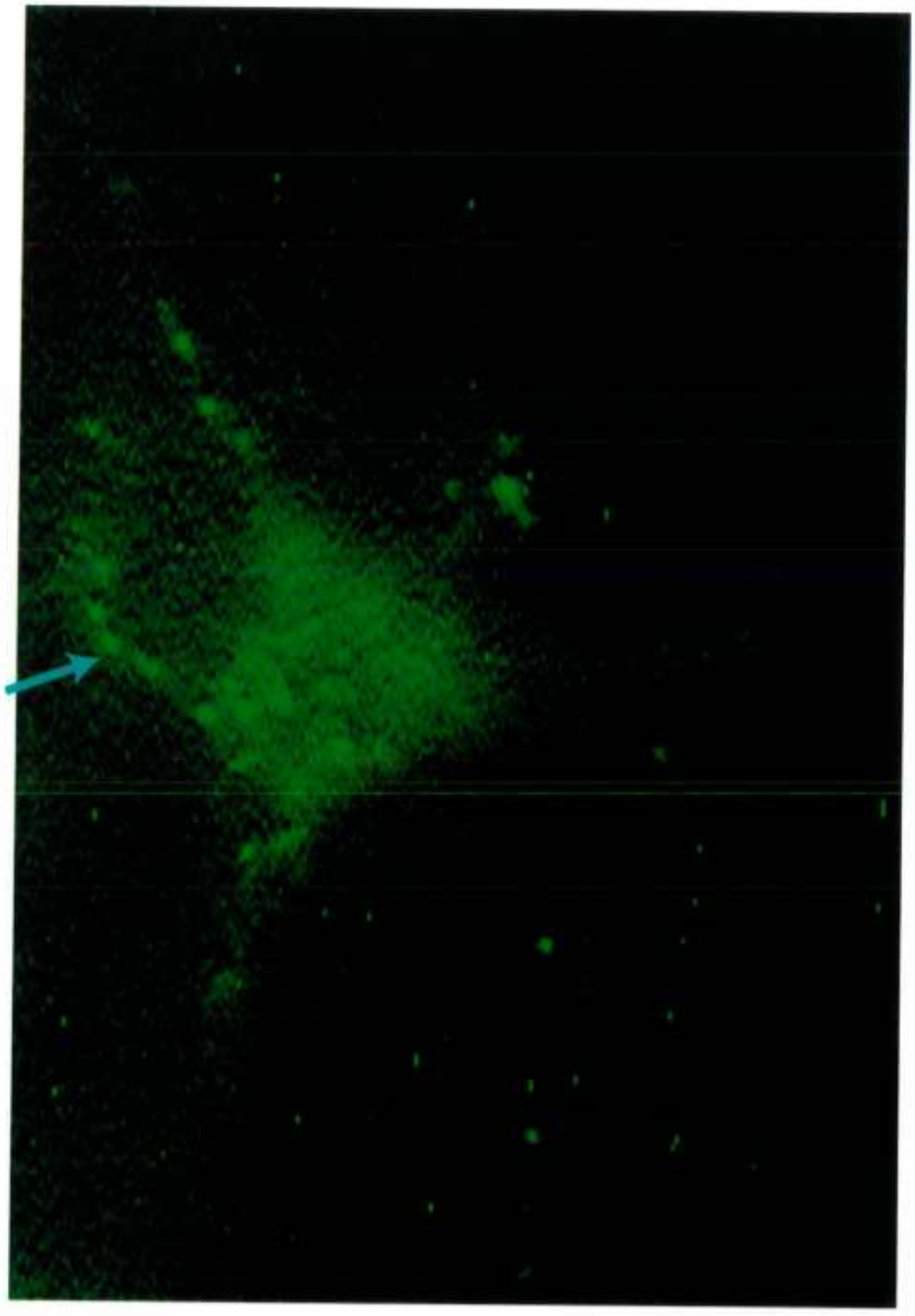

Functionally, a number of possible actions of substance P are possible (Gilbert et al. 1998). In another pilot study, I tested for possible substance P synaptic release electrophysiologically. ST evoked EPSCs were measured before and after exposure to non-selective neurokinin antagonists in the slice. Interestingly, application of these antagonists had variable effects on EPSC amplitude (increases and decreases). These electrophysiological experiments were performed early in my graduate studies before I developed strategies for clearly identifying ST evoked monosynaptic responses in second-order neurons. Therefore, some of the variability in these responses might reflect a recorded mix of second and higher order neurons. This may be critical since it is well known that a substantial fraction of substance P within NTS is not associated with visceral afferent endings, e.g. (Gillis et al. 1980). Where the post-synaptic receptors are located is fundamental to answering questions about function. Sampling across multiple sub-populations of NTS neurons can account for the multiple responses to the same experimental paradigm. The cellular mechanisms of these peptides use in modulating the first synapse and second-order neurons remains an important topic and needs to be studied more thoroughly.

Adenosine- Tri- Phosphate (ATP)

Some of the neurotransmitters released from presynaptic endings feedback to have substantial effects on presynaptic release properties. One example from my studies suggests just such a role for ATP at NTS sensory synapses. Microinjection studies had suggested that ATP and purinergic receptors had substantial effects in medial NTS (Barraco et al. 1996;Scislo et al. 1997;Scislo and O'Leary 1998;Scislo et al. 1998), although which neurons were involved was unknown. We evaluated whether ATP could act at the primary synapse in NTS. A non-hydrolysable, mixed agonist for P2X1 and P2X3 receptors dramatically increased the number of evoked synaptic responses in the slice. This suggested a potential pre-synaptic action, but could not resolve potential indirect effects within the slice. Thus, interpretation was complicated and difficult. We turned to an ongoing collaboration with the lab of Norio Akaike in Fukuoka, Japan. These experiments were conducted in Japan in dissociated NTS neurons and the results were clearly consistent with a selective presynaptic action at P2X receptors on sensory terminals. VR-1 appears to co-localize with P2X receptors on these medial NTS neurons. Co-release of ATP and glutamate, both of which may act at presynaptic receptors, is an intriguing mechanism of sensory modulation. Furthermore, if ATP is release synaptically, then the cleavage of ATP into adenosine will likely produce a host of other effects as well. Postsynaptic effects of adenosine could act as an anterograde mechanism of synaptic modulation and might have actions at postsynaptic potassium channels.

Conclusion

When I started working in NTS, the knowledge base about synaptic transmission was limited. Techniques at the time could not provide the resolution required to answer many of the specific cellular questions. My major contribution has been to develop a visualized preparation that combines electrophysiological access with an anatomical reference to the sensory afferents of the baroreflex. The clear advantage of this preparation is that visualization of the neurons provides the ability to identify both the projections to the cell through an anterograde fluorescent label and where the neurons project to by retrograde tracing in a viable slice. This identification has elucidated characteristics of the presynaptic afferents and characteristics of the second-order NTS neurons important in sensory processing. This information places the neurons under study within the context of their physiological role and provides a platform for unraveling the complexity of thousands of neurons with multiple functions within a small nucleus, NTS.

Reference List

1. Aars, H., Myhre, L., and Haswell, B. The function of baroreceptor C fibres in the rabbit's aortic nerve. Acta Physiol.Scand. 102: 84-93, 1978.

2. Allen, A. M., Adams, J. M., and Guyenet, P. G. Role of the spinal cord in generating the 2- to 6-Hz rhythm in rat sympathetic outflow. Am.J.Physiol.Regul.Integr.Comp.Physiol. 264: R938-R945, 1993.

3. Andresen, M. C., Doyle, M. W., Jin, Y.-H., and Bailey, T. W. Cellular mechanisms of baroreceptor integration at the nucleus tractus solitarius.New York Academy of Sciences. 2001.

4. Andresen, M. C., Krauhs, J. M., and Brown, A. M. Relationship of aortic wall baroreceptor properties during development in normotensive and spontaneously hypertensive rats. Circ.Res. 43: 728-738, 1978.

5. Andresen, M. C. and Kunze, D. L. Nucleus tractus solitarius: gateway to neural circulatory control. Annu.Rev.Physiol. 56: 93-116, 1994.

6. Andresen, M. C. and Mendelowitz, D. Sensory afferent neurotransmission in caudal nucleus tractus solitarius - common denominators. Chemical Senses 21: 387-395, 1996.

7. Andresen, M. C. and Yang, M. Arterial baroreceptor resetting: Contributions of chronic and acute processes. Clin.Exper.Pharmacol.Physiol. 15 (suppl.): 19-30, 1989.

8. Andresen, M. C. and Yang, M. Non-NMDA receptors mediate sensory afferent synaptic transmission in medial nucleus tractus solitarius. Am.J.Physiol.Heart Circ.Physiol. 259: H1307-H1311, 1990.

9. Andresen, M. C. and Yang, M. Dynamics of sensory afferent synaptic transmission in aortic baroreceptor regions of nucleus tractus solitarius. J.Neurophysiol. 74: 1518-1528, 1995.

10. Aylwin, M. L., Horowitz, J. M., and Bonham, A. C. NMDA receptors contribute to primary visceral afferent transmission in the nucleus of the solitary tract. J.Neurophysiol. 77: 2539-2548, 1997.

11. Bailey, T. W., Jin, Y.-H., Doyle, M. W., Chang, K. S. K., and Andresen, M. C. Medial nucleus tractus solitarius (mNTS) neurons with c-fiber sensory inputs preferentially express large voltage activated transient outward currents. FASEB Journal 15, A. 2001. Ref Type: Abstract

12. Barraco, R. A., O'Leary, D. S., Ergene, E., and Scislo, T. J. Activation of purinergic receptor subtypes in the nucleus tractus solitarius elicits specific regional vascular response patterns. J.Auton.Nerv.Syst. 59: 113-124, 1996.

13. Berger, A. J. and Averill, D. B. Projection of single pulmonary stretch receptors to solitary tract region. Journal.of Neurophysiology. 49: 819-830, 1983.

14. Brattström, A., De Jong, W., and De Wied, D. Vasopressin microinjections into the nucleus tractus solitarii decrease heart rate and blood pressure in anaesthetized rats. J.Hypertension 6: S521-S524, 1988.

15. Brooks, P. A., Glaum, S. R., Miller, R. J., and Spyer, K. M. The actions of baclofen on neurones and synaptic transmission in the nucleus tractus solitarii of the rat *in vitro*. J.Physiol.(Lond.) 457: 115-129, 1992.

16. Burnstock, G. P2X receptors in sensory neurones. Br.J.Anaesth. 84: 476-488, 2000.

17. Caterina, M. J. and Julius, D. Sense and specificity: a molecular identity for nociceptors. Curr.Opin.Neurobiol. 9: 525-530, 1999.

18. Caterina, M. J., Leffler, A., Malmberg, A. B., Martin, W. J., Trafton, J., Petersen-Zeitz, K. R., Koltzenburg, M., Basbaum, A. I., and Julius, D. Impaired nociception and pain sensation in mice lacking the capsaicin receptor. Science 288: 306-313, 2000.

19. Caterina, M. J., Schumacher, M. A., Tominaga, M., Rosen, T. A., Levine, J. D., and Julius, D. The capsaicin receptor: a heat-activated ion channel in the pain pathway. Nature 389: 816-824, 1997.

20. Cerne, R. and Randic, M. Modulation of AMPA and NMDA responses in rat spinal dorsal horn neurons by *trans*-1-aminocyclopentane-1,3-dicarboxylic acid. Neurosci.Lett. 144: 180-184, 1992.

21. Champagnat, J., Denavit-Saubie, M., Grant, K., and Shen, K. F. Organization of synaptic transmission in the mammalian solitary complex, studied in vitro. J.Physiol.(Lond.) 381: 551-573, 1986.

22. Champagnat, J., Siggins, G. R., Koda, L. Y., and Denavit-Saubie, M. Synaptic responses of neurons of the nucleus tractus solitarius in vitro. Brain Res. 325: 49-56, 1985.

23. Chan, R. K., Peto, C. A., and Sawchenko, P. E. Fine structure and plasticity of barosensitive neurons in the nucleus of solitary tract. J.Comp Neurol. 422: 338-351, 2000.

24. Chen, C. C., England, S., Akopian, A. N., and Wood, J. N. A sensory neuron-specific, proton-gated ion channel. Proc.Natl.Acad.Sci.U.S.A 95: 10240-10245, 1998.

25. Ciriello, J. Brainstem projections of aortic baroreceptor afferent fibers in the rat. Neurosci.Lett. 36: 37-42, 1983.

26. Coleridge, H. M. and Coleridge, J. C. G. Cardiovascular afferents involved in regulation of peripheral vessels. Annu.Rev.Physiol. 42: 413-427, 1980.

27. Collingridge, G. L. The brain slice preparation: A tribute to the pioneer Henry McIlwain. J.Neurosci.Methods 59: 5-9, 1995.

28. Collingridge, G. L. and Bliss, T. V. P. Memories of NMDA receptors and LTP. Trends Neurosci. 18: 54-56, 1995.

29. Colombari, E., Menani, J. V., and Talman, W. T. Commissural NTS contributes to pressor responses to glutamate injected into the medial NTS of awake rats. Am.J.Physiol.Regul.Integr.Comp.Physiol. 270: R1220-R1225, 1996.

30. Conti, F. and Weinberg, R. J. Shaping excitation at glutamatergic synapses. Trends Neurosci. 22: 451-458, 1999.

31. Cook, S. P. and McCleskey, E. W. ATP, pain and a full bladder. Nature 407: 951-952, 2000.

32. Cook, S. P., Rodland, K. D., and McCleskey, E. W. A memory for extracellular Ca^{2+} by speeding recovery of P2X receptors from desensitization. J.Neurosci. 18: 9238-9244, 1998.

33. Cotman, C. W., Monaghan, D. T., and Ganong, A. H. Excitatory amino acid neurotransmission: NMDA receptors and Hebb-type synaptic plasticity. Annu.Rev.Neurosci. 11: 61-80, 1988.

34. De Paula, P. M., Castania, J. A., Bonagamba, L. G. H., Salgado, H. C., and Machado, B. H. Hemodynamic responses to electrical stimulation of the aortic depressor nerve in awake rats. Am.J.Physiol.Regul.Integr.Comp.Physiol. 277: R31-R38, 1999.

35. Dekin, M. S. and Getting, P. A. In vitro characterization of neurons in the ventral part of the nucleus tractus solitarius. II. Ionic basis for repetitive firing patterns. J.Neurophysiol. 58: 215, 1987.

36. Deuchars, J., Li, Y. W., Kasparov, S., and Paton, J. F. Morphological and electrophysiological properties of neurones in the dorsal vagal complex of the rat activated by arterial baroreceptors. J.Comp Neurol. 417: 233-249, 2000.

37. Donnerer, J. and Lembeck, F. Capsaicin-induced reflex fall in rat blood pressure is mediated by afferent substance P-containing neurones via a reflex centre in the brain stem. Naunyn-Schmiedeberg's Arch.Pharmacol. 324: 293-295, 1983.

38. Douglas, W. W. and Ritchie, J. M. Cardiovascular reflexes produced by electrical excitation of non-medullated afferents in the vagus, carotid sinus and aortic nerves. J.Physiol.(Lond.) 134: 167-178, 1956.

39. Douglas, W. W. and Ritchie, J. M. Mammalian nonmyelinated nerve fibers. Physiol.Rev. 42: 297-334, 1962.

40. Doyle, M. W. and Andresen, M. C. Propofol modulates synaptic transmission within medial nucleus tractus solitarius (mNTS). FASEB Journal 11, A. 1997.
Ref Type: Abstract

41. Doyle, M. W. and Andresen, M. C. Reliability of monosynaptic transmission in brain stem neurons in vitro. J.Neurophysiol. 85: 2213-2223, 2001.

42. Doyle, M. W., Schild, J. H., Yang, M., and Andresen, M. C. Cyclothiazide fails to remove frequency dependent depression of primary sensory synaptic transmission in rat medial nucleus tractus solitarius (mNTS). Soc.Neurosci.Abstr. 23, A. 1997.
Ref Type: Abstract

43. Drewe, J. A., Childs, G. V., and Kunze, D. L. Synaptic transmission between dissociated adult mammalian neurons and attached synaptic boutons. Science 241: 1810-1813, 1988.

44. Fan, W. and Andresen, M. C. Differential frequency-dependent reflex integration of myelinated and nonmyelinated rat aortic baroreceptors. Am.J.Physiol.Heart Circ.Physiol. 275: H632-H640, 1998.

45. Fan, W., Schild, J. H., and Andresen, M. C. Graded and dynamic reflex summation of myelinated and unmyelinated rat aortic baroreceptors.
Am.J.Physiol.Regul.Integr.Comp.Physiol. 277: R748-R756, 1999.

46. Felder, R. B. Excitatory and inhibitory interactions among renal and cardiovascular afferent nerves in dorsomedial medulla. Am.J.Physiol.Regul.Integr.Comp.Physiol. 250: R580-R588, 1986.

47. Felder, R. B. and Mifflin, S. W. Modulation of carotid sinus afferent input to nucleus tractus solitarius by parabrachial nucleus stimulation. Circ.Res. 63: 35-49, 1988.

48. Feldman, P. D. and Felder, R. B. Effects of gamma-aminobutyric acid and glycine on synaptic excitability of neurones in the solitary tract nucleus. Neuropharmacology 30: 225-236, 1991.

49. Ferster, D. and Spruston, N. Cracking the neuronal code. Science 270: 756-757, 1995.

50. Foreman, R. D. Mechanisms of cardiac pain. Annu.Rev.Physiol. 61: 143-167, 1999.

51. Foreman, R. D. Integration of viscerosomatic sensory input at the spinal level. Prog.Brain Res. 122: 209-221, 2000.

52. Franz, G. Nonlinear rate sensitivity of the carotid sinus reflex as a consequence of static and dynamic nonlinearities in baroreceptor behavior. Ann.NY Acad.Sci. 156: 811-824, 1969.

53. Gil, Z., Connors, B. W., and Amitai, Y. Efficacy of thalamocortical and intracortical synaptic connections: quanta, innervation, and reliability. Neuron 23: 385-397, 1999.

54. Gilbert, R., Ryan, J. S., Horackova, M., Smith, F. M., and Kelly, M. E. M. Actions of substance P on membrane potential and ionic currents in guinea pig stellate ganglion neurons. Am.J.Physiol.Cell Physiol. 274: C892-C903, 1998.

55. Gillis, R. A., Helke, C. J., Hamilton, B. L., Norman, W. P., and Jacobowitz, D. M. Evidence that substance P is a neurotransmitter of baro- and chemoreceptor afferents in nucleus tractus solitarius. Brain Res. 181: 476-481, 1980.

56. Gordon, F. J. and Leone, C. Non-NMDA receptors in the nucleus of the tractus solitarius play the predominant role in mediating aortic baroreceptor reflexes. Brain Res. 568: 319-322, 1991.

57. Granata, A. R. and Kitai, S. T. Intracellular study of nucleus parabrachialis and nucleus tractus solitarii interconnections. Brain Res. 492: 281-292, 1989.

58. Gross, P. M., Wall, K. M., Pang, J. J., Shaver, S. W., and Wainman, D. S. Microvascular specializations promoting rapid interstitial solute dispersion in nucleus tractus solitarius. Am.J.Physiol.Regul.Integr.Comp.Physiol. 259: R1131-R1138, 1990.

59. Gross, P. M., Wall, K. M., Wainman, D. S., and Shaver, S. W. Subregional topography of capillaries in the dorsal vagal complex of rats: II. Physiological properties. J.Comp.Neurol. 306: 83-94, 1991.

60. Gu, J. G., Albuquerque, C., Lee, C. J., and MacDermott, A. B. Synaptic strengthening through activation of Ca^{2+}-permeable AMPA receptors. Nature 381: 793-796, 1996.

61. Gu, J. G. G. and MacDermott, A. B. Activation of ATP P2X receptors elicits glutamate release from sensory neuron synapses. Nature 389: 749-753, 1997.

62. Guo, A., Vulchanova, L., Wang, J., Li, X., and Elde, R. Immunocytochemical localization of the vanilloid receptor 1 (VR1): relationship to neuropeptides, the $P2X_3$ purinoceptor and IB4 binding sites. Eur.J.Neurosci. 11: 946-958, 1999.

63. Hall, M. E., Greer, R. A., and Stewart, J. M. Effects of L-glutamate, substance P and substance P(1-7) on cardiovascular regulation in the nucleus tractus solitarius. Regul.Pept. 46: 102-109, 1993.

64. Helke, C. J., Jacobowitz, D. M., and Thoa, N. B. Capsaicin and potassium evoked substance P release from the nucleus tractus solitarius and spinal trigeminal nucleus in vitro. Life Sci. 29: 1779-1785, 1981.

65. Helliwell, R. J. A., McLatchie, L. M., Clarke, M., Winter, J., Bevan, S., and McIntyre, P. Capsaicin sensitivity is associated with the expression of the vanilloid (capsaicin) receptor (VR1) mRNA in adult rat sensory ganglia. Neuroscience Letters 250: 177-180, 1998.

66. Holzer, P. Capsaicin: Cellular targets, mechanisms of action, and selectivity for thin sensory neurons. Pharmacol.Rev. 43: 143-201, 1991.

67. Huangfu, D. H. and Guyenet, P. G. Autoactivity of A5 neurons: role of subthreshold oscillations and persistent Na^+ current. Am.J.Physiol.Heart Circ.Physiol. 273: H2280-H2289, 1997.

68. Hudspeth, A. J. and Tanaka, K. Sensory systems - Editorial overview. Curr.Opin.Neurobiol. 8: 443-446, 1998.

69. Ito, S. and Sved, A. F. Tonic glutamate-mediated control of rostral ventrolateral medulla and sympathetic vasomotor tone. Am.J.Physiol.Regul.Integr.Comp.Physiol. 273: R487-R494, 1997.

70. Janig, W. and Habler, H. J. Specificity in the organization of the autonomic nervous system: a basis for precise neural regulation of homeostatic and protective body functions. Prog.Brain Res. 122: 351-367, 2000.

71. Janig, W., Khasar, S. G., Levine, J. D., and Miao, F. J. The role of vagal visceral afferents in the control of nociception. Prog.Brain Res. 122: 273-287, 2000.

72. Jonas, P. and Spruston, N. Mechanisms shaping glutamate-mediated excitatory postsynaptic currents in the CNS. Curr.Opin.Neurobiol. 4: 366-372, 1994.

73. Jung, R. and Katona, P. G. Cardiovascular and respiratory responses to slow ramp carotid sinus pressures in the dog. J.Appl.Physiol. 68: 1465-1474, 1990.

74. Kalia, M. and Richter, D. Rapidly adapting pulmonary receptor afferents: II. Fine structure and synaptic organization of central terminal processes in the nucleus of the tractus solitarius. J.Comp.Neurol. 274: 574-594, 1988.

75. Kasparov, S. and Paton, J. F. Differential effects of angiotensin II in the nucleus tractus solitarii of the rat - plausible neuronal mechanisms. J.Physiol (Lond) 521 Pt 1: 227-238, 1999.

76. Kerkut, G. and Wheal, H. V. Electrophysiology of isolated mammalian CNS preparations. New York, Academic Press. 1981, 1-402.

77. Kobayashi, M., Cheng, Z. B., Tanaka, K., and Nosaka, S. Is the aortic depressor nerve involved in arterial chemoreflexes in rats? J.Auton.Nerv.Syst. 78: 38-48, 1999.

78. Kollai, M., Jokkel, G., Bonyhay, I., Tomcsanyi, J., and Naszlady, A. Relation between baroreflex sensitivity and cardiac vagal tone in humans. Am.J.Physiol.Heart Circ.Physiol. 266: H21-H27, 1994.

79. Koyama, S., Kubo, C., Rhee, J. S., and Akaike, N. Presynaptic serotonergic inhibition of GABAergic synaptic transmission in mechanically dissociated rat basolateral amygdala neurons. J.Physiol (Lond) 518: 525-538, 1999.

80. Kunze, D. L. Reflex discharge patterns of cardiac vagal efferent fibres. J.Physiol.(Lond.) 222: 1-15, 1972.

81. Kunze, D. L. and Andresen, M. C. Arterial baroreceptors: Excitation and modulation. In Zucker, I. H. and Gilmore, J. P. eds. Reflex Control of the Circulation. Boca Raton, CRC Press. 1991, 141-166.

82. Lawrence, A. J. and Jarrott, B. Neurochemical modulation of cardiovascular control in the nucleus tractus solitarius. Prog.Neurobiol. 48: 21-53, 1996.

83. Lawson, S. N. Morphological and biochemical cell types of sensory neurons. In Scott, S. A. ed. Sensory neurons: diversity, development, and plasticity. New York, Oxford University Press. 1992, 27-59.

84. Leone, C. and Gordon, F. J. Is L-glutamate a neurotransmitter of baroreceptor information in the nucleus of tractus solitarius? J.Pharmacol.Exp.Ther. 250: 953-962, 1989.

85. Levy, M. and Martin, P. Neural control of the heart. In Berne, R. M. ed. Handbook of Physiology Section 2: The Cardiovascular System, Volume 1 Heart. Bethesda, American Physiological Society. 1979, 581-620.

86. Lichtman, J. W., Wilkinson, R. S., and Rich, M. M. Multiple innervation of tonic endplates revealed by activity-dependent uptake of fluorescent probes. Nature 314: 357-359, 1985.

87. Llewellyn-Smith, I. J. and Burnstock, G. Ultrastructural localization of $P2X_3$ receptors in rat sensory neurons. NeuroReport 9: 2545-2550, 1998.

88. Loewy, A. D. Central autonomic pathways. In Loewy, A. D. and Spyer, K. M. eds. Central regulation of autonomic functions. New York, Oxford. 1990, 88-103.

89. Loewy, A. D. and Spyer, K. M. Vagal preganglionic neurons. In Loewy, A. D. and Spyer, K. M. eds. Central regulation of autonomic functions. New York, Oxford. 1990, 68-87.

90. Lorez, H. P., Haeusler, G., and Aeppli, L. Substance P neurones in medullary baroreflex areas and baroreflex function of capsaicin-treated rats. Comparison with other primary afferent systems. Neuroscience 8: 507-523, 1983.

91. Mantyh, P. W., DeMaster, E., Malhotra, A., Ghilardi, J. R., Rogers, S. D., Mantyh, C. R., Liu, H., Basbaum, A. I., Vigna, S. R., Maggio, J. E., and Simone, D. A. Receptor endocytosis and dendrite reshaping in spinal neurons after somatosensory stimulation. Science 268: 1629-1632, 1995.

92. Mantyh, P. W. and Hunt, S. P. Hot peppers and pain. Neuron 21: 644-645, 1998.

93. Matsuguchi, H., Sharabi, F. M., Gordon, F. J., Johnson, A. K., and Schmid, P. G. Blood pressure and heart rate responses to microinjections of vasopressin into the nucleus tractus solitarus region of the rat. Neuropharmacology 21: 687-693, 1982.

94. Matsumura, K., Averill, D. B., and Ferrario, C. M. Angiotensin II acts at AT_1 receptors in the nucleus of the solitary tract to attenuate the baroreceptor reflex. Am.J.Physiol.Regul.Integr.Comp.Physiol. 275: R1611-R1619, 1998.

95. McAllen, R. M. and Spyer, K. M. The baroreceptor input to cardiac vagal motoneurones. J.Physiol.(Lond.) 282: 365-374, 1978.

96. McCleskey, E. W. and Gold, M. S. Ion channels of nociception. Annu.Rev.Physiol. 61: 835-856, 1999.

97. Mendelowitz, D. Firing properties of identified parasympathetic cardiac neurons in nucleus ambiguus. Am.J.Physiol.Heart Circ.Physiol. 271: H2609-H2614, 1996.

98. Mendelowitz, D. and Kunze, D. L. Characterization of calcium currents in aortic baroreceptor neurons. J.Neurophysiol. 68: 509-517, 1992.

99. Mendelowitz, D., Yang, M., Andresen, M. C., and Kunze, D. L. Localization and retention in vitro of fluorescently labeled aortic baroreceptor terminals on neurons from the nucleus tractus solitarius. Brain Res. 581: 339-343, 1992.

100. Menetrey, D. and Basbaum, A. I. Spinal and trigeminal projections to the nucleus of the solitary tract: a possible substrate for somatovisceral and viscerovisceral reflex activation. J.Comp.Neurol. 255: 439-450, 1987.

101. Mezey, E., Toth, Z. E., Cortright, D. N., Arzubi, M. K., Krause, J. E., Elde, R., Guo, A., Blumberg, P. M., and Szallasi, A. Distribution of mRNA for vanilloid receptor subtype 1 (VR1), and VR1- like immunoreactivity, in the central nervous system of the rat and human. Proc.Natl.Acad.Sci.USA 97: 3655-3660, 2000.

102. Michael, G. J. and Priestley, J. V. Differential expression of the mRNA for the vanilloid receptor subtype 1 in cells of the adult rat dorsal root and nodose ganglia and its downregulation by axotomy. J.Neurosci. 19: 1844-1854, 1999.

103. Mifflin, S. W. and Felder, R. B. An intracellular study of time-dependent cardiovascular afferent interactions in nucleus tractus solitarius. J.Neurophysiol. 59: 1798-1813, 1988.

104. Mifflin, S. W. and Felder, R. B. Synaptic mechanisms regulating cardiovascular afferent inputs to solitary tract nucleus. Am.J.Physiol.Heart Circ.Physiol. 259: H653-H661, 1990.

105. Miles, R. Frequency dependence of synaptic transmission in nucleus of the solitary tract in vitro. J.Neurophysiol. 55: 1076-1090, 1986.

106. Mitsikostas, D. D., Del Rio, M. S., Waeber, C., Huang, Z. H., Cutrer, F. M., and Moskowitz, M. A. Non-NMDA glutamate receptors modulate capsaicin induced c-*fos* expression within trigeminal nucleus caudalis. Br.J.Pharmacol. 127: 623-630, 1999.

107. Miura, M. Postsynaptic potentials recorded from nucleus of the solitary tract and its subjacent reticular formation elicited by stimulation of the carotid sinus nerve. Brain Res. 100: 437-440, 1975.

108. Neff, R. A., Mihalevich, M., and Mendelowitz, D. Stimulation of NTS activates NMDA and non-NMDA receptors in rat cardiac vagal neurons in the nucleus ambiguus. Brain Res. 792: 277-282, 1998.

109. North, R. A. and Surprenant, A. Pharmacology of cloned P2X receptors. Annu.Rev.Pharmacol.Toxicol. 40: 563-580, 2000.

110. Nowak, L., Bregestovski, P., Ascher, P., Herbet, A., and Prochiantz, A. Magnesium gates glutamate-activated channels in mouse central neurones. Nature 307: 462-465, 1984.

111. Ohta, H. and Talman, W. T. Both NMDA and non-NMDA receptors in the NTS participate in the baroreceptor reflex in rats. Am.J.Physiol.Regul.Integr.Comp.Physiol. 267: R1065-R1070, 1994.

112. Palkovits, M. Distribution of neuroactive substances in the dorsal vagal complex of the medulla oblongata. Neurochem.Int. 7: 213-219, 1985.

113. Paton, J. F. R., Ramirez, J.-M., and Richter, D. W. Functionally intact in vitro preparation generating respiratory activity in neonatal and mature mammals. Pflügers Arch. 428: 250-260, 1994.

114. Qu, L., McQueeney, A. J., and Barnes, K. L. Presynaptic or postsynaptic location of receptors for angiotensin II and substance P in the medial solitary tract nucleus. J.Neurophysiol. 75: 2220-2228, 1996.

115. Randich, A., Ren, K., and Gebhart, G. F. Electrical stimulation of cervical vagal afferents.II.Central relays for behavioral antinociception and arterial blood pressure decreases. J.Neurophysiol. 64: 1115-1124, 1990.

116. Reis, D. J. and Talman, W. T. Brain lesions and hypertension. In Jong, W. d. e. ed. Handbook of Hypertension Experimental and Genetic Models of Hypertension. New York, Elsevier Science Publishers. 1984, 451-473.

117. Rhee, J.-S., Wang, Z. M., Nabekura, J., Inoue, K., and Akaike, N. ATP facilitates spontaneous glycinergic IPSC frequency at dissociated dorsal horn interneurone synapses. J.Physiol.(Lond.) 542: 471-483, 2000.

118. Sabatini, B. L. and Regehr, W. G. Timing of neurotransmission at fast synapses in the mammalian brain. Nature 384: 170-172, 1996.

119. Sabatini, B. L. and Regehr, W. G. Timing of synaptic transmission. Annu.Rev.Physiol 61: 521-542, 1999.

120. Sandkuhler, J., Chen, J. G., Cheng, G., and Randic, M. Low-frequency stimulation of afferent Adelta-fibers induces long-term depression at primary afferent synapses with substantia gelatinosa neurons in the rat. J Neurosci 17: 6483-6491, 1997.

121. Saper, C. B. Pain as a visceral sensation. Prog.Brain Res. 122: 237-243, 2000.

122. Sapru, H. N., Gonzalez, E., and Krieger, A. J. Aortic nerve stimulation in the rat: Cardiovascular and respiratory responses. Brain Res.Bull. 6: 393-398, 1981.

123. Sapru, H. N. and Krieger, A. J. Carotid and aortic chemoreceptor function in the rat. J.Appl.Physiol. 42: 344-348, 1977.

124. Scheuer, D. A., Zhang, J., Toney, G. M., and Mifflin, S. W. Temporal processing of aortic nerve evoked activity in the nucleus of the solitary tract. J.Neurophysiol. 76: 3750-3757, 1996.

125. Schild, J. H., Clark, J. W., Canavier, C. C., Kunze, D. L., and Andresen, M. C. Afferent synaptic drive of rat medial nucleus tractus solitarius neurons: Dynamic simulation of graded vesicular mobilization, release, and non-NMDA receptor kinetics. J.Neurophysiol. 74: 1529-1548, 1995.

126. Schild, J. H., Doyle, M. W., Yang, M., and Andresen, M. C. Desensitization is not essential for use dependent depression of sensory synaptic transmission in medial nucleus tractus solitarius (mNTS). Soc.Neurosci.Abstr. 23, A. 1997.
Ref Type: Abstract

127. Schild, J. H., Khushalani, S., Clark, J. W., Andresen, M. C., Kunze, D. L., and Yang, M. An ionic current model for neurons in the rat medial nucleus tractus solitarius receiving sensory afferent input. J.Physiol.(Lond.) 469: 341-363, 1993.

128. Schild, J. H. and Kunze, D. L. Experimental and modeling study of Na^+ current heterogeneity in rat nodose neurons and its impact on neuronal discharge. J.Neurophysiol. 78: 3198-3209, 1997.

129. Scislo, T. J., Augustyniak, R. A., Barraco, R. A., Woodbury, D. J., and O'Leary, D. S. Activation of P_{2x}-purinoceptors in the nucleus tractus solitarius elicits differential inhibition of lumbar and renal sympathetic nerve activity. J.Auton.Nerv.Syst. 62: 103-110, 1997.

130. Scislo, T. J., Ergene, E., and O'Leary, D. S. Impaired arterial baroreflex regulation of heart rate after blockade of P_2-purinoceptors in the nucleus tractus solitarius. Brain Research Bulletin 47: 63-67, 1998.

131. Scislo, T. J. and O'Leary, D. S. Differential control of renal vs. adrenal sympathetic nerve activity by NTS A2a and P2x purinoceptors. Am.J.Physiol 275: H2130-H2139, 1998.

132. Scislo, T. J. and O'Leary, D. S. Differential role of ionotropic glutamatergic mechanisms in responses to NTS P(2x) and A(2a) receptor stimulation. Am.J.Physiol Heart Circ.Physiol 278: H2057-H2068, 2000.

133. Seagard, J. L., Dean, C., and Hopp, F. A. Discharge patterns of baroreceptor-modulated neurons in the nucleus tractus solitarius. Neurosci.Lett. 191: 13-18, 1995.

134. Seagard, J. L., Dean, C., and Hopp, F. A. Role of glutamate receptors in transmission of vagal cardiac input to neurones in the nucleus tractus solitarii in dogs. Journal of Physiology 520: 243-253, 1999.

135. Seagard, J. L., Van Brederode, J. F. M., Dean, C., Hopp, F. A., Gallenberg, L. A., and Kampine, J. P. Firing characteristics of single-fiber carotid sinus baroreceptors. Circ.Res. 66: 1499-1509, 1990.

136. Shaver, S. W., Pang, J. J., Wall, K. M., Sposito, N. M., and Gross, P. M. Subregional topography of capillaries in the dorsal vagal complex of rats: I. Morphometric properties. J.Comp.Neurol. 306: 73-82, 1991.

137. Snedecor, G. W. and Cochran, W. G. Statistical Methods. Ames, Iowa, Iowa State University Press. 1980, 385-388.

138. Snider, W. D. and McMahon, S. B. Tackling pain at the source: New ideas about nociceptors. Neuron 20: 629-632, 1998.

139. Spyer, K. M. The central nervous organization of reflex circulatory control. In Loewy, A. D. and Spyer, K. M. eds. Central Regulation of Autonomic Functions. New York, Oxford University Press. 1990, 168-188.

140. Sved, A. F. and Curtis, J. T. Amino acid neurotransmitters in nucleus tractus solitarius: An in vivo microdialysis study. J.Neurochem. 61: 2089-2098, 1993.

141. Szallasi, A. and Blumberg, P. M. Vanilloid (Capsaicin) receptors and mechanisms. Pharmacol.Rev. 51: 159-212, 1999.

142. Takano, K., Stanfield, P. R., Nakajima, S., and Nakajima, Y. Protein kinase C-mediated inhibition of an inward rectifier potassium channel by substance P in nucleus basalis neurons. Neuron 14: 999-1008, 1995.

143. Takano, K., Yasufuku-Takano, J., Kozasa, T., Singer, W. D., Nakajima, S., and Nakajima, Y. $G_{q/11}$ and PLC-β1 mediate the substance P-induced inhibition of an inward rectifier K^+ channel in brain neurons. J.Neurophysiol. 76: 2131-2136, 1996.

144. Talman, W. T., Perrone, M. H., and Reis, D. J. Evidence for L-glutamate as the neurotransmitter of baroreceptor afferent nerve fibers. Science 209: 813-815, 1980.

145. Tell, F. and Bradley, R. M. Whole-cell analysis of ionic currents underlying the firing pattern of neurons in the gustatory zone of the nucleus tractus solitarii. J.Neurophysiol. 71: 479-492, 1994.

146. Thomas, S., Virginio, C., North, R. A., and Surprenant, A. The antagonist trinitrophenyl-ATP reveals co-existence of distinct P2X receptor channels in rat nodose neurones. Journal of Physiology 509: 411-417, 1998.

147. Thomson, A. M. Facilitation, augmentation and potentiation at central synapses. Trends Neurosci. 23: 305-312, 2000.

148. Thomson, A. M., West, D. C., and Deuchars, J. Properties of single axon excitatory postsynaptic potentials elicited in spiny interneurons by action potentials in pyramidal neurons in slices of rat neocortex. Neuroscience 69: 727-738, 1995.

149. Thoren, P. N. Role of cardiac vagal c-fibers in cardiovascular control. Rev.Physiol.Biochem.Pharmacol. 86: 1-94, 1979.

150. Thoren, P. N., Andresen, M. C., and Brown, A. M. Resetting of aortic baroreceptors with non-myelinated afferent fibers in spontaneously hypertensive rats. Acta Physiol.Scand. 117: 91-97, 1983.

151. Thoren, P. N. and Jones, J. Characteristics of aortic baroreceptor C-fibers in the rabbit. Acta Physiol.Scand. 99: 448-456, 1977.

152. Thoren, P. N., Saum, W. R., and Brown, A. M. Characteristics of rat aortic baroreceptors with nonmedullated afferent nerve fibers. Circ.Res. 40: 231-237, 1977.

153. Titz, S. and Keller, B. U. Rapidly deactivating AMPA receptors determine excitatory synaptic transmission to interneurons in the nucleus tractus solitarius from rat. J.Neurophysiol. 78: 82-91, 1997.

154. Tominaga, M., Caterina, M. J., Malmberg, A. B., Rosen, T. A., Gilbert, H., Skinner, K., Raumann, B. E., Basbaum, A. I., and Julius, D. The cloned capsaicin receptor integrates multiple pain-producing stimuli. Neuron 21: 531-543, 1998.

155. Trussell, L. O. Synaptic mechanisms for coding timing in auditory neurons. Annu.Rev.Physiol 61: 477-496, 1999.

156. Undem, B. J. and Weinreich, D. Electrophysiological properties and chemosensitivity of guinea pig nodose ganglion neurons in vitro. J.Auton.Nerv.Syst. 44: 17-34, 1993.

157. Van Giersbergen, P. L. M., Palkovits, M., and De Jong, W. Involvement of neurotransmitters in the nucleus tractus solitarii in cardiovascular regulation. Physiol.Rev. 72: 789-824, 1992.

158. Virginio, C., North, R. A., and Surprenant, A. Calcium permeability and block at homomeric and heteromeric $P2X_2$ and $P2X_3$ receptors, and P2X receptors in rat nodose neurones. Journal of Physiology 510: 27-35, 1998.

159. Von Gersdorff, H., Schneggenburger, R., Weis, S., and Neher, E. Presynaptic depression at a calyx synapse: The small contribution of metabotropic glutamate receptors. J.Neurosci. 17: 8137-8146, 1997.

160. Vorobjev, V. S. Vibrodissociation of sliced mammalian nervous tissue. J.Neurosci.Methods 38: 145-150, 1991.

161. Vulchanova, L., Riedl, M. S., Shuster, S. J., Buell, G., Surprenant, A., North, R. A., and Elde, R. Immunohistochemical study of the P2X2 and P2X3 receptor subunits in rat and monkey sensory neurons and their central terminals. Neuropharmacology 36: 1229-1242, 1997.

162. Waxman, S. G., Dib-Hajj, S., Cummins, T. R., and Black, J. A. Sodium channels and pain. Proc.Natl.Acad.Sci.USA 96: 7635-7639, 1999.

163. Willis, W. D., Jr. Neurobiology: Cold, pain and the brain. Nature 373: 19-20, 1995.

164. Willis, W. D., Jr. and Coggeshall, R. E. Dorsal root ganglion cells and their processes.Sensory mechanisms of the spinal cord. New York, Plenum Press. 1991a, 47-78.

165. Willis, W. D., Jr. and Coggeshall, R. E. Peripheral nerves and sensory receptors.Sensory mechanisms of the spinal cord. New York, Plenum Press. 1991b, 13-45.

166. Wood, J. N. II. Genetic approaches to pain therapy. Am.J.Physiol Gastrointest.Liver Physiol 278: G507-G512, 2000.

167. Yao, S. T., Barden, J. A., Finkelstein, D. I., Bennett, M. R., and Lawrence, A. J. Comparative study on the distribution patterns of P2X(1)-P2X(6) receptor immunoreactivity in the brainstem of the rat and the common marmoset (Callithrix jacchus): association with catecholamine cell groups. J.Comp Neurol. 427: 485-507, 2000.

168. Yoshimura, M. and Jessell, T. M. Primary afferent-evoked synaptic responses and slow potential generation in rat substantia gelatinosa neurons in vitro. J.Neurophysiol. 62: 96-108, 1989.

169. Zhang, J. and Mifflin, S. W. Differential roles for NMDA and non-NMDA receptor subtypes in baroreceptor afferent integration in the nucleus of the solitary tract of the rat. Journal of Physiology 511: 733-745, 1998a.

170. Zhang, J. and Mifflin, S. W. Receptor subtype specific effects of GABA agonists on neurons receiving aortic depressor nerve inputs within the nucleus of the solitary tract. J.Auton.Nerv.Syst. 73: 170-181, 1998b.

171. Zhang, J. and Mifflin, S. W. Integration of aortic nerve inputs in hypertensive rats. Hypertension 35: 430-436, 2000.